Protein-Polyelectrolyte Complex: Versatile Techniques for Protein Handling

TAKAAKI KURINOMARU

Doctoral Program in Applied Physics

Submitted to the Graduate School of
Pure and Applied Sciences
in Partial Fulfillment of the Requirements
for the Degree of Doctor of Philosophy in
Engineering

at the
University of Tsukuba

Contents

Chapter 1. General Introduction

1.1. Protein: function, structure, and application

Proteins express many of the phenomena of living systems, such as metabolism, immunity, and signal transmission. Compared with other materials, many protein functions are highly selective and precise. For example, enzymes are biocatalysts that regulate a variety of chemical reactions with high specificity under mild conditions, and antibodies recognize and capture target molecules (antigen) with a high degree of specificity. These protein functions are closely related to thei unique three-dimensional structures. Proteins consist of one or multiple polypeptide chains composed of 20 types of L-α-amino acid. Many proteins fold into their native structure in aqueous solution [1]. Typically, hydrophobic amino acids are buried within the interior of the protein and hydrophilic amino acids are exposed to the aqueous medium. The complex folding structures of proteins contribute to their specific functions. For example, enzymes have a substrate-binding pocket and active site, and antibodies are typically Y-shaped with a disulfide bond between two heavy chains and two light chains [2].

Charged amino acids are also important factors in protein function. Four types of charged amino acid are exposed on the protein surface, i.e., cationic lysine (Lys) and arginine (Arg), and anionic asparagine acid (Asp) and glutamic acid (Glu). As charged amino acids are exposed on the protein surface, folding protein molecules have a roughly positive or negative charge. The surface charge of a protein is mainly determined by the isoelectric point (*p*I) and pH—when pH < *p*I, the protein has a positive charge, and vice versa. Note that the *p*I is typically calculated from the amount of amino acids in the protein. These charged amino acids play an important role in protein stability and function [3–10]. For example, superoxide dismutase (SOD) can take up anionic $O_2^{-}\cdot$ toward the active site due to the local cationic amino acid residues, resulting in superior catalytic efficiency ($k_{cat}/K_M \approx 10^9\ M^{-1}s^{-1}$) [3].

Progress in the field of recombinant DNA technology and biotechnology has markedly increased the number of proteins available for various research fields, including biology, bioengineering, and biomedicine. In particular, there have been great advances in biomedicines, including enzymes and antibodies, over the past two decades because of their high target specificity and biocompatibility. At present, more than 200 different biomedicines are approved by the US Food and Drug Administration [11], and used in the treatment of several diseases, including cancer [12, 13], autoimmune diseases [14], rheumatoid arthritis [15], and acute lymphocytic leukemia [16]. In contrast to small molecule drugs, the markets for which have remained at the same level due to patent expiration, it is expected that the market for biomedicines will grow up continuously in future.

1.2. Challenges in protein handling

Despite the significant advances in protein production, the application of proteins has been challenging due to their intrinsic instability. In general, the native structure of a protein is affected by physical and chemical stress in solution, such as heat, pH, pressure, organic solvent, agitation, and proteases, resulting in denaturation of its three-dimensional structure. Denaturated proteins not only lose of their functions but also irreversibly aggregate because the hydrophobic amino acid residues are exposed to the aqueous medium. The formation of protein aggregates is a serious problem for protein handling in various fields, e.g, aggregates of therapeutic proteins are generally unacceptable as protein drugs [17]. Methods for stabilization of proteins are important to enhance their application.

To overcome the problems associated with instability of proteins in solution, various solution additives have been used. Proteins can be stabilized by long term storage- and thermal-induced aggregation in the presence of solution additives, typically with small molecular weight, such as arginine [18, 19], amino acid alkyl esters [20], oligoamine compounds [21–23], sugars [24–26], and detergents [27]. However, high concentrations of solution additives are required to suppress inactivation and aggregation of protein. These high concentrations of additives frequently lead to high viscosity and cytotoxicity. In addition, most solution

additives other than detergents cannot protect against the effects of mechanical stress, such as agitation, which is associated with degradation of therapeutic proteins during transport.

The functionalization of proteins using mutagenesis or chemical modification is another approach to enhance their stability and regulate their activities [7–10, 28]. Conjugation of polymers onto the protein surface is a promising strategy for this purpose [29–31]. Conjugation of poly(ethylene glycol) (PEG) is the most notable strategy for stabilization of therapeutic proteins due to the steric shield of PEG [32–37]. Recently, conjugation of functional polymers onto proteins has been shown to provide novel functions, such as enhancement of enzyme activity [38] and stilum-responsiveness [39–41]. However, conjugation of polymers requires chemical reaction for covalent attachment of the polymer to the protein, which is both time-consuming and costly. In addition, the reduction of intrinsic protein activity often occurs with the conjugation of polymers.

1.3. Protein-polyelectrolyte complex (PPC)

Polyelectrolytes, charged polymers, have great potential as alternative protein stabilizing and functionalizing agents. The polyelectrolytes interact with complementary charged proteins, resulting in the formation of protein-polyelectrolyte complex (PPC). PPC have the following three features:

(i) Simple preparation: Complex formation between proteins and polyelectrolytes occurs spontaneously because the driving force is non-covalent interaction, such as electrostatic interactions, hydrophobic interactions, van der Waals forces, and hydrogen bonds. That is, PPC solutions can be prepared by mixing protein and polyelectrolyte solutions without the need for special equipment. Thus, the preparation of PPC is easier than that of protein-polymer conjugates, which requires a complex procedure of chemical modification. The complementary charge combination should be selected for preparation of PPC, i.e., cationic proteins are used with anionic polyelectrolytes, and vice versa.

(ii) Various states: PPC can exist in several states depending on a number of facors, such as pH, temperature, pressure, ionic strength, stoichiometric ratio, and the types of protien and polyelectrolyte [42,

43]. These states can be roughly classified as soluble PPC and insoluble PPC. Soluble PPC have a surplus charge associated with dispersion in aqueous medium and a size of about < 100 nm, while insoluble PPC with a size of > 100 nm has less charge. Insoluble PPC frequently self-assemble, resulting in precipitate, cocervate, and gel formation [42, 43]. Furthermore, novel types of PPC have been reported using unique polyelectrolytes, including spherical polyelectrolyte brush [44] and polyion complex micelles [45–47].

(iii) Reversibility: PPC are generally reversible because their non-covalent interactions are weaker than the covalent interactions of protein-polymer conjugations. For example, the salts at high ionic concentration shield the electrostatic interaction between proteins and polyelectrolytes, resulting in disruption of PPC [48, 49]. The salt-responsiveness of PPC is generally independent of the state of the PPC. Similarly, the reversibility of the PPC has been reported using several methods, including protein [50, 51], polyelectrolytes [52–54], and pulse electric field [55].

Although there have been a number of fundamental studies of PPC, they have been used in few practical applications. There have been few reports regarding the formation of PPC tailored to achieve on/off switching of enzyme activities [53, 54] and thermal stabilization [52]. Recently, the on/off switching of enzyme activity using PPC was applied to a sensor array for detection of protein ratio in serum [50, 51]. Therefore, the development of a protein handling method using PPC would be useful for elucidating the utility of proteins in various fields.

1.4. Objective of this study

In this study, three protein-handling methods were developed using PPC to facilitate practical application of proteins. Chapter 2 descrives a novel soluble PPC with PEGylated polyelectrolyte that can regulate the activity of unstable enzymes and stabilize oligomeric protein against stress. Chapter 3 presents an enzyme hyperactivation phenomenon that enables enhancement of enzyme activity. Chapter 4 discusses a precipitation-redissolution method for preparing high-concentration protein formulations. The last two

chapters present an overview and discussion of this research, as well as a discussion of future work to be performed.

1.5. References

[1] Anfinsen, C. B. Principles that Govern the Folding of Protein Chains. *Science.* **1973**, *181*, 223-230.

[2] Wang, W.; Singh, S.; Zeng, D. L.; King, K.; Nema, S. Antibody Structure, Instability, and Formulation. *J. Pharm. Sci.* **2007**, *96*, 1-26.

[3] Getzoff, E. D.; Tainer, J. A.; Weiner, P. K.; Kollman, P. A.; Richardson, J. S.; Richardson, D. C. Electrostatic Recognition between Superoxide and Copper, Zinc Superoxide Dismutase. *Nature.* **1983**, *306*, 287-290.

[4] Quinn, D. M. Acetylcholinesterase: Enzyme Structure, Reaction Dynamics, and Virtual Transition States. *Chem. Rev.* **1987**, *87*, 955-979.

[5] Wade, R. C.; Gabdoulline, R. R.; Luty, B. A. Species Dependence of Enzyme-Substrate Encounter Rates for Triose Phosphate Isomerases. *Proteins* **1998**, *31*, 406-416.

[6] Jogl, G.; Rozovsky, S.; McDermott, A.E.; Tong, L. Optimal Alignment for Enzymatic Proton Transfer: Structure of the Michaelis Complex of Triosephosphate Isomerase at 1.2-Å Resolution. *Proc. Natl. Acad. Sci. U. S. A.* **2003**, *100*, 50-55.

[7] Getzoff, E. D.; Cabelli, D. E.; Fisher, C. L.; Parge, H. E.; Viezzoli, M. S.; Banci, L.; Hallewell, R. A. Faster Superoxide Dismutase Mutants Designed by Enhancing Electrostatic Guidance. *Nature.* **1992**, *358*, 347-351.

[8] Shiraki, K.; Norioka, S.; Li, S.; Sakiyama, F. Contribution of an Imidazole-Indole Stack to High Catalytic Potency of a Lysine-Specific Serine Protease, *Achromobacter* Protease I. *J. Biochem.* **2002**, *131*, 213-218.

[9] Shiraki, K.; Sakiyama, F. Histidine 210 Mutant of a Trypsin-Type *Achromobacter* Protease I Shows Broad Optimum pH Range. *J. Biosci. Bioeng.* **2002**, *93*, 331-333.

[10] Shiraki, K.; Norioka, S.; Li, S.; Yokota, K.; Sakiyama, F. Electrostatic Role of Aromatic Ring Stacking in the pH-Sensitive Modulation of a Chymotrypsin-Type Serine Protease, *Achromobacter* Protease I. *Eur. J. Biochem.* **2002**, *269*, 4152-4158.

[11] Walsh, G. Biopharmaceutical Benchmarks 2010. *Nat. Biotechnol.* **2010**, *28*, 917-924.

[12] Weiner, L. M.; Surana, R.; Wang, S. Monoclonal Antibodies: Versatile Platforms for Cancer Immunotherapy. *Nat. Rev. Immunol.* **2010**, *10*, 317-327.

[13] Sliwkowski, M. X.; Mellman, I. Antibody Therapeutics in Cancer. *Science.* **2013**, *341*, 1192-1198.

[14] Chan, A. C.; Carter, P. J. Therapeutic Antibodies for Autoimmunity and Inflammation. *Nat. Rev. Immunol.* **2010**, *10*, 301-316.

[15] Wells, A. F.; Jodat, N.; Schiff, M. A critical Evaluation of the Role of Subcutaneous Abatacept in the Treatment of Rheumatoid Arthritis: Patient Considerations. *Biologics* **2014**, *8*, 41-55.

[16] Panetta, J. C.; Gajjar, A.; Hijiya, N.; Hak, L. J.; Cheng, C.; Liu, W.; Pui, C. H.; Relling, M. V. Comparison of Native *E. coli* and PEG Asparaginase Pharmacokinetics and Pharmacodynamics in Pediatric Acute Lymphoblastic Leukemia. *Clin. Pharmacol. Ther.* **2009**, *86*, 651-658.

[17] Wang, W. Protein Aggregation and its Inhibition in Biopharmaceutics. *Int. J. Pharm.* **2005**, *289*, 1-30.

[18] Shiraki, K.; Kudou, M.; Fujiwara, S.; Imanaka, T.; Takagi, M. Biophysical Effect of Amino Acids on the Prevention of Protein Aggregation. *J. Biochem.* **2002**, *132*, 591-595.

[19] Arakawa, T.; Tsumoto, K. The Effects of Arginine on Refolding of Aggregated Proteins: Not Facilitate Refolding, but Suppress Aggregation. *Biochem. Biophys. Res. Commun.* **2003**, *304*, 148-152.

[20] Shiraki, K.; Kudou, M.; Sakamoto, R.; Yanagihara, I.; Takagi, M. Amino Acid Esters Prevent Thermal Inactivation and Aggregation of Lysozyme. *Biotechnol. Prog.* **2005**, *21*, 640-643.

[21] Kudou, M.; Shiraki, K.; Fujiwara, S.; Imanaka, T.; Takagi, M. Prevention of Thermal Inactivation and Aggregation of Lysozyme by Polyamines. *Eur. J. Biochem.* **2003**, *270*, 4547-4554.

[22] Okanojo, M.; Shiraki, K.; Kudou, M.; Nishikori, S.; Takagi, M. Diamines Prevent Thermal Aggregation and Inactivation of Lysozyme. *J. Biosci. Bioeng.* **2005**, *100*, 556-561.

[23] Hirano, A.; Hamada, H.; Shiraki, K. Trans-Cyclohexanediamines Prevent Thermal Inactivation of Protein: Role of Hydrophobic and Electrostatic Interactions. *Protein J.* **2008**, *27*, 253-257.

[24] Allison, S. D.; Chang, B.; Randolph, T. W.; Carpenter, J. F. Hydrogen Bonding between Sugar and Protein is Responsible for Inhibition of Dehydration-Induced Protein Unfolding. *Arch. Biochem. Biophys.* **1999**, *365*, 289-298.

[25] Rajagopal, K.; Wood, J.; Tran, B.; Patapoff, T. W.; Nivaggioli, T. Trehalose Limits BSA Aggregation in Spray-Dried Formulations at High Temperatures: Implications in Preparing Polymer Implants for Long-Term Protein Delivery. *J. Pharm. Sci.* **2013**, *102*, 2655-2666.

[26] Sasahara, K.; McPhie, P.; Minton, A. P. Effect of Dextran on Protein Stability and Conformation Attributed to Macromolecular Crowding. *J. Mol. Biol.* **2003**, *326*, 1227-1237.

[27] Wang, W.; Wang, Y. J.; Wang, D. Q. Dual Effects of Tween 80 on Protein Stability. *Int. J. Pharm.* **2008**, *347*, 31-38.

[28] Kotzia, G. A.; Labrou, N. E. Engineering Thermal Stability of L-Asparaginase by *in vitro* Directed Evolution. *FEBS. J.* **2009**, *276*, 1750-1761.

[29] Frokjaer, S.; Otzen, D. E. Protein Drug Stability: A Formulation Challenge. *Nat. Rev. Drug. Discov.* **2005**, *4*, 298-306.

[30] Duncan, R. The Dawning Era of Polymer Therapeutics. *Nat. Rev. Drug. Discov.* **2003**, *2*, 347-360.

[31] Nguyen, T. H.; Kim, S. H.; Decker, C. G.; Wong, D. Y.; Loo, J. A.; Maynard, H. D. A Heparin-Mimicking Polymer Conjugate Stabilizes Basic Fibroblast Growth Factor. *Nat. Chem.* **2013**, *5*, 221-227.

[32] Veronese, F. M. Peptide and Protein PEGylation: A Review of Problems and Solutions. *Biomaterials.* **2001**, *22*, 405-417.

[33] Roberts, M. J.; Bentley, M. D.; Harris, J. M. Chemistry for Peptide and Protein PEGylation. *Adv. Drug. Deliv. Rev.* **2002**, *54*, 459-476.

[34] Harris, J. M.; Chess, R. B. Effect of Pegylation on Pharmaceuticals. *Nat. Rev. Drug. Discov.* **2003**, *2*, 214-221.

[35] Veronese, F. M.; Pasut, G. PEGylation, Successful Approach to Drug Delivery. *Drug. Discov. Today.* **2005**, *10*, 1451-1458.

[36] Alconcel, S. N. S.; Baas, A. S.; Maynard, H. D. FDA-Approved Poly(ethylene glycol)–Protein Conjugate Drugs. *Polym. Chem.* **2011**, *2*, 1442–1448.

[37] Pfister, D.; Morbidelli, M. Process for Protein PEGylation. *J. Control. Release* **2014**, *180C*, 134-149.

[38] Murata, H.; Cummings, C. S.; Koepsel, R. R.; Russell, A. J. Polymer-Based Protein Engineering can Rationally Tune Enzyme Activity, pH-Dependence, and Stability. *Biomacromolecules* **2013**, *14*, 1919-1926.

[39] Shimoboji, T.; Larenas, E.; Fowler, T.; Kulkarni, S.; Hoffman, A. S.; Stayton, P. S. Photoresponsive Polymer-Enzyme Switches. *Proc. Natl. Acad. Sci. U. S. A.* **2002**, *99*, 16592-16596.

[40] Shimoboji, T.; Larenas, E.; Fowler, T.; Hoffman, A. S.; Stayton, P. S. Temperature-Induced Switching of Enzyme Activity with Smart Polymer-Enzyme Conjugates. *Bioconjug. Chem.* **2003**, *14*, 517-525.

[41] Cummings, C.; Murata, H.; Koepsel, R.; Russell, A. J. Tailoring Enzyme Activity and Stability Using Polymer-Based Protein Engineering. *Biomaterials* **2013**, *34*, 7437-7443.

[42] Cooper, C. L.; Dubin, P. L.; Kayitmazer, A. B.; Turksen, S. Polyelectrolyte–protein complexes *Curr. Opin. Colloid Interface Sci.* **2005***, 10*, 52-78.

[43] Kayitmazer, A. B.; Seeman, D.; Minsky, B. B.; Dubin, P. L.; Xu, Y. Protein–Polyelectrolyte Interactions *Soft Matter* **2013**, *9*, 2553-2583.

[44] Ballauff, M.; Borisov, O. Polyelectrolyte Brushes *Curr. Opin. Colloid Interface Sci.* **2006**, *211*, 316-323.

[45] Kataoka, K.; Harada, A.; Nagasaki, Y. Block Copolymer Micelles for Drug Delivery: Design, Characterization and Biological Significance. *Adv. Drug. Deliv. Rev.* **2001**, *47*, 113-131.

[46] Kakizawa, Y.; Kataoka, K. Block Copolymer Micelles for Delivery of Gene and Related Compounds. *Adv. Drug. Deliv. Rev.* **2002**, *54*, 203-222.

[47] Osada, K.; Christie, R. J.; Kataoka, K. Polymeric Micelles from Poly(ethylene glycol)-Poly(amino acid) Block Copolymer for Drug and Gene Delivery. *J. R. Soc. Interface 6. Suppl.* **2009**, *3*, S325-339.

[48] Carlsson, F.; Malmsten, M.; Linse, P. Protein-Polyelectrolyte Cluster Formation and Redissolution: a Monte Carlo study. *J. Am. Chem. Soc.* **2003**, *125*, 3140-3149.

[49] Ni, R.; Cao, D.; Wang, W. Release of Lysozyme from the Branched Polyelectrolyte-Lysozyme Complexation. *J. Phys. Chem. B* **2008**, *112*, 4393-4400.

[50] Tomita, S.; Yoshimoto, K. Polyion Complex Libraries Possessing Naturally Occurring Differentiation for Pattern-Based Protein Discrimination. *Chem. Commun.* **2013**, *49*, 10430-10432.

[51] Tomita, S.; Soejima, T.; Shiraki, K.; Yoshimoto, K. Enzymatic Fingerprinting of Structurally Similar Homologous Proteins Using Polyion Complex Library Constructed by Tuning PEGylated Polyamine Functionalities. *Analyst* **2014**, *139*, 6100-6103.

[52] Ganguli, S.; Yoshimoto, K.; Tomita, S.; Sakuma, H.; Matsuoka, T.; Shiraki, K.; Nagasaki, Y. Regulation of Lysozyme Activity Based on Thermotolerant Protein/Smart Polymer Complex Formation. *J. Am. Chem. Soc.* **2009**, *131*, 6549-6553.

[53] Tomita, S.; Ito, L.; Yamaguchi, H.; Konishi, G.; Nagasaki, Y.; Shiraki, K. Enzyme Switch by Complementary Polymer Pair System (CPPS) *Soft Matter* **2010**, *6*, 5320-5326.

[54] Tomita, S.; Shiraki, K. Poly(acrylic acid) is a Common Noncompetitive Inhibitor for Cationic Enzymes with High Affinity and Reversibility. *J. Polym. Sci. Part A: Polym. Chem.* **2011**, *49*, 3835-3841.

[55] Harada, A.; Kataoka, K. Switching by Pulse Electric Field of the Elevated Enzymatic Reaction in the Core of Polyion Complex Micelles. *J. Am. Chem. Soc.* **2003**, *125*, 15306-15307.

Chapter 2. PEGylated Polyelectrolyte

2.1. Improved Complementary Polymer Pair System: Switching for Enzyme Activity by PEGylated Polymers

2.1.1. Introduction

On/off switching of enzymatic activity holds a great deal of potential for various applications, including biosensors, bioreactors, and high performance protein delivery systems. Several attempts have been made to regulate enzymatic activity. Strategies typically involve covalent modifications of a ligand [1] and stimuli-responsive polymers [2,3] in close proximity to the active site of enzymes. These strategies facilitate many potential uses for enzymes because the activities of these modified enzymes can be easily switched by appropriate signals, such as heavy metal ions, light, or temperature. On the other hand, noncovalent approaches involve the use of artificial reversible inhibitors, such as polymeric substrate analogues,4 molecular clips and tweezers [5], gold nanoparticles [6−11], and micelles [12−14]. However, these methods are still time-consuming and costly.

Recently, our group have developed a convenient technique, the complementary polymer pair system (CPPS), which allows the control of enzymatic activity by a pair of oppositely charged polymers [15−17]. For example, an enzyme with a cationic surface is inactivated by the addition of an anionic polymer due to binding through electrostatic interactions, followed by reactivation of enzyme activity by the addition of a cationic polymer. This simple and inexpensive system was applied successfully to several model enzymes, such as ribonuclease A, lysozyme, trypsin, and cellulase with cationic poly(allylamine) (PAA) and anionic poly(acrylic acid) (PAAc). However, the system could not be used for switching of α-amylase. This failure was concluded to be the result of irreversible denaturation of enzymes due to the formation of aggregates

between α-amylase and PAA [16].

To apply CPPS to enzymes that are liable to undergo aggregate formation, I focused on charged polymers modified with poly(ethylene glycol) (PEG), as the modification of PEG (PEGylation) is a well-used strategy to avoid aggregate formation of polyion complexes [18−25]. Here, I investigated the improved CPPS that allows us to switch the activity of large and unstable anionic enzymes, α-amylase (*p*I = 4.2) and β-galactosidase (*p*I = 5.1) (Figure 2.1.1A), using the designed and synthesized cationic copolymer with poly(ethylene glycol) backbone, poly(*N,N*-diethylaminoethyl methacrylate)-*block*-poly(ethylene glycol) (PEAMA-*b*-PEG) (Figure 2.1.1B). In contrast to PAA, both enzymes were inactivated by PEAMA-*b*-PEG with the formation of water-dispersed complexes, and subsequently the activity of the enzymes was successfully recovered from the complex by the addition of PAAc (Figure 2.1.1C).

2.1.2. Materials and Methods

Materials

Aspergillus oryzae α-amylase was purchased from Fluka Chemica GmbH (Buchs, Switzerland). Escherichia coli β-galactosidase and 3-(*N*-morpholino)propanesulfonic acid (MOPS) were from Sigma Chemical. Co. (St. Louis, MO). *p*-Nitrophenyl-α-D-maltoside (PNPM), *o*-nitrophenyl-β-D-galactopyranoside (ONPG), and PAAc with an average molecular weight of 5000 were from Wako Pure Chemical Ind., Ltd. (Osaka, Japan). PAA with an average molecular weight of 5000 was acquired from Nitto Boseki Co., Ltd. (Fukushima, Japan). PEAMA-*b*-PEG was synthesized as reported previously [26,27]. All chemicals used were of high quality analytical grade and were used as received.

Protein Concentration

Protein concentrations were determined from the absorbance at 280 nm using a spectrophotometer (V-630; Jasco Corp., Tokyo, Japan), with extinction coefficients of 106,160 M^{-1} cm^{-1} (α-amylase) or 1,046,760 M^{-1}

cm^{-1} (β-galactosidase) [28].

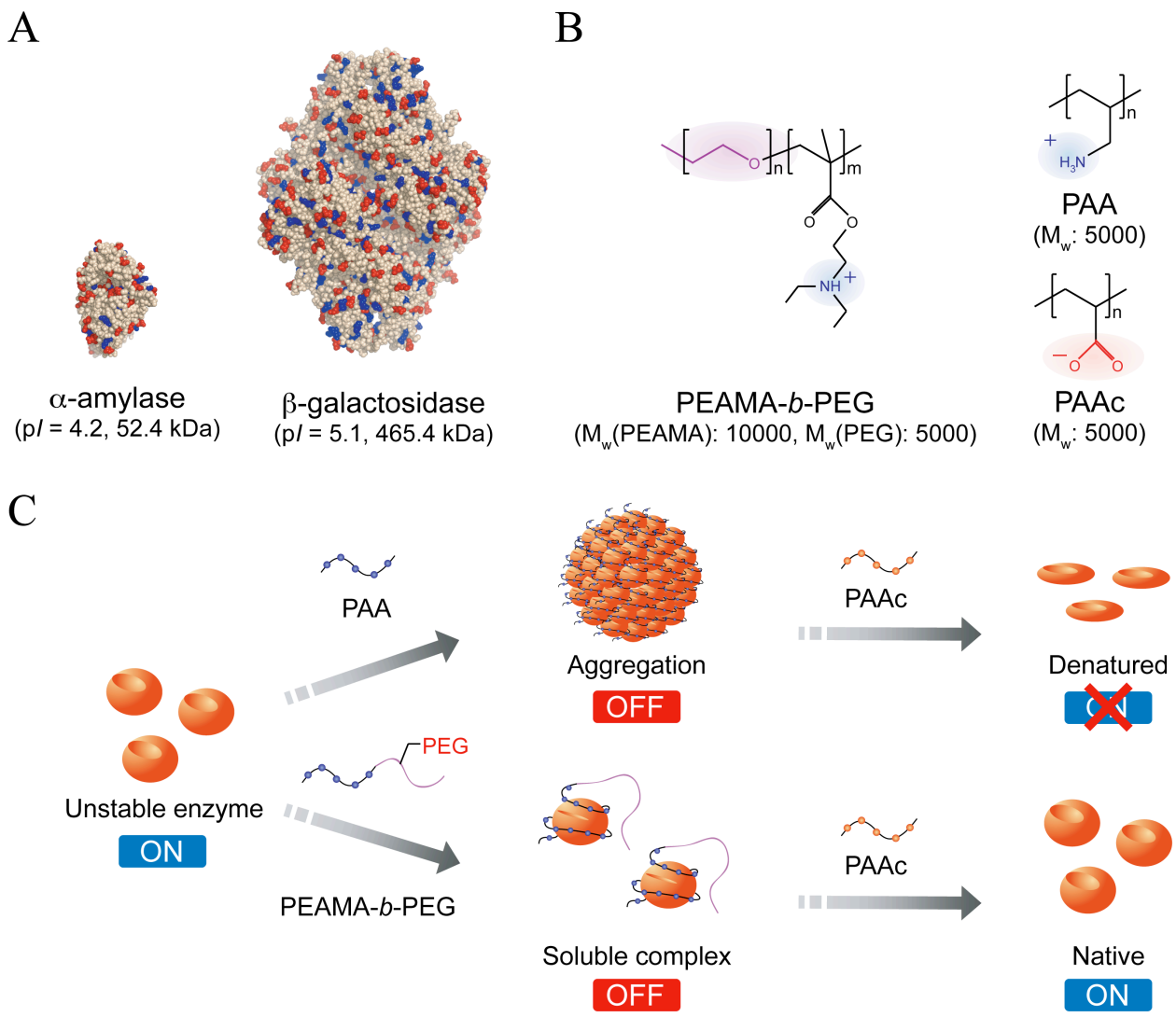

Figure 2.1.1. (A) Tertiary structures of enzymes (PDB entries: α-amylase, 6TAA; β-galactosidase, 3MUY). **(B)** Chemical structures of polymers. **(C)** Schematic illustration of improved CPPS.

Enzyme Assay

Enzyme assay for α-amylase was performed as follows. A substrate solution of 150 μL containing 1.0 mM PNPM and 10 mM MOPS buffer (pH 7.0) was mixed with 150 μL of 4.0 μM α-amylase solution. The initial reaction velocities were determined from the slope of the initial increase in the absorbance intensity at 410 nm. Enzyme assay for β-galactosidase was performed as follows. A substrate solution of 200 μL containing

10 mM ONPG and 10 mM MOPS buffer (pH 7.0) was mixed with 100 μL of 23 nM β-galactosidase solutions. The initial reaction velocities were determined from the slope of the initial increase in the absorbance intensity at 410 nm.

Inactivation of Enzymes by Polymers

Various concentrations of PEAMA-*b*-PEG and PAA were added to solutions containing enzymes (4.0 μM α-amylase or 23 nM β-galactosidase) and 10 mM MOPS buffer (pH 7.0). After incubation at 25 ^{o}C for 2 h without shaking, the enzyme activity was measured. PEAMA-*b*-PEG and PAA have 12 and 70 positive charges at pH 7.0, respectively; α-amylase and β-galactosidase have 24 and 149 negative charges at pH 7.0, respectively.

Reactivation of Enzymes by PAAc

Reactivation of enzymes was performed by adding PAAc to enzyme/polymer complex solution. Solutions of 180 μL containing enzymes (4.0 μM α-amylase or 23 nM β-galactosidase) and 10 mM MOPS buffer (pH 7.0) were incubated with PEAMA-*b*-PEG (15 μM for α-amylase or 2.0 μM for β-galactosidase) or PAA (40 μM for α-amylase or 1.0 μM for β-galactosidase) at 25 ^{o}C for 24 h, and then aliquots of 20 μL containing various concentrations of PAAc and 10 mM MOPS buffer (pH 7.0) were added to the samples. After incubation at 25 ^{o}C for 2 h, the samples were centrifuged at 15000g for 15 min at 25 ^{o}C. The enzyme activity of supernatant was then measured.

Circular Dichroism

Circular dichroism (CD) experiments were performed in a 1 mm (α-amylase) or 10 mm (β-galactosidase) path- length quartz cuvette using a spectropolarimeter (J-720; Jasco Corp). Solutions of 1800 μL containing enzymes (4.0 μM α-amylase or 23 nM β-galactosidase) and 10 mM MOPS buffer (pH 7.0) were incubated with PEAMA-*b*-PEG (15 μM for α-amylase or 2.0 μM for β-galactosidase) or PAA (40 μM for α-amylase

or 1.0 μM for β-galactosidase) at 25 °C for 24 h, and then aliquots of 200 μL containing PAAc (25 μM for α-amylase/PEAMA-*b*-PEG, 40 μM for α-amylase/PAA, 2.0 μM for β-galactosidase/PEAMA-*b*-PEG, or 0.3 μM for β-galactosidase/PAA) and 10 mM MOPS buffer (pH 7.0) were added to the samples. After incubation at 25 °C for 2 h, the samples were centrifuged at 15000g for 15 min, and the spectra of supernatant were measured at 25 °C. The CD spectra of the samples were corrected by subtracting the corresponding spectra of buffers in the absence of enzymes.

Dynamic Light Scattering

Dynamic light scattering (DLS) experiments were performed using a light scattering photometer (Zetasizer Nano ZS; Malvarn Instruments, Worcestershire, UK). The size of enzyme/polymer complexes was determined as follows. Solutions containing enzymes (4.0 μM α-amylase or 230 nM β-galactosidase) and 10 mM MOPS buffer (pH 7.0) were incubated with PEAMA-*b*-PEG (15 μM for α-amylase or 20 μM for β-galactosidase) or PAA (40 μM for α-amylase or 10 μM for β-galactosidase) at 25 °C for 24 h, and then DLS measurements were carried out at 25 °C.

2.1.3. Results and Discussion

Inactivation of Enzymes by Polymers

Previously, our group reported that CPPS failed in on/off switching of α-amylase activity due to the formation of aggregates between the anionic enzyme and cationic PAA [16]. To confirm the versatility of improved CPPS, on-off swiching experiments for α-amylase and β-galactosidase as a model for large and unstable anionic enzymes were compared using newly synthesized PEAMA-*b*-PEG and previously reported PAA. Figure 2.1.2A shows the enzyme activity of α-amylase when 4.0 μM enzyme was mixed with PEAMA-*b*-PEG or PAA. The enzyme activity decreased concomitantly with concentrations of both PEAMA-*b*-PEG and PAA; the enzymatic activity was fully inactivated with addition of 15 μM (3.75 equiv)

PEAMA-*b*-PEG and 40 μM (10 equiv) PAA. Interestingly, the solution containing α-amylase and PEAMA-*b*-PEG was a clear liquid, although addition of PAA caused the formation of visible aggregates. A similar pattern of PEAMA-*b*-PEG and PAA was observed for β-galactosidase (Figure 2.1.2B). The enzyme activity of β-galactosidase dropped to almost zero in the presence of 2.0 μM (87 equiv) PEAMA-*b*-PEG and 1.0 μM (43 equiv) PAA, while the solutions containing β-galactosidase and both polymers were not turbid. These results indicated that cationic polymers bind strongly to the anionic surface of enzymes, resulting in full inactivation of the enzymes.

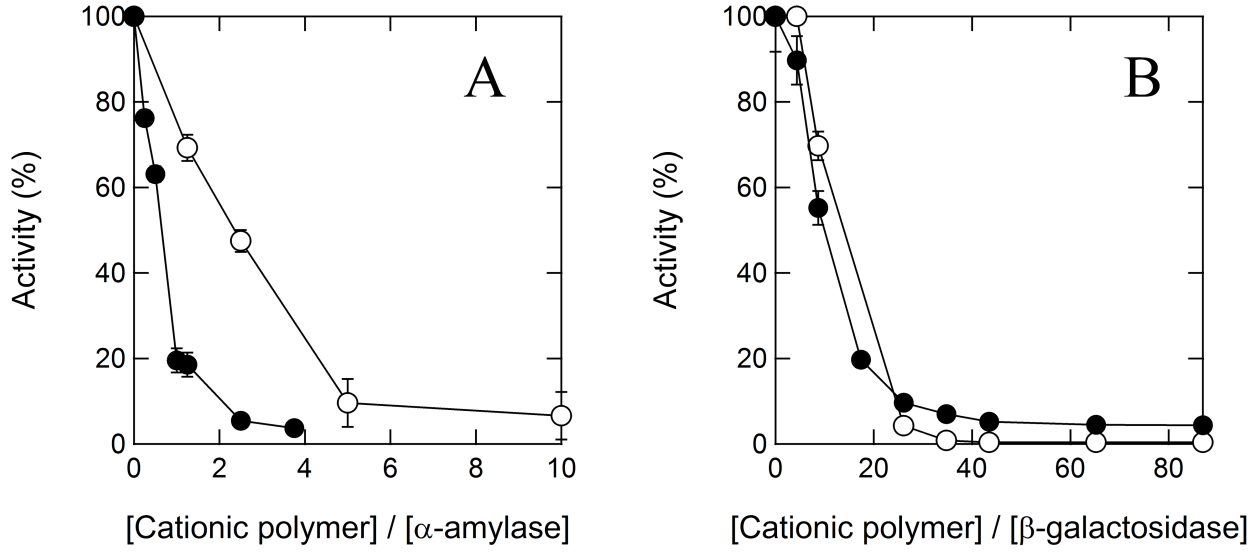

Figure 2.1.2. Inactivation of anionic enzymes by cationic polymers. Various concentrations of PEAMA-*b*-PEG (closed circles) or PAA (open circles) were added to solution containing 4.0 μM α-amylase **(A)** or 23 nM β-galactosidase **(B)**.

Reactivation of Enzymes by PAAc

α-Amylase and β-galactosidase were inactivated by incubation with PEAMA-*b*-PEG and PAA for 24 h, and then the inactivated enzymes were titrated with PAAc. The addition of PAAc to the complex between 4.0 μM α-amylase and 15 μM PEAMA-*b*-PEG resulted in 85% recovery of the activity, while the recovery of α-amylase inhibited by PAA reached only 10% in the presence of 20 μM PAAc (Figure 2.1.3A). Similarly,

23 nM β-galactosidase inhibited by 2.0 μM PEAMA-*b*-PEG was fully recovered by the addition of 1.6 μM PAAc (Figure 2.1.3B). On the other hand, the addition of PAAc to the solution containing β-galactosidase/PAA complexes did not show full recovery of enzyme activity. Therefore, I hypothesized that the enzyme inactivation by PEAMA-*b*-PEG had a favorable effect on the conformation of the enzymes, resulting in highly reversible inhibition.

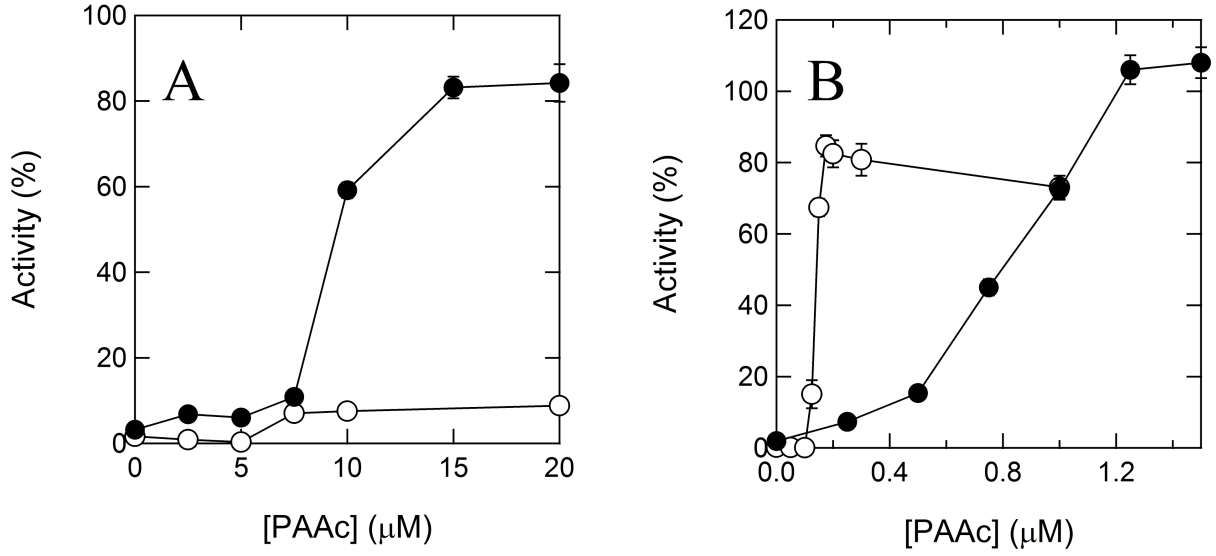

Figure 2.1.3. Reactivation of inhibited anionic enzymes by PAAc. Various concentrations of PAAc were added to solutions containing 4.0 μM α-amylase and 15 μM PEAMA-*b*-PEG (closed circles) or 40 μM PAA (open circles) **(A)**; 23 nM β-galactosidase and 2.0 μM PEAMA-*b*-PEG (closed circles) or 1.0 μM PAA (open circles) **(B)**.

Secondary Structure of Enzyme/Polymer Complex

To evaluate the conformational changes in the enzymes, CD spectra of the enzyme/polymer complexes were measured (Figure 2.1.4). As anticipated, a slight change was observed in the far-UV CD spectrum of 4.0 μM α-amylase with the addition of 15 μM PEAMA-*b*-PEG (Figure 2.1.4A). In addition, the far-UV CD spectrum was maintained after the addition of 25 μM PAAc. Thus, the secondary structure of α-amylase did not change significantly in the processes of activity switching by PEAMA-*b*-PEG and PAAc. In contrast, the

far-UV CD spectrum of 4.0 μM α-amylase disappeared remarkably with the addition of 40 μM PAA (Figure 2.1.4B). Although PAAc was added to the solution with α-amylase/PAA complex, the far-UV CD spectrum showed less recovery, suggesting that PAA induced a marked conformational change in the secondary structure. A similar tendency was observed for β-galactosidase. In contrast to PAA, the far-UV CD spectrum of 23 nM β-galactosidase did not change when the enzyme was inactivated by 2.0 μM PEAMA-*b*-PEG and reactivated by 2.0 μM PAAc (Figure 2.1.4C,D). These observations suggested that complex formation between PEAMA-*b*-PEG and both enzymes did not strongly affect the secondary structures of the enzymes. Thus, the enzyme inactivation by PEAMA-*b*-PEG is likely coupled with local structural changes rather than complete unfolding. These weak and multiple bindings may result in non-competitive inhibition of the enzymatic activity from a kinetic viewpoint [17].

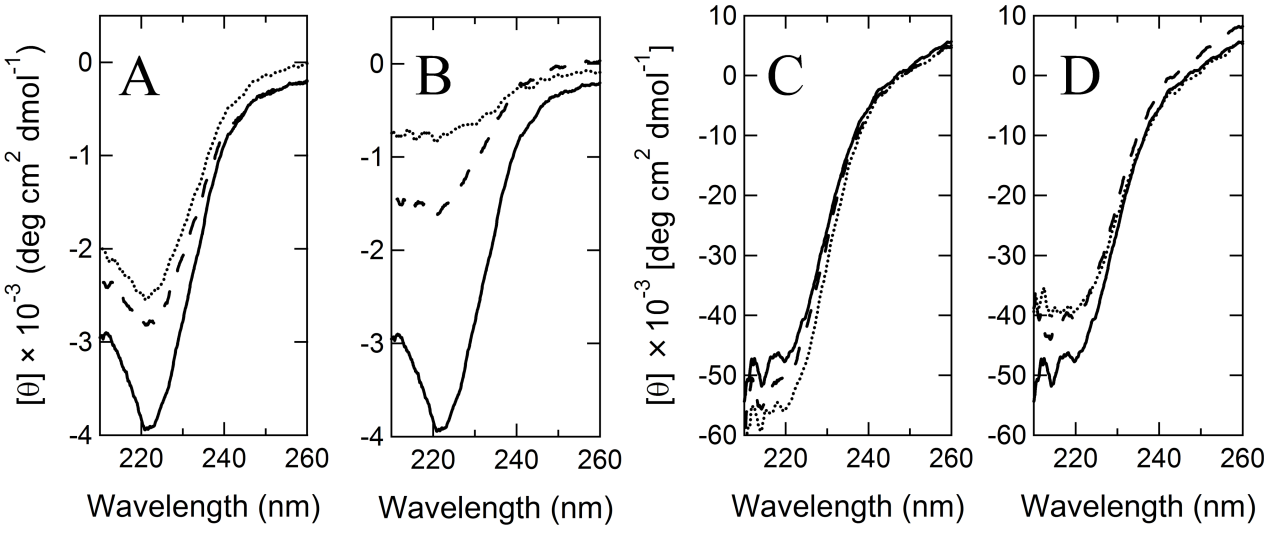

Figure 2.1.4. Far-UV CD spectra of anionic enzymes in the absence or presence of polymers. 4.0 μM α-amylase was mixed with 15 μM PEAMA-*b*-PEG **(A)** or 40 μM PAA **(B)**, and then PAAc (25 μM for PEAMA-*b*-PEG, 40 μM for PAA) was added to the solutions. 23 nM β-galactosidase was mixed with 2.0 μM PEAMA-*b*-PEG **(C)** or 1.0 μM PAA **(D)**, and then PAAc (2.0 μM for PEAMA-*b*-PEG 0.3 μM for PAA) was added to the solutions. Native enzymes, solid lines; inactivated enzymes, dotted lines; recovered enzymes, broken lines.

Size of Enzyme/Polymer Complex

It is possible that PEAMA-*b*-PEG inactivates anionic enzymes with the formation of nonaggregated complexes, resulting in a lower degree of enzyme secondary structure disruption. To evaluate this suggestion, DLS was used to determine the hydrodynamic radius (R_h) of the complexes between anionic enzymes and cationic polymers preincubated for 24 h. Figure 2.1.5 shows a representative result of the particle size distribution for α-amylase and β-galactosidase in the absence and presence of cationic polymers. The R_h values of α-amylase and β-galactosidase were 5.9 and 13.3 nm, respectively. The addition of 15 μM PEAMA-*b*-PEG to 4.0 μM α-amylase slightly increased R_h to 9.7 nm, whereas the mixture of 4.0 μM α-amylase and 40 μM PAA showed $R_h \approx 500$ nm, indicating that PAA but not PEAMA-*b*-PEG formed a large aggregate with α-amylase. Likewise, the mixture of 230 nM of β-galactosidase and 20 μM PEAMA-*b*-PEG showed R_h of 47.5 nm, while that with 10 μM PAA showed $R_h \approx 1900$ nm. Therefore, It was suggested that the PEG segment of PEAMA-*b*-PEG is crucial for dispersion of the complex between cationic PEAMA-*b*-PEG and anionic enzymes.

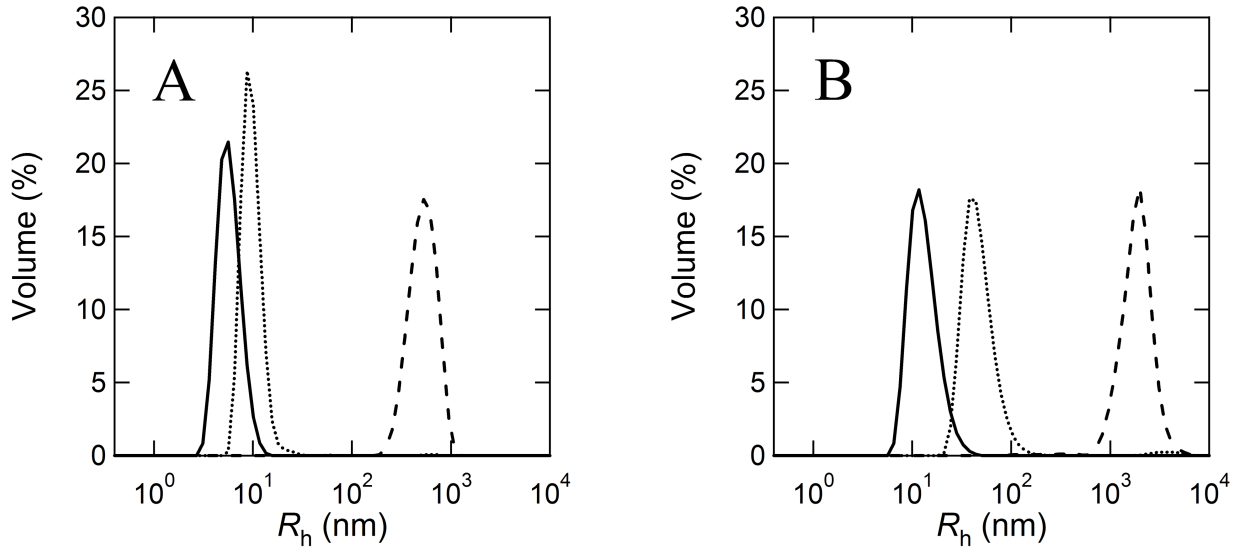

Figure 2.1.5. Hydrodynamic radii (R_h) of anionic enzymes in the absence or presence of cationic polymers. 4.0 μM α-amylase **(A)** and 230 nM β-galactosidase **(B)** were inactivated by PEAMA-*b*-PEG (15 μM for α-amylase, 20 μM for β-galactosidase) or PAA (40 μM for α-amylase, 10 μM for β-galactosidase). None, solid lines; PEAMA-*b*-PEG, dotted lines; PAA, broken lines.

PEG is a nonionic water-soluble polymer with high flexibility and large excluded volume. Therefore, PEG provides the water- dispersed properties for a pair of oppositely charged PEGylated block copolymers by the formation of a corona of PEG segments surrounding the core of water-incompatible segment [18−25] similar to the present case. DLS measurement revealed that R_h values of α-amylase and β-galactosidase with PEAMA-*b*-PEG were increased by 1.6- and 3.6-fold compared to those in the absence of these polymers, respectively (Figure 2.1.5), indicating that PEAMA-*b*-PEG likely formed micelle-like complexes [29] with β-galactosidase but not α-amylase. On the other hand, PAA inactivated anionic enzymes with the formation of aggregates due to the lack of a soluble PEG segment, leading to the irreversible denaturation of the enzyme. The conformational changes were probably due to the strong physical stress between the aggregates of enzyme/PAA complexes.

2.1.4. Conclusion

In summary, the novel cationic copolymer PEAMA-*b*-PEG was developed to establish CPPS for large and unstable enzymes. PEAMA-*b*-PEG successfully inactivated anionic enzymes with the formation of water-dispersed complexes. The complexation between PEAMA-*b*-PEG and enzymes had little influence on the conformation of enzymes, and hence the enzyme activity was fully recovered by the addition of anionic PAAc. It is expected that cationic unstable and aggregated enzymes would be switched on/off by PEGylated anionic polymers. Soluble complex formation between PEGylated charged polymer and enzymes linked to fully reversible inactivation of enzymes would expand the potential of enzymes in biomedical and biotechnological fields.

2.1.5. References

[1] Corey, D. R.; Schultz, P. G. Introduction of a Metal-Dependent Regulatory Switch into an Enzyme. *J. Biol. Chem.* **1989**, *264*, 3666−3669.

[2] Shimoboji, T.; Larenas, E.; Fowler, T.; Kulkarni, S.; Hoffman, A. S.; Stayton, P. S. Photoresponsive Polymer-Enzyme Switches. *Proc. Natl. Acad. Sci. U. S. A.* **2002**, *99*, 16592−16596.

[3] Shimoboji, T.; Larenas, E.; Fowler, T.; Hoffman, A. S.; Stayton, P. S. Temperature-Induced Switching of Enzyme Activity with Smart Polymer-Enzyme Conjugates. *Bioconjugate Chem.* **2003**, *14*, 517−525.

[4] Wenck, K.; Koch, S.; Renner, C.; Sun, W.; Schrader, T. A Noncovalent Switch for Lysozyme. *J. Am. Chem. Soc.* **2007**, *129*, 16015−16019.

[5] Talbiersky, P.; Bastkowski, F.; Klarner, F. G.; Schrader, T. Molecular Clip and Tweezer Introduce New Mechanisms of Enzyme Inhibition. *J. Am. Chem. Soc.* **2008**, *130*, 9824−9828.

[6] Fischer, N. O.; Verma, A.; Goodman, C. M.; Simard, J. M.; Rotello, V. M. Reversible "Irreversible" Inhibition of Chymotrypsin Using Nanoparticle Receptors. *J. Am. Chem. Soc.* **2003**, *125*, 13387−13391.

[7] Hong, R.; Fischer, N. O.; Verma, A.; Goodman, C. M.; Emrick, T.; Rotello, V. M. Control of Protein Structure and Function through Surface Recognition by Tailored Nanoparticle Scaffolds. *J. Am. Chem. Soc.* **2004**, *126*, 739−743.

[8] Verma, A.; Simard, J. M.; Worrall, J. W.; Rotello, V. M. Tunable Reactivation of Nanoparticle-Inhibited β-Galactosidase by Glutathione at Intracellular Concentrations. *J. Am. Chem. Soc.* **2004**, *126*, 13987−13991.

[9] Bayraktar, H.; Ghosh, P. S.; Rotello, V. M.; Knapp, M. J. Disruption of Protein-Protein Interactions Using Nanoparticles: Inhibition of Cytochrome c Peroxidase. *Chem. Commun.* **2006**, *13*, 1390−1392.

[10] Miranda, O. R.; Chen, H. T.; You, C. C.; Mortenson, D. E.; Yang, X. C.; Bunz, U. H.; Rotello, V. M. Enzyme-Amplified Array Sensing of Proteins in Solution and in Biofluids. *J. Am. Chem. Soc.* **2010**, *132*, 5285−5289.

[11] Miranda, O. R.; Li, X.; Garcia-Gonzalez, L.; Zhu, Z. J.; Yan, B.; Bunz, U. H.; Rotello, V. M. Colorimetric Bacteria Sensing Using a Supramolecular Enzyme-Nanoparticle Biosensor. *J. Am. Chem. Soc.* **2011**, *133*, 9650−9653.

[12] Harada, A.; Kataoka, K. On-Off Control of Enzymatic Activity Synchronizing with Reversible Formation of Supramolecular Assembly from Enzyme and Charged Block Copolymers. *J. Am. Chem. Soc.* **1999**, *121*, 9241−9242.

[13] Harada, A.; Kataoka, K. Switching by Pulse Electric Field of the Elevated Enzymatic Reaction in the Core of Polyion Complex Micelles. *J. Am. Chem. Soc.* **2003**, *125*, 15306−15307.

[14] Sandanaraj, B. S.; Vutukuri, D. R.; Simard, J. M.; Klaikherd, A.; Hong, R.; Rotello, V. M.; Thayumanavan, S. Noncovalent Modification of Chymotrypsin Surface Using an Amphiphilic Polymer Scaffold: Implications in Modulating Protein Function. *J. Am. Chem. Soc.* **2005**, *127*, 10693−10698.

[15] Ganguli, S.; Yoshimoto, K.; Tomita, S.; Sakuma, H.; Matsuoka, T.; Shiraki, K.; Nagasaki, Y. Regulation of Lysozyme Activity Based on Thermotolerant Protein/Smart Polymer Complex Formation. *J. Am. Chem. Soc.* **2009**, *131*, 6549−6553.

[16] Tomita, S.; Ito, L.; Yamaguchi, H.; Konishi, G.; Nagasaki, Y.; Shiraki, K. Enzyme Switch by Complementary Polymer Pair System (CPPS). *Soft Matter* **2010**, *6*, 5320−5326.

[17] Tomita, S.; Shiraki, K. Poly(acrylic acid) is a Common Noncompetitive Inhibitor for Cationic Enzymes with High Affinity and Reversibility. *J. Polym. Sci., Part A: Polym. Chem.* **2011**, *49*, 3835−3841.

[18] Kabanov, A. V.; Vinogradov, S. V.; Suzdaltseva, Y. G.; Alakhov, V. Y. Water-Soluble Block Polycations as Carriers for Oligonucleotide Delivery. *Bioconjugate Chem.* **1995**, *6*, 639−643.

[19] Harada, A.; Kataoka, K. Formation of Polyion Complex Micelles in an Aqueous Milieu from a Pair of Oppositely-Charged Block Copolymers with Poly(ethy1ene glycol) Segments. *Macromolecules* **1996**, *28*, 5294−5299.

[20] Kabanov, A. V.; Bronich, T. K.; Kabanov, V. A.; Yu, K.; Eisenberg, A. Soluble Stoichiometric Complexes from Poly(*N*-ethyl-4-vinylpyridinium) Cations and Poly(ethylene oxide)-*block*-polymethacrylate Anions. *Macromolecules* **1996**, *29*, 6797−6802.

[21] Kataoka, K.; Togawa, H.; Harada, A.; Yasugi, K.; Matsumoto, T.; Katayose, S. Spontaneous Formation of Polyion Complex Micelles with Narrow Distribution from Antisense Oligonucleotide and Cationic Block Copolymer in Physiological Saline. *Macromolecules* **1996**, *29*, 8556−8557.

[22] Batrakova, E. V.; Li, S.; Reynolds, A. D.; Mosley, R. L.; Bronich, T. K.; Kabanov, A. V.; Gendelman, H. E. A Macrophage-Nanozyme Delivery System for Parkinson's Disease. *Bioconjugate Chem.* **2007**, *18*, 1498−1506.

[23] Lee, Y.; Ishii, T.; Cabral, H.; Kim, H. J.; Seo, J. H.; Nishiyama, N.; Oshima, H.; Osada, K.; Kataoka, K. Charge-Conversional Polyionic Complex Micelles-Efficient Nanocarriers for Protein Delivery into Cytoplasm. *Angew. Chem., Int. Ed.* **2009**, *48*, 5309−5312.

[24] Wang, Y.; Han, P.; Xu, H.; Wang, Z.; Zhang, X.; Kabanov, A. V. Photocontrolled Self-Assembly and Disassembly of Block Ionomer Complex Vesicles: A Facile Approach toward Supramolecular Polymer Nanocontainers. *Langmuir* **2010**, *26*, 709−715.

[25] Lee, Y.; Ishii, T.; Kim, H. J.; Nishiyama, N.; Hayakawa, Y.; Itaka, K.; Kataoka, K. Efficient Delivery of Bioactive Antibodies into the Cytoplasm of Living Cells by Charge-Conversional Polyion Complex Micelles. *Angew. Chem., Int. Ed.* **2010**, *49*, 2552−2555.

[26] Tamura, A.; Oishi, M.; Nagasaki, Y. Enhanced Cytoplasmic Delivery of siRNA Using a Stabilized Polyion Complex Based on PEGylated Nanogels with a Cross-Linked Polyamine Structure. *Biomacromolecules* **2009**, *10*, 1818−1827.

[27] Tamura, A.; Oishi, M.; Nagasaki, Y. Efficient siRNA Delivery Based on PEGylated and Partially Quaternized Polyamine Nanogels: Enhanced Gene Silencing Activity by the Cooperative Effect of Tertiary and Quaternary Amino Groups in the Core. *J. Controlled Release* **2010**, *146*, 378−387.

[28] Pace, C. N.; Vajdos, F.; Fee, L.; Grimsley, G.; Gray, T. How to Measure and Predict the Molar Absorption Coefficient of a Protein. *Protein Sci.* **1995**, *4*, 2411−2423.

[29] Harada, A.; Kataoka, K. Novel Polyion Complex Micelles Entrapping Enzyme Molecules in the Core: Preparation of Narrowly-Distributed Micelles from Lysozyme and Poly(ethylene glycol)-Poly(aspartic acid) Block Copolymer in Aqueous Medium. *Macromolecules* **1998**, *31*, 288−294.

2.2. Noncovalent PEGylation of L-Asparaginase Using PEGylated Polyelectrolyte

2.2.1. Introduction

Progress in the fields of recombinant technology and biotechnology has markedly increased the numbers of therapeutic proteins [1]. Many therapeutic proteins have large and multidomain structures consisting of homo- or heteropolypeptide chains. The formation of quaternary structures is required for bioactivity of multidomain enzymes, such as tetrameric L-asparaginase (ASNase), tetrameric uricase, and trimeric arginase [2]. In comparison with single-domain proteins, multidomain proteins are prone to aggregation and are inactivated by common stresses, such as changes in temperature, pH shift, and mechanical stress [3]. Aggregation is the most serious problem for therapeutic proteins causing loss of their bioactivities, and therefore such aggregates in therapeutic proteins are generally unacceptable [4]. Accordingly, a method for stabilization of multidomain proteins is important for pharmaceutics.

Covalent attachment of polymers to the protein surface is one strategy for stabilization of proteins [3,5,6]. Especially, conjugation of poly(ethylene glycol) (PEGylation) is the most promising method for protein therapy [7–12]. PEG is a hydrophilic, nonionic, and nontoxic polymer that provides a steric shield for proteins, resulting in improvement of the pharmacological properties of the proteins. In addition, PEGylation also protects proteins against aggregation and protease digestion *in vitro* [13–15]. At present, 12 types of PEGylated therapeutic protein have been approved by the United States Food and Drug Administration [12], and are used for several diseases, such as severe combined immunodeficiency disease, acute lymphoblastic leukemia, and refractory chronic gout [11]. However, covalent PEGylation requires chemical reaction for conjugation of PEG to proteins, which is both time consuming and costly.

Noncovalent PEGylation has been suggested as an alternative method for stabilizing proteins using

PEG [16–21]. A common strategy for noncovalent PEGylation involves designing functional PEG derivatives that bind to proteins. For example, Mueller et al. [17,18,21] synthesized several PEG derivatives conjugated with hydrophobic ligands, which reduced the aggregation of salmon calcitonin and lysozyme. Similarly, PEG derivatives conjugated with sugars [19], biotin [16], and nitrilotriacetic acid [20] have also been designed. However, there have been few studies regarding noncovalent PEGylation of therapeutic proteins.

PEGylated polyelectrolytes are also PEG derivatives. The polyelectrolyte interacts strongly with complementary charged proteins through multiple electrostatic interactions, resulting in the formation of various types of protein-polyelectrolyte complex (PPC) [22–28]. I have recently shown that PEGylated polyelectrolyte could form a water-soluble PPC with α-amylase and β-galactosidase due to the PEG segment of the polyelectrolyte [25]. Here, stabilization of therapeutic protein through noncovalent PEGylation using PEGylated polyelectrolytes was investigated. ASNase was selected as a model therapeutic protein which used in acute lymphoblastic leukemia. Anionic ASNase and cationic poly(ethylene glycol)-*block*-poly(*N,N*-dimethylaminoethyl methacrylate) (PEG-*b*-PAMA) formed a water-soluble PPC with maintenance of the original secondary structure and enzyme activity of ASNase. As expected, PEG-*b*-PAMA protected ASNase against protease digestion and shaking-induced inactivation. It is important to note that these protective effects of PEG-*b*-PAMA were comparable to those of commercial PEGylated ASNase (PEG-ASNase).

2.2.2. Materials and Methods

Materials

L-Asparaginase from *Escherichia coli* was from Kyowa Hakko Kirin Company Ltd. (Tokyo, Japan). Nessler's reagent, 3-(*N*-morpholino)propanesulfonic acid (MOPS), poly(ethylene glycol)-L-asparaginase (PEG-ASNase) from *Escherichia coli*, and trypsin from bovine pancreas were from Sigma Chemical Company (St. Louis, Missouri). Poly(*N,N*-dimethylaminoethyl methacrylate) (PAMA) with average

molecular weight (M_w) 4.2 kDa, PEG-*b*-PAMA with average M_w (PEG) 5.0 and M_w (PAMA) 5.5 kDa were from Polymer Source Inc. (Dorval, QC, Canada). Ammonium sulfate, L-asparagine (L-Asn), PEG with average M_w 7.5 kDa, and trichloroacetic acid (TCA) were from Wako Pure Chemical. Ind., Ltd. (Osaka, Japan). Phenylmethyl- sulfonyl fluoride (PMSF) was from Nacalai Tesque (Kyoto, Japan). These chemicals were of high-quality analytical grade and were used as received.

Protein Concentrations

The concentrations of proteins were determined from the absorbance at 280 nm using a spectrophotometer (V-630; Japan Spectroscopic Company, Ltd., Tokyo, Japan) with extinction coefficients of 94,020 M^{-1} cm^{-1} (ASNase and PEG-ASNase) or 37,650 M^{-1} cm^{-1} (trypsin) [29].

Dynamic Light Scattering

Dynamic light scattering (DLS) experiments were performed using a Zetasizer Nano ZS light scattering photometer (Malvern Instruments, Worcestershire, UK) equipped with a 4 mW He-Ne ion laser (λ = 633 nm). The sizes of the protein with polymer were determined as follows. Solutions containing 1.0 μM ASNase, 0-100 μM polymers, and 10 mM MOPS buffer (pH 7.0) were placed in a 1-cm path length disposable cuvette, and DLS measurements were performed at 25°C at a detection angle of 173°. The viscosity of the solutions was approximated by the value of the 10 mM MOPS solution (η = 0.87 cP). All results are presented as the averages of three independent experiments.

Circular Dichroism

Circular dichroism (CD) experiments were performed in a 1-mm path length quartz cuvette using a J-720 spectropolarimeter (Japan Spectroscopic Company, Ltd.). Solutions containing 1.0 μM ASNase, 0-40 μM polymers, and 10 mM MOPS buffer (pH 7.0) were prepared, and the spectra were measured at 25°C. The CD spectra of the samples were corrected by subtracting the corresponding spectra of the buffers in the absence

of proteins.

Enzyme Assay

The enzyme activities of ASNase and PEG-ASNase were measured as follows. An aliquot of 50 μL of the protein solution was incubated with 950 μL of the substrate solution containing 22 mM L-Asn, 10 mM MOPS (pH 7.0) at 37^{o}C for 2.0 min (ASNase) or 10 min (PEG-ASNase). The reaction was stopped by the addition of 250 μL of 3.0 M TCA in the assay mixture. Subsequently, the sample was mixed with Nessler's reagent to measure the ammonia released after L-Asn hydrolysis. The absorbance was monitored spectrophotometrically at 450 nm. The concentration of ammonia produced by the enzymatic reaction was determined from a reference curve using ammonium sulfate as a standard. One unit of enzyme activity was defined as the amount of enzyme required to produce 1.0 μmol ammonia per min at 37^{o}C.

Proteolytic Degradation by Trypsin

Trypsin solution of 1.0 μM was prepared by dissolving the lyophilized trypsin in cold 1.0 mM HCl. An aliquot of 5.0 μL of trypsin solution was added to 500 μL protein solutions (ASNase: 1.0 μM ASNase, 0-40 μM polymers, 10 mM MOPS, pH 7.0; PEG-ASNase: 1.0 μM PEG-ASNase, 10 mM MOPS, pH 7.0) at 37^{o}C. After incubation for respective periods, enzyme activities of ASNase were measured by above-mentioned assay.

SDS-PAGE

An aliquot of 5.0 μL of trypsin solution was added to 500 μL protein solutions (ASNase: 1.0 μM ASNase, 0-40 μM polymers, 10 mM MOPS, pH 7.0; PEG-ASNase: 1.0 μM PEG-ASNase, 10 mM MOPS, pH 7.0) at 37^{o}C. After incubation for 2.0 h, 5.0 μL of 100 mM PMSF in ethanol was added to stop the trypsin digestion reaction. The samples were then mixed with an equal volume of loading buffer containing 4.0% (w/v) SDS, 20% sucrose, 0.010% (w/v) bromophenol blue, and 125 mM Tris-HCl (pH 6.8). The samples were boiled for

15 min followed by loading on a 14% PAGE with a standard ladder marker, which was obtained from Bio-Rad Laboratories (Hercules, California). After gel electrophoresis, the gels were stained with silver nitrate.

Shaking Treatment

Aliquots of 1.2 mL of protein solutions (ASNase: 1.0 μM ASNase, 0-40 μM polymers, 10 mM MOPS, pH 7.0; PEG-ASNase: 1.0 μM PEG-ASNase, 10 mM MOPS, pH 7.0) were added to 2.0 mL microcentrifuge tubes (Thermo Scientific, Waltham, Mas- sachusetts). The samples were then shaken at 500 rpm for 0-6 h. The enzyme activities and sizes of the samples were measured by the assay described above.

Heat Treatment

Protein solutions (ASNase: 1.0 μM ASNase, 0-40 μM polymers, 10 mM MOPS, pH 7.0; PEG-ASNase: 1.0 μM PEG-ASNase, 10 mM MOPS, pH 7.0) were heated at 60^{o}C for 0-2 h. The enzyme activities and sizes of the samples were measured by the assay described above.

2.2.3. Results

Preparation and Characterization of ASNase/PEG-*b*-PAMA Complexes

Figure 2.2.1A shows the chemical structures of polymers used in this study. Cationic PEG-*b*-PAMA had PEG and PAMA regions with average M_w of 5.0 and 5.5 kDa, respectively. Two types of homopolymer were also used for control experiments: cationic PAMA with an average M_w of 4.2 kDa and nonionic PEG with an average M_w of 7.5 kDa, which were similar to PEG-*b*-PAMA. Anionic ASNase, which is used in treatment of acute lymphoblastic leukemia, was selected as a multidomain therapeutic protein.

I demonstrated previously that cationic PEGylated polyelectrolytes bind to anionic proteins, resulting in the formation of water-dispersed PPCs [25]. Therefore, a PPC between cationic PEG-*b*-PAMA

and anionic ASNase was prepared, as illustrated in Figure 2.2.1B. Figure 2.2.2A shows the hydrodynamic diameter (D_h) of ASNase in the absence or presence of polyelectrolytes. The D_h of ASNase alone was 11.1 nm, but increased to >1000 nm with the addition of 1.0 μM PEG-*b*-PAMA. When further PEG-*b*-PAMA was added to ASNase solution, the D_h decreased with increasing concentration of PEG-*b*-PAMA, and then reached a plateau of 22 nm at around 40 μM PEG-*b*-PAMA. In contrast, the D_h of ASNase increased sharply with increasing concentration of cationic PAMA with a plateau of >1000 nm at around 30 μM PAMA. The D_h of PEG-*b*-PAMA and PAMA alone could not be detected by DLS. These results indicated that ASNase formed a soluble PPC with PEG-*b*-PAMA, whereas ASNase formed an aggregative PPC with PAMA.

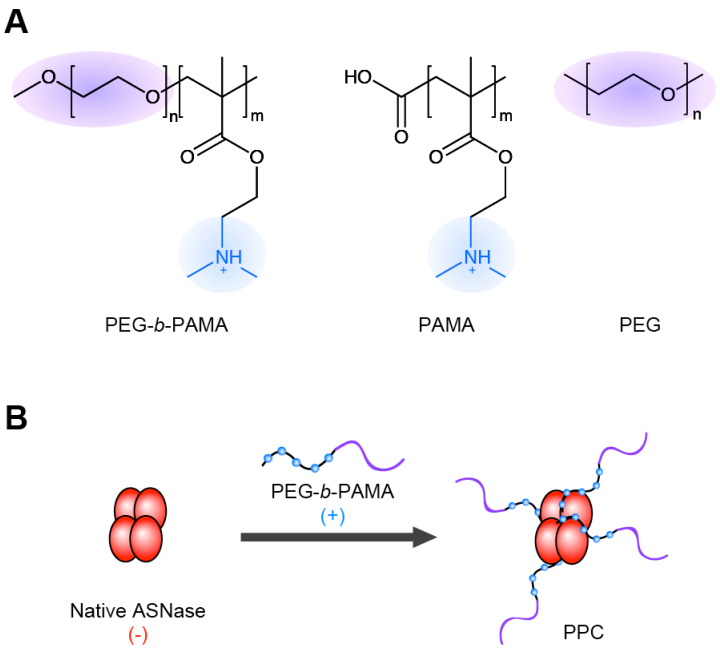

Figure 2.2.1. (A) Chemical structures of polymers. **(B)** Schematic illustration of PPC with PEG-*b*-PAMA.

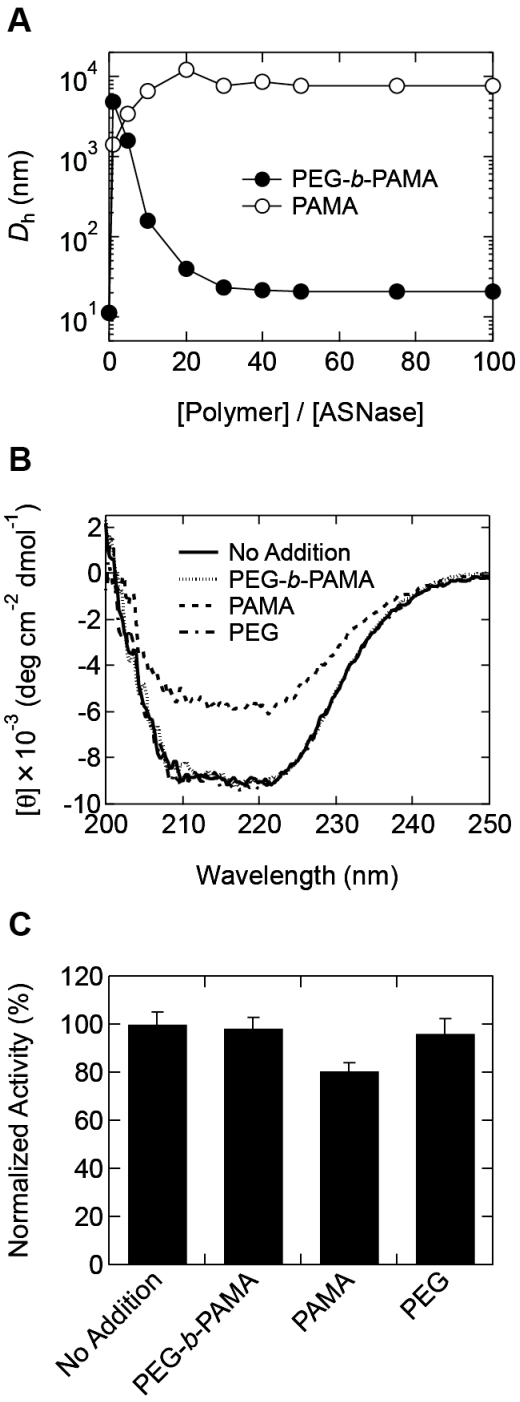

Figure 2.2.2. Characterization of ASNase/PEG-*b*-PAMA complexes. **(A)** Hydrodynamic diameter (D_h) variations of the ASNase in the presence of polymers at various [polymer]/[ASNase] ratios. **(B)** Far-UV CD spectra of ASNase in the absence or presence of polymers at [ASNase]/[polymer] = 1:40. **(C)** Normalized enzyme activity of the ASNase in the absence or presence of polymers at [ASNase]/[polymer] = 1:40.

Subsequently, the structure and enzyme activity of ASNase in the presence of polymers were characterized. Far-UV CD spectra of ASNase in the presence of PEG-*b*-PAMA and PEG were identical to those of the native ASNase, whereas those of ASNase in the presence of PAMA decreased (Figure 2.2.2B). These results indicated that PAMA denatured the ASNase in aggregate form, as shown in Figure 2.2.2A. Furthermore, PEG-*b*-PAMA as well as PEG did not affect the enzyme activity of ASNase, whereas it decreased in the presence of PAMA (Figure. 2.2.2C). These results indicated that ASNase retained the original properties of secondary structure and enzyme activity after the formation of a PPC with PEG-*b*-PAMA.

Stress Tolerance of ASNase Formed PPC with PEG-*b*-PAMA

PEGylation is one of the major strategies to stabilize pharmaceutical proteins *in vivo* due to the steric hindrance of PEG segments on the protein surface [7–12]. It is of interest to determine whether noncovalent interaction between ASNase and PEG-*b*-PAMA stabilizes the proteins to the same extent as in covalently conjugated PEGylated proteins toward various stresses, including proteolytic degradation and agitation. Therefore, commercially available PEG-ASNase was prepared as a model PEGylated protein.

Figure 2.2.3A shows the enzyme activities of ASNase in the absence or presence of polymers preincubated with trypsin, which hydrolyzes peptide bonds at the carboxyl end of basic amino acids in the proteins. The residual activity of native ASNase was 15%, indicating that ASNase was inactivated by trypsin proteolysis. Similarly, ASNase in the presence of PAMA and PEG was inactivated by trypsin proteolysis. In contrast, the addition of PEG-*b*-PAMA showed a protective effect against trypsin proteolysis. The residual activity of ASNase/PEG-*b*-PAMA was 81%, which was higher than that of PEG-ASNase (47%).

The proteolytic digestion of ASNase by trypsin was further evaluated by SDS-PAGE (Figure 2.2.3B). Without trypsin treatment, only a band of monomeric size (35 kDa) was observed under all conditions. After trypsin digestion, the band of 35 kDa disappeared in the samples of ASNase alone, ASNase with PAMA, and ASNase with PEG. In contrast, the band of 35 kDa remained in the presence of

PEG-*b*-PAMA after trypsin treatment, corresponding with the residual activity (Figure. 2.2.3A). These results indicated that the PPC with PEG-*b*-PAMA had a protective effect against proteolysis by trypsin.

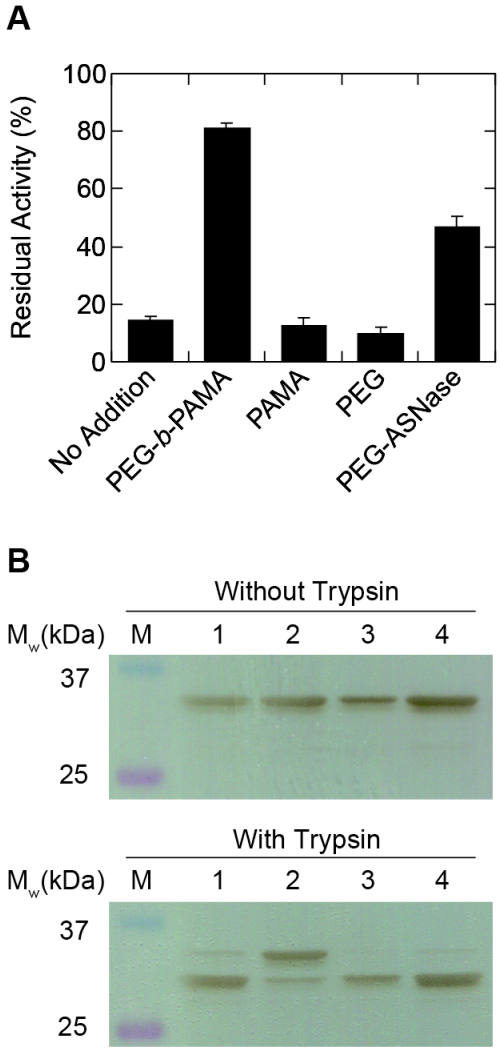

Figure 2.2.3. Proteolytic digestion of ASNase with polymer. **(A)** Residual activity of ASNase with polymers and PEG–ASNase after trypsin treatment. **(B)** SDS-PAGE of ASNase/polymer preincubated with or without trypsin treatment. Lane 1, native ASNase; lane 2, ASNase/PEG-*b*-PAMA; lane 3, ASNase/PAMA; lane 4, ASNase/PEG; M, standard ladder marker.

The protective effects of PEGylated polyelectrolyte against shaking were then evaluated. A solution of native ASNase shaken at 500 rpm for 6 h showed visible suspension and the enzyme activity

disappeared completely (Figure 2.2.4). DLS measurements indicated that D_h of native ASNase after shaking was >1000 nm (Table 2.2.1), suggesting that the native ASNase was inactivated due to aggregation induced by shaking. In contrast, the residual activity of ASNase with polymers remained above 75%, and that of PEG-ASNase remained at 47%. It is interesting to note that D_h of ASNase/PEG-*b*-PAMA after shaking remained constant, whereas those of other samples were above 1000 nm (Table 2.2.1). These results indicated that the PEGylated polyelectrolytes inhibited shaking-induced protein aggregation.

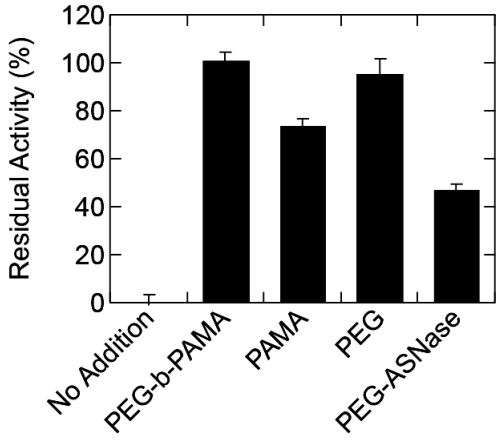

Figure 2.2.4. Residual activities of ASNase with polymers and PEG-ASNase after the shaking at 500 rpm for 6 h.

Finally, the effects of PEGylated polyelectrolyte against heat-induced inactivation of ASNase were confirmed. Heating temperature was chosen 60^{o}C because of the ASNase did not inactivated below 40^{o}C (data not shown). The residual activities of native ASNase and PEG-ASNase were 55% and 38%, respectively (Figure 2.2.5). With the addition of nonionic PEG, there was a slight change in the residual activity to 60%. In contrast, the addition of cationic polyelectrolytes, PEG-*b*-PAMA and PAMA, the enzyme activities decreased about 10%. The ASNase and polyelectrolyte solutions after heating showed visible aggregates with D_h values >330 nm (Table 2.2.1). These results suggested that polyelectrolytes accelerated the heat-induced inactivation of ASNase.

Table 2.2.1. Hydrodynamic Diameters (D_h) of ASNase in the Absence or Presence of Polymers.

	D_h (nm)[a]		
	No Stress	Shaking	Heating
No Addition	10.8 ± 0.06 (0.20)	> 1000 (0.92)	10.1 ± 0.13 (0.29)
PEG-*b*-PAMA	26.2 ± 0.28 (0.46)	28.9 ± 0.38 (0.67)	330 ± 2.61 (0.18)
PAMA	> 1000 (1.00)	> 1000 (1.00)	> 1000 (0.88)
PEG	11.3 ± 0.02 (0.22)	> 1000 (0.84)	13.3 ± 0.40 (0.47)
PEG-ASNase	24.5 ± 0.18 (0.25)	> 1000 (1.00)	28.0 ± 3.01 (0.59)

Parentheses show polydispersity index (PDI).

[a]Z-average size.

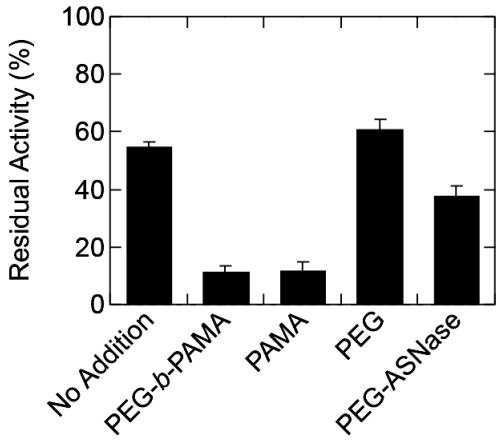

Figure 2.2.5. Residual activity of ASNase with polymers and PEG-ASNase after heat treatment at 60◦C for 2 h.

2.2.4. Discussion

This study showed stabilization of therapeutic proteins using PEGylated polyelectrolytes, as summarized below. PEGylated cationic PEG-*b*-PAMA and anionic ASNase formed soluble complexes without conformational changes, whereas non-PEGylated PAMA formed aggregative complexes with conformational changes (Figures 2.2.2A,B), corresponding to the results reported previously [25]. This is because the electrostatic interactions between proteins and polyelectrolytes are driving forces that stabilize PPC, which was also supported by the control data in which noncharged PEG alone did not affect the size of ASNase (Table 2.2.1). In is interesting to note that the D_h of ASNase with PEG-*b*-PAMA was identical to that of PEG-ASNase (Table 2.2.1), suggesting that the conformation of the PPC with PEG-*b*-PAMA may be similar to that of PEGylated proteins.

Several authors, including our group, reported previously that cationic polyelectrolytes can bind to anionic enzymes, resulting in inhibition of enzyme activities [23,25,30,31]. However, the results of the present study showed that the enzyme activity of ASNase did not change despite PPC formation (Figure 2.2.2C). This unexpected difference in inhibition of polyelectrolytes may be due to several factors, such as the types of compounds, pH of the solution, and the method used for enzyme assay. Although it is difficult to determine whether polyelectrolytes inhibit the enzyme activity, PPC is more favorable for enzyme activity of ASNase than PEG-ASNase because the covalent PEGylation produces a decrease in activity of proteins [7–12]. Under the present experimental condition, the enzyme activities of native ASNase and PEG-ASNase were about 35 and 10 U/mL, respectively.

PEG-conjugated proteins are protected from proteolytic digestion by proteases *in vitro* and *in vivo*. In fact, the residual activity of PEG-ASNase toward trypsin was higher than that of native ASNase (Figure 2.2.3). In this study, PEG-*b*-PAMA protected ASNase from proteolytic digestion to a comparable extent to PEG-ASNase, whereas the PAMA and PEG did not (Figure 2.2.3). These results indicated that binding of PEG-*b*-PAMA to the surface of ASNase provided a shield. It was suggested that the protective mechanism of PPC with PEG-*b*-PAMA is similar to that of PEGylated proteins, that is, steric hindrance of PEG on

ASNase/PEG-*b*-PAMA complex inhibits access to protease.

Shaking is one of the major causes of protein aggregation [3,4]. Aggregation by shaking is primarily attributable to the con- tact of proteins and air-water interfaces [4]. Our results indicated that native ASNase also formed visible aggregates on shaking stress (Table 2.2.1), resulting in inactivation of the enzyme (Figure 2.2.4). In contrast, the solutions of ASNase with polymer and PEG-ASNase were clear and retained enzyme activity. It is emphasized that the D_h of ASNase/PEG-*b*-PAMA after shaking remained constant, even though DLS measurement is sensitive to small amounts of aggregates. It is possible that the steric hindrance of PEG on the ASNase/PEG-*b*-PAMA complex conferred protection from the contact of air-water interfaces for the protein.

The data for heat treatment on ASNase are complex, and it is difficult to understand the mechanism compared to other types of stress. Briefly, PEG-*b*-PAMA and PAMA accelerated irreversible inactivation of ASNase against heat treatment, whereas the others did not (Figure 2.2.5). This result was inconsistent with a previous report in which PEGylated polyelectrolyte stabilized hen egg white lysozyme against heat-induced inactivation [22]. It was suggested that the inconsistency resulted from monomeric or oligomeric forms of the proteins as follows. The tetrameric ASNase loses enzyme activity due to dissociation of subunits during heat treatment at 60^{o}C, and then the enzyme activity is restored by decreasing temperature due to the reassociation of subunits [13,32] Furthermore, the denaturation temperature of ASNase is 62^{o}C, which was independent even in the presence of polymers. Accordingly, the polyelectrolytes are thought to inhibit the reassociation of ASNase through electrostatic interaction, resulting in irreversible inactivation of ASNase.

In summary, I showed that PEGylated polyelectrolytes stabilize the therapeutic protein, ASNase. PEG-*b*-PAMA successfully protected ASNase against trypsin digestion and shaking-induced aggregation due to PPC formation. The stabilizing effects of PPC with PEG-*b*-PAMA were similar to those of covalent PEGylated ASNase, suggesting that noncovalent PEGylation occurred with PEGylated polyelectrolytes. Other therapeutic proteins with multidomain structures would be stabilized by PEGylated polyelectrolytes. I believe that complex formation between PEGylated polyelectrolytes and proteins will expand the

applications of therapeutic proteins, such as formulation and drug delivery systems.

2.2.5. References

[1] Leader, B.; Baca, Q. J.; Golan, D. E. Protein Therapeutics: a Summary and Pharmacological Classification. *Nat. Rev. Drug. Discov.* **2008**, *7*, 21-39.

[2] Pasut, G.; Sergi, M.; Veronese, F. M. Anti-Cancer PEG-Enzymes: 30 Years Old, but Still a Current Approach. *Adv. Drug. Deliv. Rev.* **2008**, *60*, 69-78.

[3] Frokjaer, S.; Otzen, D. E. Protein Srug Stability: a Formulation Challenge. *Nat. Rev. Drug. Discov.* **2005**, *4*, 298-306.

[4] Wang, W. Protein Aggregation and its Inhibition in Biopharmaceutics. *Int. J. Pharm.* **2005**, *289*, 1-30.

[5] Duncan, R. The Dawning Era of Polymer Therapeutics. *Nat. Rev. Drug. Discov.* **2003**, *2*, 347-360.

[6] Nguyen, T. H.; Kim, S. H.; Decker, C. G.; Wong, D. Y.; Loo, J. A.; Maynard, H. D. A Heparin-Mimicking Polymer Conjugate Stabilizes Basic Fibroblast Growth Factor. *Nat. Chem.* **2013**, *5*, 221-227.

[7] Veronese, F. M. Peptide and Protein PEGylation: a Review of Problems and Solutions. *Biomaterials* **2001**, *22*, 405-417.

[8] Roberts, M. J.; Bentley, M. D.; Harris, J. M. Chemistry for Peptide and Protein PEGylation. *Adv. Drug. Deliv. Rev.* **2002**, *54*, 459-476.

[9] Harris, J. M.; Chess, R. B. Effect of Pegylation on Pharmaceuticals. *Nat. Rev. Drug. Discov.* **2003**, *2*, 214-221.

[10] Veronese, F. M.; Pasut, G. PEGylation, Successful Approach to Drug Delivery. *Drug. Discov. Today* **2005**, *10*, 1451-1458.

[11] Alconcel, S. N. S.; Baas, A. S.; Maynard, H. D. FDA-Approved Poly(ethylene glycol)–Protein Conjugate Drugs. *Polym. Chem.* **2011**, *2*, 1442–1448.

[12] Pfister, D.; Morbidelli, M. Process for Protein PEGylation. *J. Control. Release.* **2014**, *180C*, 134-149.

[13] Soares, A.L.; Guimaraes, G. M.; Polakiewicz, B.; de, Moraes Pitombo R. N.; Abrahao-Neto, J. Effects of Polyethylene Glycol Attachment on Physicochemical and Biological Stability of *E. coli* L-Asparaginase. *Int. J. Pharm.* **2002**, *237*, 163-170.

[14] Kodera, Y.; Sekine, T.; Yasukohchi, T.; Kiriu, Y.; Hiroto, M.; Matsushima, A.; Inada, Y. Stabilization of L-Asparaginase Modified with Comb-Shaped Poly(ethylene glycol) Derivatives, *in vivo* and *in vitro*. *Bioconjug. Chem.* **1994**, *5*, 283-286.

[15] Hinds, K.; Koh, J. J.; Joss, L.; Liu, F.; Baudys, M.; Kim, S. W. Synthesis and Characterization of Poly(ethylene glycol)-Insulin Conjugates. *Bioconjug. Chem.* **2000**, *11*, 195-201.

[16] Lee, H.; Park, T. G. A Novel Method for Identifying PEGylation Sites of Protein Using Biotinylated PEG Derivatives. *J. Pharm. Sci.* **2003**, *92*, 97-103.

[17] Mueller, C.; Capelle, M. A.; Arvinte, T.; Seyrek, E.; Borchard, G. Noncovalent Pegylation by Dansyl-Poly(ethylene glycol)s as a New Means against Aggregation of Salmon Calcitonin. *J. Pharm. Sci.* **2011**, *100*, 1648-1662.

[18] Mueller, C.; Capelle, M. A.; Arvinte, T.; Seyrek, E.; Borchard, G. Tryptophan-mPEGs: Novel Excipients that Stabilize Salmon Calcitonin against Aggregation by Non-covalent PEGylation. *Eur. J. Pharm. Biopharm.* **2011**, *79*, 646-657.

[19] Khondee, S.; Olsen, C. M.; Zeng, Y.; Middaugh, C. R.; Berkland, C. Noncovalent PEGylation by Polyanion Complexation as a Means to Stabilize Keratinocyte Growth Factor-2 (KGF-2). *Biomacromolecules* **2011**, *12*, 3880-3894.

[20] Mero, A.; Ishino, T.; Chaiken, I.; Veronese, F. M.; Pasut, G. Multivalent and Flexible PEG-Nitrilotriacetic Acid Derivatives for Non-Covalent Protein Pegylation. *Pharm. Res.* **2011**, *28*, 2412-2421.

[21] Mueller, C.; Capelle, M. A.; Seyrek, E.; Martel, S.; Carrupt, P. A.; Arvinte, T.; Borchard, G. Noncovalent PEGylation: Different Effects of Dansyl-, L-Tryptophan-, Phenylbutylamino-, Benzyl-

and Cholesteryl-PEGs on the Aggregation of Salmon Calcitonin and Lysozyme. *J. Pharm. Sci.* **2012**, *101*, 1995-2008.

[22] Ganguli, S.; Yoshimoto, K.; Tomita, S.; Sakuma, H.; Matsuoka, T.; Shiraki, K.; Nagasaki, Y. Regulation of Lysozyme Activity Based on Thermotolerant Protein/Smart Polymer Complex Formation. *J. Am. Chem. Soc.* **2009**, *131*, 6549-6553.

[23] Tomita, S.; Ito, L.; Yamaguchi, H.; Konishi, G.; Nagasaki, Y.; Shiraki, K. Enzyme Switch by Complementary Polymer Pair System (CPPS). *Soft Matter* **2010**, *6*, 5320-5326

[24] Tomita, S.; Shiraki, K. Poly(acrylic acid) is a Common Noncompetitive Inhibitor for Cationic Enzymes with High Affinity and Reversibility. *J. Polym. Sci. Part A: Polym. Chem.* **2011**, *49*, 3835-3841.

[25] Kurinomaru, T.; Tomita, S.; Kudo, S.; Ganguli, S.; Nagasaki, Y.; Shiraki, K.. Improved Complementary Polymer Pair System: Switching for Enzyme Activity by PEGylated Polymers. *Langmuir* **2012**, *28*, 4334-4338.

[26] Kayitmazer, A. B.; Seeman, D.; Minsky, B. B.; Dubin, P. L.; Xu, Y.. Protein–Polyelectrolyte Interactions. *Soft Matter* **2013**, *9*, 2553-2583.

[27] Kurinomaru, T.; Tomita, S.; Hagihara, Y.; Shiraki, K. Enzyme Hyperactivation System Based on a Complementary Charged Pair of Polyelectrolytes and Substrates. *Langmuir* **2014**, *30*, 3826-3831.

[28] Kurinomaru, T.; Maruyama, T.; Izaki, S.; Handa, K.; Kimoto, T.; Shiraki, K.. Protein-Poly(amino acid) Complex Precipitation for High-Concentration Protein Formulation. *J. Pharm. Sci.* **2014**, *8*, 2248-2254.

[29] Pace, C. N.; Vajdos, F.; Fee, L.; Grimsley, G.; Gray, T. How to Measure and Predict the Molar Absorption Coefficient of a Protein. *Protein. Sci.* **1995**, *4*, 2411-2423.

[30] Tamura, A.; Ikeda, G.; Seo, J.H.; Tsuchiya, K.; Yajima, H.; Sasaki, Y.; Akiyoshi, K.; Yui, N. Molecular Logistics Using Cytocleavable Polyrotaxanes for the Reactivation of Enzymes Delivered in Living Cells. *Sci. Rep.* **2013**, *3*, 2252.

[31] Tomita, S.; Yoshimoto, K. Polyion Complex Libraries Possessing Naturally Occurring Differentiation for Pattern-Based Protein Discrimination. *Chem. Commun.* **2013**, *49*, 10430-10432.

[32] Stecher, A. L.; de, Deus P. M.; Polikarpov, I.; Abrahao-Neto, J. Stability of L-Asparaginase: an Enzyme Used in Leukemia Treatment. *Pharm. Acta. Helv.* **1999**, *74*, 1-9.

Chapter 3. Enzyme Hyperactivation

3.1. Enzyme Hyperactivation System Based on a Complementary Charged Pair of Polyelectrolytes and Substrates

3.1.1. Introduction

The control of enzyme activity through noncovalent interaction has attracted widespread attention not only in biological studies, but also in innovative applications such as biosensors [1−3]. These artificial modulators are classified as inhibitors or activators. Several artificial inhibitors have been designed: for example, polymeric substrate analogs [4], dendrimers [5], molecular clips and tweezers [6], gold nanoparticles [7−10], and graphene oxides [11]. The binding of inhibitors to enzyme surfaces typically results in a decrease in enzyme activity. Our group have recently demonstrated that charged polyelectrolytes function as reversible inhibitors of various enzymes via a so called complementary polymer pair system (CPPS) [12−15]. Briefly, the formation of noncovalent complexes between enzymes and polyelectrolytes results in the complete prevention of enzyme activity; the subsequent addition of another charged polyelectrolyte can restore the enzyme activity by removing the binding polyelectrolytes from the enzyme. By contrast, artificial activators, such as polymer micelles [16−22], thermoresponsive microgels [23], gold nanoparticles [24,25], and graphene oxides [26], have been reported to increase enzyme activity through noncovalent interactions. However, strategies for the development of artificial modulators have typically focused on the binding of artificial modulators to enzyme surfaces.

Here, I developed a unique hyperactivation system for enzymes that focuses on the electrostatic nature of both the polyelectrolytes and substrates. In this system, enzyme activation occurs immediately

when a polyelectrolyte is added to an enzyme solution containing a substrate whose electric charge is opposite that of the polyelectrolyte. In other words, a complementary charged pair is designed between the substrate and polyelectrolyte in addition to between the polyelectrolyte and enzyme. The enzyme activity of α-chymotrypsin (ChT) for a cationic substrate increased 7-fold in the presence of anionic poly(acrylic acid) (PAAc) and for an anionic substrate increased 18-fold in the presence of cationic poly(allylamine) (PAA) at pH 7.0. Analysis of salt and pH effects, enzyme kinetics, dynamic light scattering (DLS), and circular dichroism (CD) suggested that the hyperactivation is due to modulation of the charge distribution of the enzyme.

3.1.2. Materials and Methods

Materials

α-Chymotrypsin (ChT) from bovine pancreas, *N*-succinyl-L-phenylalanine-*p*-nitroanilide (SPNA), and 3-(*N*-morpholino)propanesulfonic acid (MOPS) were from Sigma Chemical Co. (St. Louis, MO). Poly(acrylic acid) (PAAc) with an average molecular weight of 5.0 kDa and dimethyl sulfoxide (DMSO) were from Wako Pure Chemical Ind., Ltd. (Osaka, Japan). Poly(allylamine) (PAA) with an average molecular weight of 5.0 kDa was from Nitto Boseki Co., Ltd. (Fukushima, Japan). Sodium chloride (NaCl) was from Nacalai Tesque, Inc. (Kyoto, Japan). *N*-Acetyl-L-phenylalanine-*p*-nitroanilide (APNA) was from Watanabe Chemical Ind., Ltd. (Hiroshima, Japan). *N*-Glycyl-L-phenylalanine-*p*-nitroanilide (GPNA) was from Bachem AG (Bubendorf, Switzerland). Ethanol was from Kanto Chemical Co., Inc. (Tokyo, Japan). All chemicals used were high-quality analytical grade and used as received.

Protein Concentration

The protein concentration of ChT was determined from the absorbance at 280 nm using a V-630 spectrophotometer (Japan Spectroscopic Co., Ltd., Tokyo, Japan) and an extinction coefficient of 50,585 M^{-1}

cm^{-1} [27].

Enzyme Assay

All substrates used in this study were insoluble in pure water, and hence 9.0 mM MOPS (pH 7.0) with 9.0% ethanol and 1.0% DMSO was used as the solvent for the enzyme assays. A 30 μL aliquot of substrate solution containing 0−30 mM substrate (GPNA, APNA, or SPNA), 90% ethanol, and 10% DMSO was mixed with 120 μL of polyelectrolyte (PAA or PAAc) in 10 mM MOPS (pH 7.0) and 150 μL of 10 μM ChT in 10 mM MOPS (pH 7.0). The initial reaction velocities v_0 were determined from the slope of the initial increase in the absorbance intensity at 410 nm. The absorbance was converted into concentration using a molar extinction coefficient for *p*-nitroaniline of 8,800 M^{-1} cm^{-1}. Normalized enzyme activity was defined as the ratio of v_0 in the presence of polyelectrolyte to v_0 with no polyelectrolyte. For the salt effect studies, all parameters were unchanged except for the concentration of NaCl. The activity of ChT in the presence of the polyelectrolytes was normalized to that without polyelectrolytes at the same salt concentration because the v_0 of ChT for substrates changed slightly with increasing NaCl concentration. For pH effect studies, all parameters were unchanged except for the addition of 6.66 mM HCl/NaOH. For kinetics studies with PAA, all parameters were unchanged except for the concentration of MOPS. At higher concentrations of SPNA, a pH shift due to protons from SPNA could not be neglected, so that a high concentration of MOPS buffer (100 mM) was used to avoid changing the pH.

Dynamic Light Scattering

Dynamic light scattering (DLS) experiments were performed using a Zetasizer Nano ZS light scattering photometer (Malvern Instruments, Worcestershire, UK) equipped with a 4 mW He−Ne ion laser (λ = 633 nm). The sizes of the enzyme with polyelectrolytes were determined as follows. Solutions containing 5.0 μM ChT, 0−5.0 μM polyelectrolytes, and 10 mM MOPS buffer (pH 7.0) were placed in a 1-cm path length disposable cuvette, and DLS measurements were performed at 25 ^{o}C at a detection angle of 173^{o}. The

viscosity of the solutions was approximated by the value of the 10 mM MOPS solution (η = 0.87 cP). All results are presented as the average values of three independent experiments.

Circular Dichroism

Circular dichroism (CD) experiments were performed in a 1-mm path length quartz cuvette using a J-720 spectropolarimeter (Japan Spectroscopic Co., Ltd., Tokyo, Japan). Solutions containing 5.0 μM ChT, 0 - 5.0 μM polyelectrolytes, and 10 mM MOPS buffer (pH 7.0) were prepared, and the spectra were measured at 25 ^{o}C. The CD spectra of the samples were corrected by subtracting the corresponding spectra of the buffers in the absence of enzymes.

3.1.3. Results

Hyperactivation of ChT by Polyelectrolytes

Figure 3.1.1a illustrates the molecular structures of the enzyme, polyelectrolytes, and substrates used in this study. α-Chymotrypsin (ChT) is classified as a serine protease that hydrolyzes peptide bonds at the carboxyl end of aromatic amino acids in a given substrate. The enzyme hyperactivation system was investigated using three types of substrates: *N*-glycyl-L-phenylalanine-*p*-nitroanilide (GPNA) as a cationic substrate, *N*-acetyl-L-phenylalanine-*p*-nitroanilide (APNA) as a neutral substrate, and *N*-succinyl-L-phenylalanine-*p*-nitroanilide (SPNA) as an anionic substrate. Note that the initial velocities (v_0) of native ChT for cationic GNPA and anionic SPNA were similar, with values of 13.6 ± 0.2 (nM/sec) and 18.4 ± 0.2 (nM/sec), respectively, whereas the activity for neutral APNA was three times higher, with a value of 43.2 ± 0.8 (nM/sec). Two types of polyelectrolytes were used: cationic PAA and anionic PAAc. Figure 3.1.1b shows the system for the hyperactivation of ChT with polyelectrolytes and charged substrates. ChT activity for the cationic substrate GPNA was enhanced by the addition of the anionic polyelectrolyte PAAc; conversely, ChT activity for the anionic substrate SPNA was enhanced by the addition of the cationic polyelectrolyte PAA.

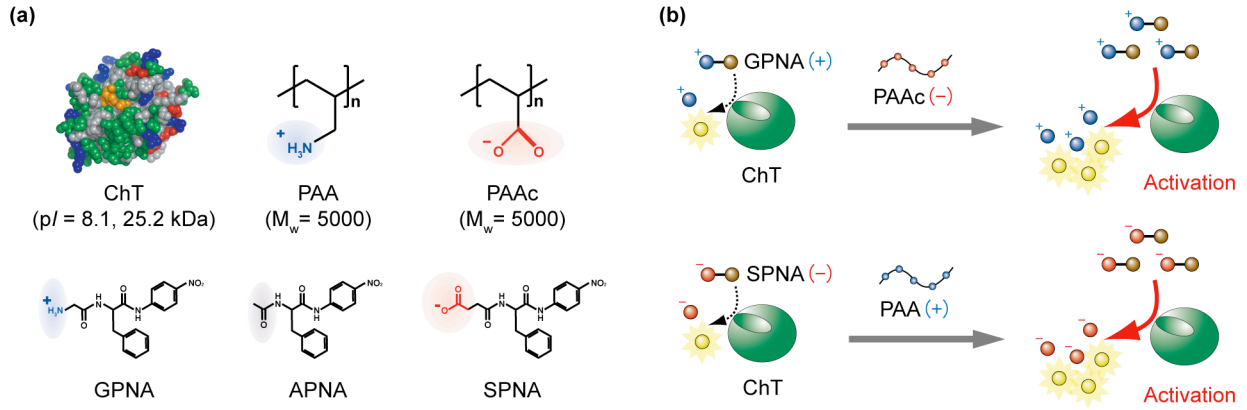

Figure 3.1.1. (a) Tertiary structure of ChT (PDB entry 4CHA) and the chemical structures of the polyelectrolytes and substrates. Color scheme for enzymes: anionic residues, red; cationic residues, blue; hydrophobic residues, gray; hydrophilic residues, green; catalytic regions, orange. **(b)** Schematic illustration of ChT hyperactivation by polyelectrolytes.

Figure 3.1.2a shows the normalized activity of ChT when 5.0 μM enzyme was mixed with various concentrations of PAAc. As expected, the ChT activity for GPNA markedly increased with increasing concentrations of PAAc; the ChT activity increased approximately 7.0-fold (96.6 nM/sec) in the presence of 5.0 μM PAAc (1.0 equiv). It should be noted that PAAc alone did not catalyze the hydrolysis of GPNA. By contrast, for the neutral substrate APNA and anionic substrate SPNA, ChT activity decreased 0.28-fold (12.1 nM/sec) and 0.05-fold (0.8 nM/sec), respectively, in the presence of PAAc. These results clearly indicate that activation of ChT by anionic PAAc occurred only for the cationic substrate. Similarly, enzyme activity was measured in the presence of cationic PAA and the three types of substrates (Figure 3.1.2b). The activity of ChT for the anionic substrate SPNA was significantly enhanced upon the addition of cationic PAA; the enzyme activity was activated approximately 18.0-fold (321.0 nM/sec) by 50.0 μM PAA (10.0 equiv), whereas hydrolysis of SPNA by PAA alone was not observed. In contrast to the effects of PAAc, ChT activities for neutral APNA and cationic GPNA increased slightly with increasing PAA concentration, up to 2.4-fold (108.0 nM/sec) and 1.5-fold (15.4 nM/sec), respectively, i.e., the effects of PAA increased in the

order GPNA < APNA ≪ SPNA. Thus, an oppositely charged polyelectrolyte and substrate pair was necessary for higher activation of ChT.

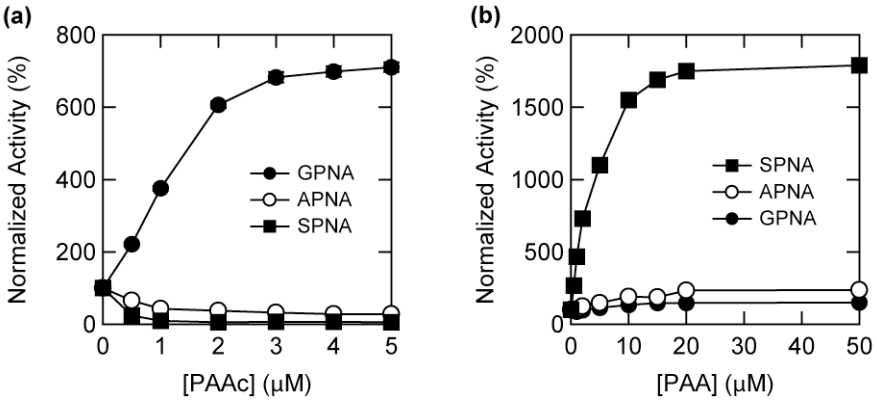

Figure 3.1.2. Normalized activity of ChT for three types of substrates in the presence of PAAc **(a)** or PAA **(b)**. Various concentrations of polyelectrolytes were added to solutions containing 5.0 μM ChT and 0.8 mM substrate. GPNA, filled circles; APNA, open circles; SPNA, filled squares.

Effect of pH and Ionic Strength

Because enzyme activity is influenced by pH [28], it is unclear from Figure 3.1.2 whether polyelectrolytes shift the optimum pH of ChT, resulting in an apparent activation of ChT. The effect of pH on enzyme activity in the presence and absence of polyelectrolytes was compared. Figure 3.1.3a shows the initial velocity (v_0) for the hydrolysis of cationic GPNA by ChT in the absence and presence of anionic PAAc as a function of pH. Although the pH profile of v_0 of ChT in the presence of PAAc slightly shifted to lower pH regions, the v_0 of ChT in the presence of PAAc was much higher than that of ChT alone. In the pH range from 5.5 to 8.5, the maximum v_0 for GPNA was 42.5 nM/sec at pH 8.5 and 227.0 nM/sec at pH 7.9 in the absence and presence of PAAc, respectively. A slight difference in the optimum pH was observed in the presence of cationic PAA and anionic SPNA (Figure 3.1.3b). PAA increased the v_0 of ChT in the presence of PAA without affecting the optimal pH of ChT. In the pH range from 5.5 to 8.5, the maximum v_0 for SPNA was 23.8 nM/sec at pH 7.7 and 856.0 nM/sec at pH 7.6 in the absence and presence of PAA, respectively.

These results demonstrate that a shift in the optimal pH was not a primary cause of the activation of ChT.

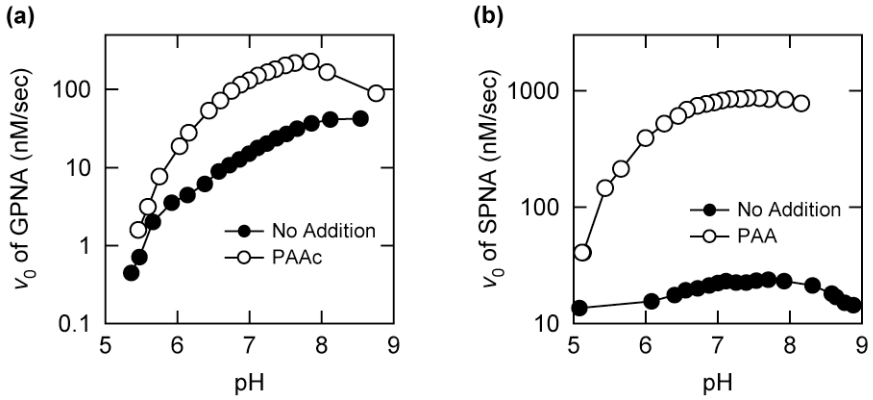

Figure 3.1.3. Initial velocity (v_0) of ChT in the absence and presence of polyelectrolytes at various pH values. **(a)** 0.8 mM GPNA was added to solutions containing 5.0 μM ChT and 0 μM (filled circles) or 5.0 μM (open circles) PAAc. **(b)** 0.8 mM SPNA was added to solutions containing 5.0 μM ChT and 0 μM (filled circles) or 50.0 μM (open circles) PAA.

Subsequently, the effects of ionic strength on the enzyme activity of ChT in the presence of polyelectrolytes were tested. Figure 3.1.4a shows the normalized activity of ChT when various concentrations of NaCl were added to a solution containing 5.0 μM enzyme and 5.0 μM PAAc. The ChT activity for cationic GPNA concomitantly decreased with increasing concentrations of NaCl; the ChT activity reached approximately 100% upon the addition of 300 mM NaCl. Likewise, the ChT activities for neutral APNA and anionic SPNA reverted to approximately 100% upon the addition of 300 mM NaCl. A similar tendency was observed for cationic PAA. The ChT activities for the three substrates in the presence of PAA also reached approximately 100% upon the addition of 300 mM NaCl (Figure 3.1.4b). These results indicate that the activation of ChT activity by polyelectrolytes is primarily attributable to electrostatic interactions.

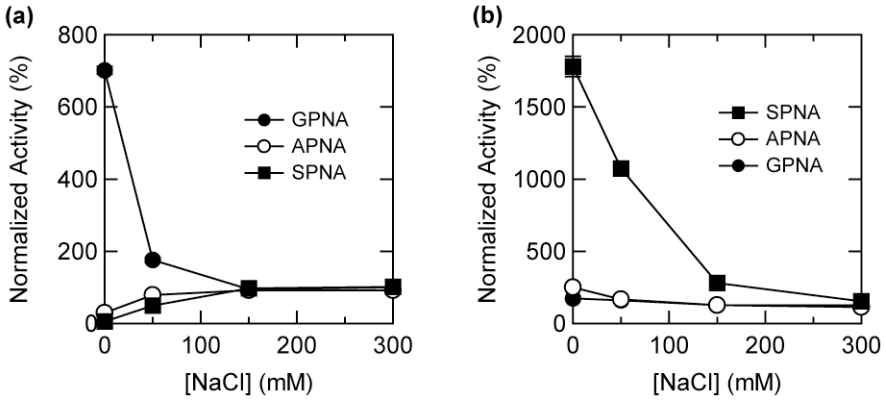

Figure 3.1.4. Normalized activity of ChT for three types of substrate in the presence of polyelectrolytes at various NaCl concentrations. **(a)** Solutions containing 5.0 μM ChT, 5.0 μM PAAc, and 0.8 mM substrate were mixed with various concentrations of NaCl. **(b)** Solutions containing 5.0 μM ChT, 50.0 μM PAA, and 0.8 mM substrate were mixed with various concentrations of NaCl. GPNA, filled circles; APNA, open circles; SPNA, filled squares.

Kinetic Analysis of ChT in the Presence of Polyelectrolytes

To obtain additional insight into the mechanism of hyperactivation, enzyme kinetic analyses were performed using various concentrations of polyelectrolytes. Figure 3.1.5a shows the Lineweaver-Burk plot of $1/v_0$ versus 1/[S] for the hydrolysis of cationic GPNA by ChT in the absence and presence of anionic PAAc. The kinetic parameters were calculated from a linear fit to the Lineweaver-Burk equation for each PAAc concentration (Table 3.1.1). The addition of PAAc to ChT significantly decreased the Michaelis constant (K_M), whereas the catalytic constant (k_{cat}) remained essentially unchanged. These results indicate that the addition of PAAc enhanced the affinity of ChT for GPNA rather than the turnover number.

A similar kinetic analysis was performed using various concentrations of cationic PAA (Figure 3.1.5b). The kinetic parameters were calculated from a linear fit to the Lineweaver-Burk equation for each PAA concentration (Table 3.1.1). The addition of PAA to ChT not only decreased K_M, similar to PAAc, but also increased k_{cat}. These results suggest different mechanisms of ChT activation by PAA and PAAc, as discussed below.

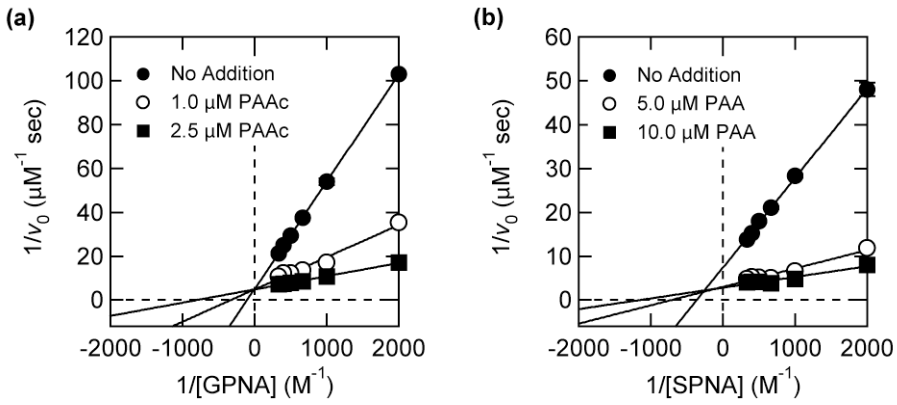

Figure 3.1.5. Lineweaver-Burk plots for the hydrolysis of substrate by ChT in the absence and presence of polyelectrolytes. **(a)** Various concentrations of GPNA were added to solutions containing 5.0 μM ChT and 0 μM (filled circles), 1.0 μM (open circles), or 2.5 μM (filled squares) PAAc. **(b)** Various concentrations of SPNA were added to solutions containing 5.0 μM ChT and 0 μM (filled circles), 5.0 μM (open circles), or 10.0 μM (filled squares) PAA. The lines represent the best fit for the data using the Lineweaver-Burk equation.

Table 3.1.1. Values for the Catalytic Constant (k_{cat}) and the Michaelis Constant (K_M) at Various Concentrations of Polyelectrolytes

Substrate	[Polyelectrolyte] (μM)	k_{cat}[a] (10^{-2} sec^{-1})	K_M[a] (mM)
GPNA	PAAc		
	0	3.98 ± 0.13	9.76 ± 0.35
	1.0	4.19 ± 1.04	3.08 ± 0.98
	2.5	4.17 ± 0.14	1.26 ± 0.07
SPNA	PAA		
	0	2.70 ± 0.11	2.76 ± 0.15
	5.0	6.70 ± 1.08	1.41 ± 0.37
	10.0	7.13 ± 0.94	0.87 ± 0.02

[a] Mean values ± standard deviation.

Size and Secondary Structure of ChT in the Presence of Polyelectrolytes

Regulation of enzyme activity by the formation of an enzyme-polyelectrolyte complex (EPC) was previously reported [12−15]. Thus, it is possible that the activation of ChT by polyelectrolytes is accompanied by EPC

formation. Figure 3.1.6 shows a representative result for the particle size distribution of ChT in the absence and presence of polyelectrolytes, as monitored by DLS. The hydrodynamic diameter (D_h) of ChT alone was 5.1 nm, whereas the D_h of the mixture of ChT and PAAc was 10.0 nm, twice that of ChT alone. By contrast, the D_h of the mixture of ChT with PAA was 6.7 nm, similar to the size of ChT alone. It is noted that the Dh of PAAc and PAA alone was not detected by DLS. These results indicated that anionic PAAc but not cationic PAA formed EPCs with cationic ChT.

Figure 3.1.7 shows the far-UV CD spectra of ChT in the presence of the polyelectrolytes. The far-UV CD spectrum of ChT in the presence of PAAc was identical to that in the absence of PAAc, indicating that the secondary structure of ChT did not significantly change, even upon complexation with PAAc. Similarly, the far-UV CD spectrum of ChT did not change, even in the presence of PAA. Thus, polyelectrolytes did not induce significant conformational changes in ChT.

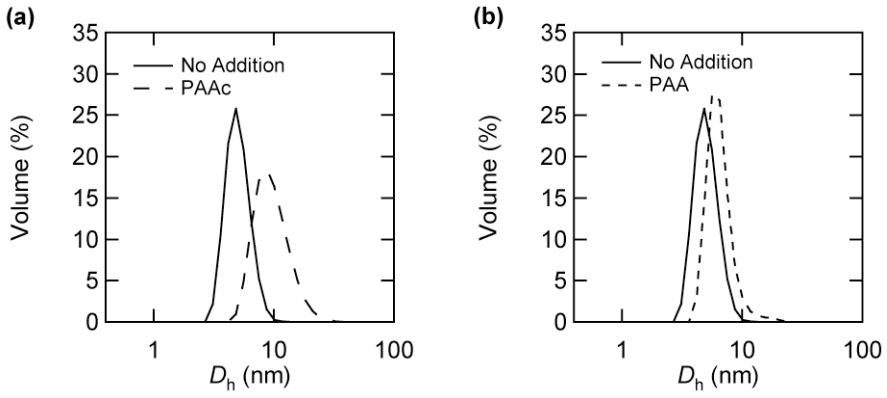

Figure 3.1.6. Hydrodynamic diameter (D_h) of ChT in the absence and presence of polyelectrolytes. 5.0 μM ChT was mixed with 5.0 μM PAAc **(a)** or 5.0 μM PAA **(b)**. Native enzymes, solid line; PAAc, broken line; PAA, dotted line.

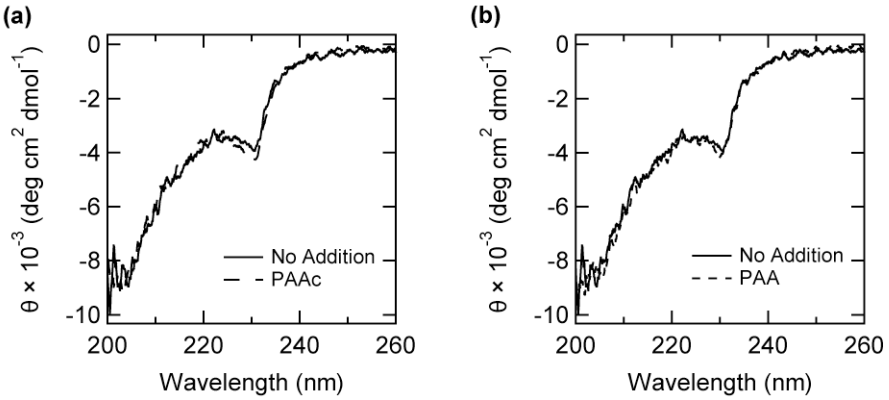

Figure 3.1.7. Far-UV CD spectra of ChT in the absence and presence of polyelectrolytes. 5.0 μM ChT was mixed with 5.0 μM PAAc **(a)** or 5.0 μM PAA **(b)**. Native enzymes, solid line; PAAc, broken line; PAA, dotted line.

3.1.4. Discussion

This study presents a novel enzyme hyperactivation system employing pairs of polyelectrolytes and substrates. Previous studies showed that anionic PAAc inhibits cationic enzymes such as ribonuclease A, lysozyme, and trypsin, whereas cationic PAA inhibits anionic enzymes such as cellulase, α-amylase, and β-galactosidase [13−15]. A significant finding of this study is that both PAAc and PAA can function not only as inhibitors but also as activators of enzymes when appropriate substrates are selected. For example, anionic PAAc activated ChT during the hydrolysis of cationic GPNA, whereas cationic PAA inhibited ChT during the hydrolysis of the same substrate (Figure 3.1.2). Thus, whether polyelectrolytes inhibit or activate reactions is determined by the charge of the substrate: i.e., ChT is activated when polyelectrolytes are complementary to the substrate. ChT activity for a cationic substrate was increased 7-fold by anionic PAAc, and ChT activity was increased 18-fold for an anionic substrate by cationic PAA at pH 7.0, an enhancement of activity greater than that of previously reported artificial activators such as quaternary ammonium salts [29,30], surfactant micelles [31−35], quaternary polyamines [36], polymer micelles [5,19,20], and gold nanoparticles [24,25].

Common mechanisms of hyperactivation by both polyelectrolytes are suggested below. Both

polyelectrolytes clearly enhanced the absolute activity of ChT for complementary charged substrates, as the enhancement of ChT activity could not be explained by a shift in the optimal pH (Figure 3.1.3). A kinetic study revealed that polyelectrolytes decreased the Michaelis constant (K_M) when functioning as activators (Table 3.1.1), indicating that the hyperactivation of ChT by polyelectrolytes was related to increased affinity of ChT for the substrate. Electrostatic interactions played a crucial role in the change in K_M because the enhancement of enzyme activity by polyelectrolytes reverted to original activity levels upon the addition of NaCl (Figure 3.1.4), which shielded the electrostatic interactions. Thus, electrostatic interactions among the enzyme, polyelectrolytes, and substrates are responsible for the enhancement of the affinity of the enzyme for the substrate.

Modulation of the charge distribution on an enzyme surface affects the diffusional association between an enzyme and its substrates. For example, the electrostatic steering of the substrate toward the active site of human superoxide dismutase was enhanced by the mutation of two charged residues in proximity to the active site, resulting in an increased rate constant for the enzyme reaction [37]. As another example, electrostatic shielding of the active site catalytic triad increased the activity of a serine protease from *Achromobacter lyticus* [28, 38, 39]. Similarly, the surfaces of ChT are likely surrounded by additional charges derived from the polyelectrolytes, thereby facilitating substrate uptake into the substrate binding site of the enzyme.

The mechanism of activation by PAAc differs from that of PAA. Such an electrostatic binding mechanism is plausible for PAAc because anionic PAAc can bind to cationic ChT (Figure 3.1.6a). The binding of charged polymers to various enzymes was also reported to accelerate the catalytic hydrolysis of substrates [16−19,21,22]. By contrast, the activity of cationic ChT or anionic substrates was increased by cationic PAA (Figure 3.1.2b), although the formation of EPCs between ChT and PAA was not clearly established (Figure 3.1.6b). These results indicate that weak interactions between PAA and ChT might exist at pH 7.0 despite their similar cationic characteristics. Interestingly, the turnover number (k_{cat}) of ChT for anionic substrates was cat increased by the addition of cationic PAA but was not affected when anionic

PAAc was combined with cationic substrates (Table 3.1.1), which may explain the difference in hyperactivation induced by PAA and PAAc (Figure 3.1.2, 3.1.3). It is possible that PAA not only increases the affinity of the enzyme for the substrate but also lowers the activation energy of the substrate or stabilizes the intermediate state in the catalytic reaction of ChT.

3.1.5. Conclusion

In summary, I have developed a hyperactivation system for ChT based on charge-complementarity between polyelectrolytes and substrates. In this system, the enzyme activity of ChT was enhanced by approximately 1 order of magnitude simply by the addition of polyelectrolytes with charges opposite to those of the substrates. Because of their simplicity, hyperactivation systems could be designed for other enzymes by combining substrates and polyelectrolytes based on charge. As the hyperactivation system does not require laborious mutagenesis or chemical modification of enzymes, I believe this system could expand the potential uses of enzymes in biomedical and biotechnological applications.

3.1.6. References

[1] Miranda, O. R.; Chen, H. T.; You, C. C.; Mortenson, D. E.; Yang, X. C.; Bunz, U. H.; Rotello, V. M. Enzyme-Amplified Array Sensing of Proteins in Solution and in Biofluids. *J. Am. Chem. Soc.* **2010**, *132*, 5285-5289.

[2] Miranda, O. R.; Li, X.; Garcia-Gonzalez, L.; Zhu, Z. J.; Yan, B.; Bunz, U. H.; Rotello, V. M. Colorimetric Bacteria Sensing Using a Supramolecular Enzyme-Nanoparticle Biosensor. *J. Am. Chem. Soc.* **2011**, *133*, 9650-9653.

[3] Tomita, S.; Yoshimoto, K. Polyion Complex Libraries Possessing Naturally Occurring Differentiation for Pattern-Based Protein Discrimination. *Chem. Commun.* **2013**, *49*, 10430-10432.

[4] Wenck, K.; Koch, S.; Renner, C.; Sun, W.; Schrader, T. A Noncovalent Switch for Lysozyme. *J. Am. Chem. Soc.* **2007**, *129*, 16015-16019.

[5] Klaikherd, A.; Sandanaraj, B. S.; Vutukuri, D. R.; Thayumanavan, S. Comparison of Facially Amphiphilic Biaryl Dendrimers with Classical Amphiphilic Ones Using Protein Surface Recognition as the Tool. *J. Am. Chem. Soc.* **2006**, *128*, 9231-9237.

[6] Talbiersky, P.; Bastkowski, F.; Klarner, F. G.; Schrader, T. Molecular Clip and Tweezer Introduce New Mechanisms of Enzyme Inhibition. *J. Am. Chem. Soc.* **2008**, *130*, 9824-9828.

[7] Fischer, N. O.; McIntosh, C. M.; Simard, J. M.; Rotello, V. M. Inhibition of Chymotrypsin through Surface Binding Using Nanoparticle-Based Receptors. *Proc. Natl. Acad. Sci. U. S. A.* **2002**, *99*, 5018-5023.

[8] Fischer, N. O.; Verma, A.; Goodman, C. M.; Simard, J. M.; Rotello, V. M. Reversible "Irreversible" Inhibition of Chymotrypsin Using Nanoparticle Receptors. *J. Am. Chem. Soc.* **2003**, *125*, 13387-13391.

[9] Verma, A.; Simard, J. M.; Rotello, V. M. Effect of Ionic Strength on the Binding of α-Chymotrypsin to Nanoparticle Receptors. *Langmuir* **2004**, *20*, 4178-4181.

[10] Hong, R.; Fischer, N. O.; Verma, A.; Goodman, C. M.; Emrick, T.; Rotello, V. M. Control of Protein Structure and Function through Surface Recognition by Tailored Nanoparticle Scaffolds. *J. Am. Chem. Soc.* **2004**, *126*, 739-743.

[11] De, M.; Chou, S. S.; Dravid, V. P. Graphene Oxide as an Enzyme Inhibitor: Modulation of Activity of α-Chymotrypsin. *J. Am. Chem. Soc.* **2011**, *133*, 17524-17527.

[12] Ganguli, S.; Yoshimoto, K.; Tomita, S.; Sakuma, H.; Matsuoka, T.; Shiraki, K.; Nagasaki, Y. Regulation of Lysozyme Activity Based on Thermotolerant Protein/Smart Polymer Complex Formation. *J. Am. Chem. Soc.* **2009**, *131*, 6549-6553.

[13] Tomita, S.; Ito, L.; Yamaguchi, H.; Konishi, G.; Nagasaki, Y.; Shiraki, K. Enzyme Switch by Complementary Polymer Pair System (CPPS). *Soft Matter* **2010**, *6*, 5320-5326.

[14] Tomita, S.; Shiraki, K., Poly(acrylic acid) is a Common Noncompetitive Inhibitor for Cationic

Enzymes with High Affinity and Reversibility. *J. Polym. Sci. Part A: Polym. Chem.* **2011**, *49*, 3835-3841.

[15] Kurinomaru, T.; Tomita, S.; Kudo, S.; Ganguli, S.; Nagasaki, Y.; Shiraki, K. Improved Complementary Polymer Pair System: Switching for Enzyme Activity by PEGylated Polymers. *Langmuir* **2012**, *28*, 4334-4338.

[16] Harada, A.; Kataoka, K. Pronounced Activity of Enzymes through the Incorporation into the Core of Polyion Complex Micelles Made from Charged Block Copolymers. *J. Control. Release* **2001**, *72*, 85-91.

[17] Harada, A.; Kataoka, K. Switching by Pulse Electric Field of the Elevated Enzymatic Reaction in the Core of Polyion Complex Micelles. *J. Am. Chem. Soc.* **2003**, *125*, 15306-15307.

[18] Kawamura, A.; Yoshioka, Y.; Harada, A.; Kono, K. Acceleration of Enzymatic Reaction of Trypsin through the Formation of Water-Soluble Complexes with Poly(ethylene glycol)-*block*-poly(α,β-aspartic acid). *Biomacromolecules* **2005**, *6*, 627-631.

[19] Sandanaraj, B. S.; Vutukuri, D. R.; Simard, J. M.; Klaikherd, A.; Hong, R.; Rotello, V. M.; Thayumanavan, S. Noncovalent Modification of Chymotrypsin Surface Using an Amphiphilic Polymer Scaffold: Implications in Modulating Protein Function. *J. Am. Chem. Soc.* **2005**, *127*, 10693-10698.

[20] Roy, R.; Sandanaraj, B. S.; Klaikherd, A.; Thayumanavan, S. Tuning Substrate Selectivity of a Cationic Enzyme Using Cationic Polymers. *Langmuir* **2006**, *22*, 7695-7700.

[21] Harada, A.; Yoshioka, Y.; Kawamura, A.; Kojima, C.; Kono, K. Effect of Polycarboxylate Blocks on the Amidase Activity of Trypsin through Complexation with PEG/Polycarboxylate Block Ionomers. *Macromol. Biosci.* **2007**, *7*, 339-343.

[22] Kawamura, A.; Harada, A.; Kono, K.; Kataoka, K. Self-Assembled Nano-Bioreactor from Block Ionomers with Elevated and Stabilized Enzymatic Function. *Bioconjug. Chem.* **2007**, *18*, 1555-1559.

[23] Welsch, N.; Wittemann, A.; Ballauff, M. Enhanced Activity of Enzymes Immobilized in Thermoresponsive Core-Shell Microgels. *J. Phys. Chem. B* **2009**, *113*, 16039-16045.

[24] Hong, R.; Emrick, T.; Rotello, V. M. Monolayer-Controlled Substrate Selectivity Using Noncovalent Enzyme-Nanoparticle Conjugates. *J. Am. Chem. Soc.* **2004**, *126*, 13572-13573.

[25] You, C. C.; Agasti, S. S.; De, M.; Knapp, M. J.; Rotello, V. M. Modulation of the Catalytic Behavior of α-Chymotrypsin at Monolayer-Protected Nanoparticle Surfaces. *J. Am. Chem. Soc.* **2006**, *128*, 14612-14618.

[26] Jin, L.; Yang, K.; Yao, K.; Zhang, S.; Tao, H.; Lee, S. T.; Liu, Z.; Peng, R. Functionalized Graphene Oxide in Enzyme Engineering: A Selective Modulator for Enzyme Activity and Thermostability. *ACS Nano* **2012**, *6*, 4864-4875.

[27] Pace, C. N.; Vajdos, F.; Fee, L.; Grimsley, G.; Gray, T. How to Measure and Predict the Molar Absorption Coefficient of a Protein. *Protein Sci.* **1995**, *4*, 2411-2423.

[28] Shiraki, K.; Norioka, S.; Li, S.; Sakiyama, F. Contribution of an Imidazole-Indole Stack to High Catalytic Potency of a Lysine-Specific Serine Protease, *Achromobacter* Protease I. *J. Biochem.* **2002**, *131*, 213-218.

[29] Viparelli, P.; Alfani, F.; Gallifuoco, A.; Cantarella, M. Effect of Quaternary Ammonium Salts on the Hydrolysis of *N*-Glutaryl-L-Phenylalanine Catalysed by α-Chymotrypsin. *J. Mol. Catal. B: Enzym.* **2004**, *28*, 101-110.

[30] Spreti, N.; Mancini, V. M.; Germani, R.; Profio, D. P.; Savelli, G. Substrate Effect on α-Chymotrypsin Activity in Aqueous Solutions of Big-Head Ammonium Salts. *J. Mol. Catal. B: Enzym.* **2008**, *50*, 1-6.

[31] Spreti, N.; Alfani, F.; Cantarella, M.; D'Amico, F.; Germani, R.; Savelli, G. α-Chymotrypsin Superactivity in Aqueous Solutions of Cationic Surfactants. *J. Mol. Catal. B: Enzym.* **1999**, *6*, 99-110.

[32] Viparelli, P.; Alfani, F.; Cantarella, M. Models for Enzyme Superactivity in Aqueous Solutions of Surfactants. *Biochem. J.* **1999**, *344*, 765-773.

[33] Spreti, N.; Di, Profio P.; Marte, L.; Bufali, S.; Brinchi, L.; Savelli, G. Activation and Stabilization of α-Chymotrypsin by Cationic Additives. *Eur. J. Biochem.* **2001**, *268*, 6491-6497.

[34] Viparelli, P.; Alfani, F.; Cantarella, M. Effect of Cationic and Non-Ionic Surfactants on the Hydrolysis

of *N*-Glutaryl-L-Phenylalanine Catalysed by Chymotrypsin Iso-Enzymes. *J. Mol. Catal. B: Enzym.* **2003**, *21*, 175-187.

[35] Celej, M. S.; D'Andrea, M. G.; Campana, P. T.; Fidelio, G. D.; Bianconi, M. L. Superactivity and Conformational Changes on α-Chymotrypsin upon Interfacial Binding to Cationic Micelles. *Biochem. J.* **2004**, *378*, 1059-1066.

[36] Gladilin, A. K.; Kudryashova, E. V.; Vakurov, A. V.; Izumrudov, V. A.; Mozhaev, V. V.; Levashov, A. V. Enzyme-Polyelectrolyte Noncovalent Complexes as Catalysts for Reactions in Binary Mixtures of Polar Organic Solvents with Water. *Biotechnol. Lett.* **1995**, *17*, 1329-1334..

[37] Getzoff, E. D.; Cabelli, D. E.; Fisher, C. L.; Parge, H. E.; Viezzoli, M. S.; Banci, L.; Hallewell, R. A. Faster Superoxide Dismutase Mutants Designed by Enhancing Electrostatic Guidance. *Nature* **1992**, *358*, 347-351.

[38] Shiraki, K.; Sakiyama, F. Histidine 210 Mutant of a Trypsin-Type *Achromobacter* Protease I Shows Broad Optimum pH Range. *J. Biosci. Bioeng.* **2002**, *93*, 331-333.

[39] Shiraki, K.; Norioka, S.; Li, S.; Yokota, K.; Sakiyama, F. Electrostatic Role of Aromatic Ring Stacking in the pH-Sensitive Modulation of a Chymotrypsin-Type Serine Protease, *Achromobacter* Protease I. *Eur. J. Biochem.* **2002**, *269*, 4152-4158.

3.2. Effects of Multivalency and Hydrophobicity of Polyamines on Enzyme Hyperactivation of α-Chymotrypsin

3.2.1. Introduction

Enzymes have attracted a great deal of interest in biomedical and bioengineering fields because of their catalytic activity under aqueous conditions. The utility of enzymes would increase dramatically if we are able to enhance their activity at will. This would require the development of methods to enable us to increase an enzyme activity above that of the native enzyme, i.e., enzyme hyperactivation (or superactivation) [1]. There have been many investigations regarding enzyme hyperactivation using surfactant micelles [1–3] or ionic liquids [4]. Other methods have also been examined, such as mutagenesis [5–7], chemical modification [8, 9], immobilization of nanomaterials [10–14], and polyion complex micelles [15–19]. However, enzyme hyperactivation remains challenging due to the lack of systematic rules.

Recently, I reported that charged polyelectrolytes markedly enhanced the enzyme activity of α-chymotrypsin (ChT) [20]. Enzyme hyperactivation using polyelectrolytes is based on a simple rule, i.e., the coexistence of a charged substrate and oppositely charged polyelectrolytes is necessary to enhance the enzyme activity of ChT. For example, the enzyme activity of ChT for cationic substrate increased in the presence of anionic poly(acrylic acid) (PAAc), whereas that for an anionic substrate increased in the presence of cationic poly(allylamine) (PAA). In addition to polyelectrolytes, charged modulators, such as quaternary ammonium salts [21, 22], surfactant micelles [23–27], polymeric micelles [11, 12], and gold nanoparticles [10, 13], have been shown to enhance ChT activity toward oppositely charged substrates. These studies suggested that the charge combination between substrate and modulator plays an important role in enzyme hyperactivation.

Polyamines, such as putrescine (Put), spermidine (Spd), and spermine (Spm), are low molecular weight linear cationic compounds that are ubiquitous to all living organisms. The functions of polyamines are varied *in vivo*, including the regulation of cell proliferation and differentiation [28, 29]. In addition, polyamines have a favorable property with protein as a solution additive *in vitro*, such as stabilization of protein against thermal aggregation and inactivation [30, 31] and solubilization of membrane proteins [32] due to their polycationic structures. In this study, I demonstrated that amine compounds, including polyamines, enhanced the enzyme activity of ChT toward anionic substrates. The enzyme activity of ChT toward anionic substrate increased 1.6 - 6.9-fold in the presence of 50 mM amine compounds at pH 7.5. The effects of amine compounds for ChT activity were depending on both the number of amines and the hydrophobicity of amine compounds. Enzyme kinetics revealed that the turnover number (k_{cat}) and specific constant (k_{cat}/K_M) of ChT for anionic substrate were increased by amine compounds, whereas the Michaelis constant (K_M) was not significantly altered. In addition, molecular dynamics (MD) simulation revealed that the amine compounds interacted weakly with ChT. It was suggested that the weak interaction between amine compounds and ChT plays an important role in enzyme hyperactivation.

3.2.2. Materials and Methods

Materials

Cadaverine dihydrochloride (Cad), α-chymotrypsin (ChT) from bovine pancreas, 3-(*N*-morpholino)propanesulfonic acid (MOPS), putrescine dihydrochloride (Put), and *N*-succinyl-L-phenylalanine-*p*-nitroanilide (SPNA) were from Sigma Chemical Co. (St. Louis, MO). Dimethyl sulfoxide (DMSO), ethylenediamine (EDA), ethylamine (EA), 1,6-hexanediamine (HDA), hydrochloric acid (HCl), 1,8-octanediamine (ODA), 1,3-propanediamine (PDA), and propylamine (PA) were from Wako Pure Chemical Ind., Ltd. (Osaka, Japan). Diethylenetriamine (DETA), and triethylenetetramine (TETA) were from Tokyo Chemical Industry Co., Ltd. (Tokyo, Japan). Sodium chloride (NaCl) was from

Nacalai Tesque (Kyoto, Japan). Spermidine trihydrochloride (Spd) and spermine tetrahydrochloride (Spm) were from MP Biomedicals (Irvine, CA). Ethanol was from Kanto Chemical Co., Inc. (Tokyo, Japan). All chemicals used were of high-quality analytical grade and used as received.

Protein Concentrations

The protein concentration of ChT was determined from the absorbance at 280 nm using a spectrophotometer (ND-1000; NanoDrop Technologies, Inc., Wilmington, DE) with an extinction coefficient of 50585 $M^{-1}cm^{-1}$ [33].

Enzyme Assay

A 30-μL aliquot of substrate solution containing 0 - 20 mM SPNA, 90% ethanol, and 10% DMSO was mixed with 260 μL of additive in 50 mM MOPS (pH 7.5) and 10 μL of 150 μM ChT in 1.0 mM HCl. The initial reaction velocities (v_0) were determined from the slope of the initial increase in the absorbance at 410 nm using a spectrophotometer (V-630; Japan Spectroscopic Co., Ltd., Tokyo, Japan). The absorbance was converted into concentration using a molar extinction coefficient for *p*-nitroanilide of 8800 M^{-1} cm^{-1}. Normalized enzyme activity was defined as the ratio of v_0 in the presence of additive to v_0 in the absence of additive.

Molecular Dynamics Simulation for Additives Surrounding ChT

The microscopic states of the amine compounds surrounding the ChT molecule were studied in a water box using molecular dynamics (MD) simulations. Three 20-ns simulations were performed for each system. The calculations were performed three times for the ChT/amine compound system with and without SPNA. The system contained one ChT molecule, 25 amine compound molecules, 0 (System 1) or 10 (System 2) SPNA molecules, 19 (monocationic additive), 44 (bicationic additive), 69 (triple cationic additive), 94 (tetracationic additive) chloride ions, and about 12500 water molecules. ChT, amine compound, and SPNA molecules

were located randomly in the water box. The concentrations of amine compounds and SPNA in MD simulations were approximately 2-fold (100 mM amine compounds) and 20-fold (40 mM SPNA) higher than those in experiments, respectively. The ChT molecules were described using the AMBER ff99SB [34] force field (GAFF). The water molecules were described using the TIP3P model [35]. The amine compounds and SPNA molecules were described using the general AMBER force field (GAFF)[36]. A restrained electrostatic potential (RESP) charge was used for the amine compounds and SPNA [37]. The simulations were conducted with the NPT ensemble (298 K, 1 bar) in a rhombic dodecahedron box with an initial length of 84 Å. The temperature was controlled using a Langevin thermostat with a viscosity of 0.5 ps^{-1}. The pressure was controlled by a Parrinello-Rahman barostat [38] with a relaxation time of 2.0 ps. The electrostatics were treated using the particle mesh Ewald (PME) method [39] with a 10 Å cutoff distance. The van der Waals interactions were expressed using the twin-range cutoff method with cutoff distances of 10 and 12 Å. The covalent bonds for the hydrogen atoms in ChT, amine compounds, and SPNA were constrained using the linear constraint solver (LINCS) [40]. The covalent bonds in the water were constrained using the SETTLE algorithm. The integration time step was 2 fs. The simulations were conducted using the GROMACS 4.5.5 simulator [41].

3.2.3. Results

Activation of ChT for Anionic Substrates by Additives

Previously, I reported that activation of α-chymotrypsin (ChT) for anionic substrate were achieved in the presence of cationic polyelectrolytes with high molecular weight (5.0 kDa) [20]. To confirm the versatility of the phenomenon, various types of monoamines, diamines, triamines, and tetramines were used (Figure 3.2.1). First, the activation of ChT activity was investigated using naturally occurring amine compounds, so-called polyamine, putrescine (Put), spermidine (Spd), and spermine (Spm). The enzyme activity of ChT was investigated in the presence of amine compounds at pH 7.5 toward the hydrolysis of anionic substrate of

SPNA. Figure 3.2.2 shows the enzyme activity of ChT when 5.0 μM enzymes was mixed with various concentration of polyamines. The ChT activity increased with increasing concentrations of polyamines; the addition of 50 mM Put, Spd, and Spm resulted in enhancement of ChT activities by 2.1-fold, 4.6-fold, and 5.6-fold, respectively. Note that the polyamines alone did not catalyze hydrolysis of the substrate, SPNA. The effects of polyamines increased in the order Put < Spd < Spm, corresponding to the number of amine groups (Put, 2; Spd, 3; Spm, 4). These results indicated that the cationic natural polyamines could enhance the enzyme activity of ChT for anionic substrates as well as cationic polyelectrolytes.

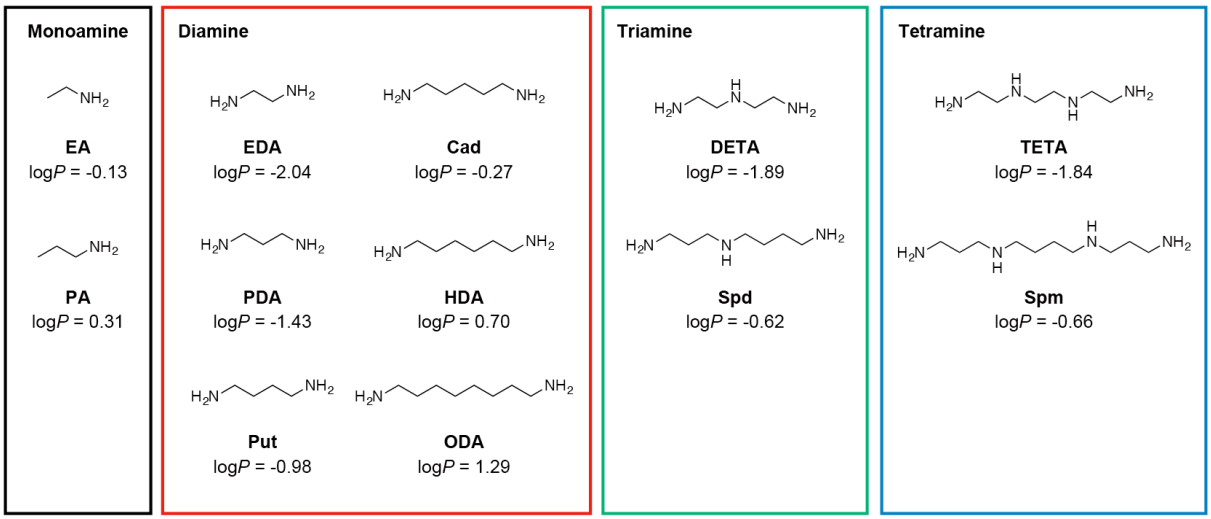

Figure 3.2.1. Chemical structures of amine compounds.

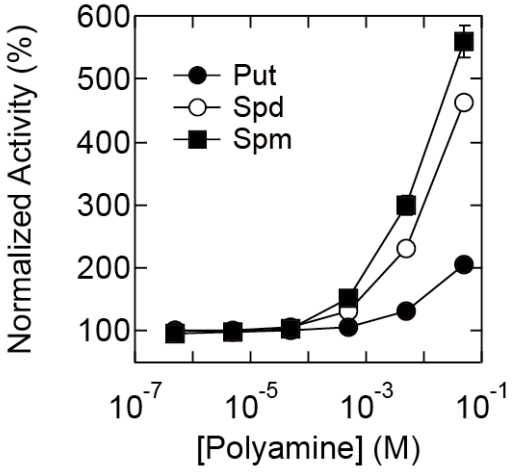

Figure 3.2.2. Normalized activities of ChT for anionic substrates in the presence of polyamines. Various concentrations of polyamine were added to solutions containing 5.0 μM ChT and 2.0 mM SPNA. Put, filled circles; Spd, open circles; Spm, filled squares.

Subsequently, similar experiments were performed using several types of amine compounds with different numbers of amine groups and alkyl chains, as shown in Figure 3.2.1. Figure 3.2.3A shows the systematic analysis of the enzyme activity of ChT in the presence of 50 mM amine compounds. The effects of diamines increased in the order EDA < PDA < Put < Cad < HDA < ODA, corresponding to the number of alkyl chains (EDA, 2; PDA, 3; Put, 4; Cad, 5; HAD, 6; ODA, 8); similar tendencies were observed with monoamines (EA < PA), triamines (DETA < Spd), and tetramines (TETA < Spm). To evaluate the relation between the activation effects of ChT and hydrophobic nature of amine compounds, the values of normalized activity were compared with *n*-octanol/water partition coefficients (log*P*) of amine compounds obtained using the program ALOPGs [42] (Figure 3.2.3B). It is clear that enhancement of ChT activity was dependent on not only the number of anime groups but also the hydrophobicity of additives.

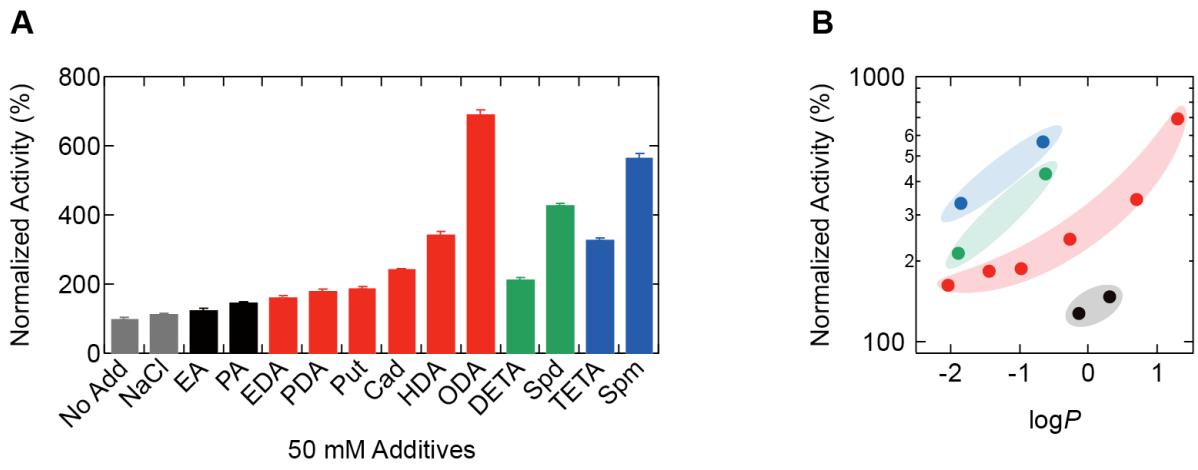

Figure 3.2.3. (A) Normalized activities of ChT upon addition of 50 mM amine compounds. **(B)** Correlation between the log*P* of amine compounds and normalized activity of ChT. Black, monoamines; red, diamines; green, triamines; blue, tetramines.

Kinetic Analysis of ChT in the Presence of Additives

To understand the molecular mechanism of enzyme activation by the amine additives, kinetic parameters were obtained and compared with the number of amine groups and the hydrophobicity of amine compounds. Figure 3.2.4 shows plots of the hydrophobicity parameter of log*P* versus parameters obtained from Michaelis-Menten kinetics in the presence of amine compounds, EDA, Put, HDA, ODA, Spd, and Spm. The values of the catalytic constant (k_{cat}) and specific constant (k_{cat}/K_M) of ChT with amine compounds were higher than those of ChT alone. These profiles were dependent on the types of amine compounds, similar to the plot of log*P* versus normalized activity (Figure 3.2.3B). In contrast, the value of the Michaelis constant (K_M) of ChT did not change significantly with amine compounds. These results indicated that the addition of amine compounds enhanced the turnover number of ChT for SPNA rather than the affinity.

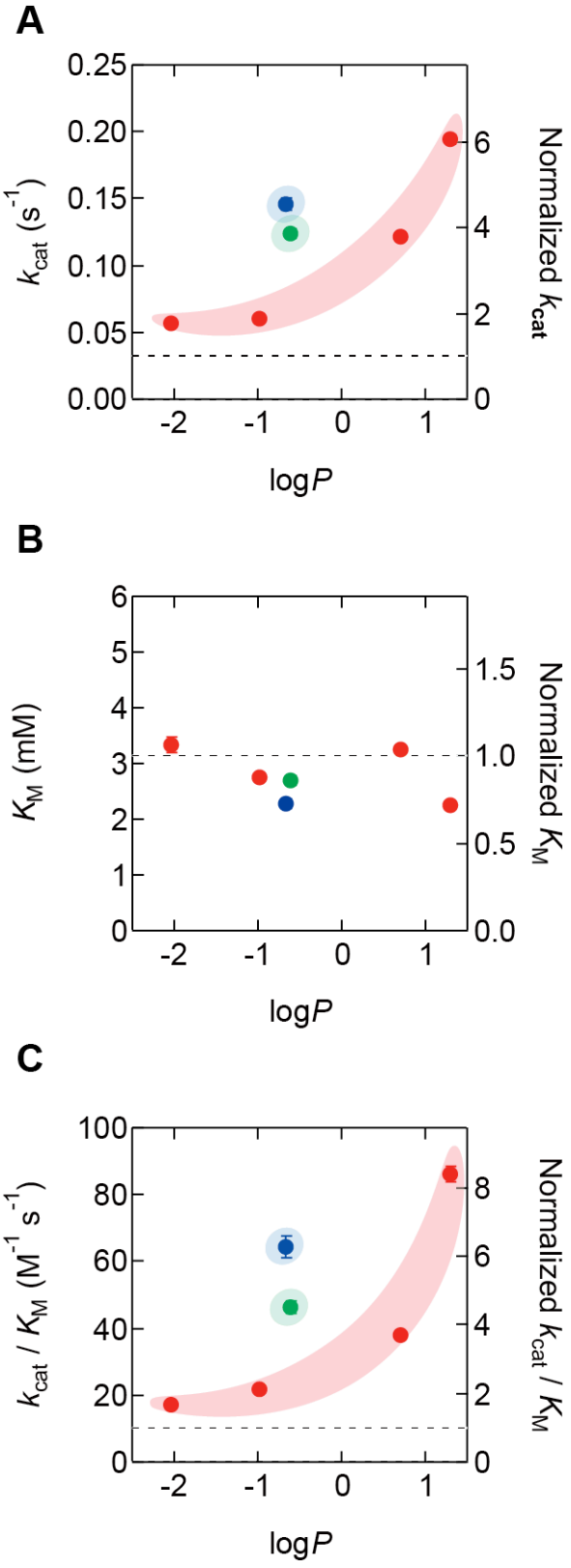

Figure 3.2.4. Correlation between the log$P$ of polyamines and kinetic parameters. **(A)** k_{cat}, **(B)** K_M, **(C)** k_{cat}/K_M. Broken lines show the value of ChT without additive. Red, diamines; green, triamines; blue, tetramines.

Molecular Dynamic Simulation of Interaction between Amine Compounds and ChT

To elucidate the behavior of amine compounds in enzyme activation, molecular dynamic (MD) simulations of the ChT-amine system were conducted (system 1). MD simulation of one ChT molecule with 25 amine molecules in water was performed in a rhombic dodecahedron box with an NPT ensemble (P = 1 bar). Note that the concentration of amine molecules in MD simulation was 2-fold (100 mM) higher than those under experimental conditions. This was because the high concentration of amine molecules increases the probability of binding rates at calculation times under 20 ns. Figure 3.2.5 shows representative snapshots of the simulation using ODA. The ODA molecules, which were initially located randomly, bound onto the surface of ChT after 20 ns, and the average number of ODA molecules was 4.7 (Table 3.2.1). A similar tendency was observed with the addition of other amine molecules from 3.7 to 6.7 molecules (Table 3.2.1). Furthermore, additional MD simulations of the ChT-amine-SPNA system (system 2) were also conducted to mimic the conditions in experimental studies. MD simulation of one ChT molecule, 25 amine molecules, and 10 SPNA molecules in water was calculated in a rhombic dodecahedron box with an NPT ensemble (P = 1 bar). Note that the concentration of SPNA in the MD simulation was 20-fold (40 mM) higher than that under experimental conditions. Similar to the results obtained in system 1, the binding of amine molecules on the ChT surface was observed. Interestingly, the average number of amine molecules in system 2 tended to be greater than that in system 1 (Table 3.2.1). Thus, these results suggested that amine molecules weakly interact with ChT at neutral pH despite their similar cationic characteristics, which may increase the catalytic activity of ChT.

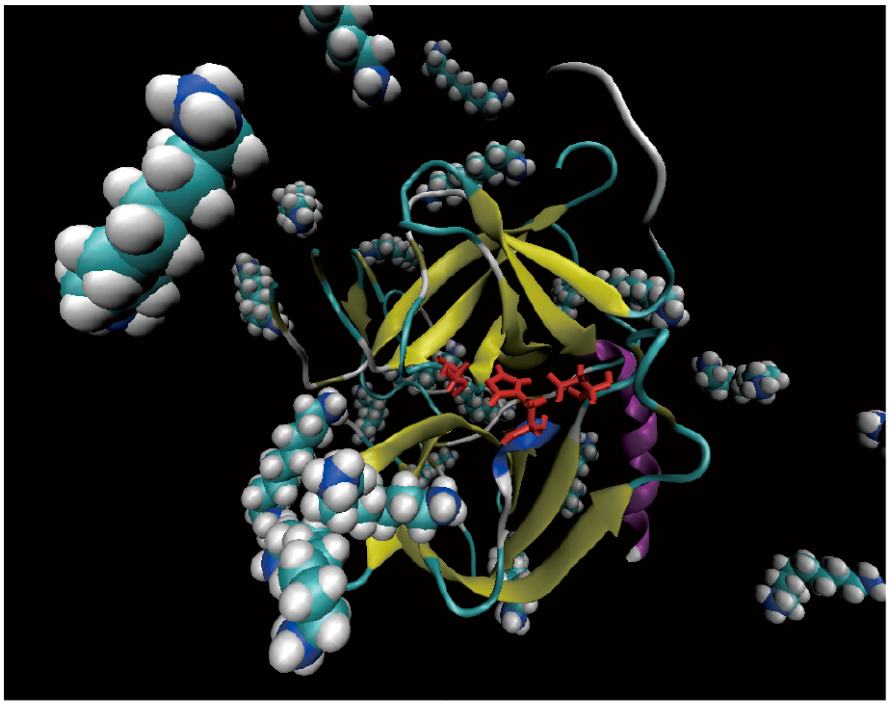

Figure 3.2.5. Snapshot of ChT and ODA molecules calculated by MD simulation. Spheres and cartoon represent ODA and ChT, respectively. The catalytic triad (His57, Asp102, and Ser195) is shown as red sticks.

3.2.4. Discussion

Several authors reported that enzyme hyperactivation of ChT was induced by a complementary charged modulator and substrate pair, i.e., anionic modulator activated ChT during hydrolysis of cationic substrates, and vice versa [10–13, 20–26]. Based on these reports, this study first demonstrated that naturally occurring polyamines and their analogs enhanced the enzyme activity of ChT toward anionic substrates (Figures 3.2.2, 3.2.3A). It is important that the enzyme hyperactivation of ChT can be occurred desirable modulators if they coexist oppositely charged substrates. This unique behavior suggests the importance of the complementary charged substrate and modulator pair, and provides novel guidelines for hyperactivation of other types of enzymes.

Figure 3.2.5. The average number of amine molecules within 4 Å of residues of ChT surfaces from MD simulation data.

	Number of amine molecules	
	System 1	System 2
Amines	ChT/Amines	ChT/Amines/SPNA
EA	3.67 ± 0.72	5.67 ± 0.72
PA	4.67 ± 0.72	5.33 ± 1.19
EDA	5.00 ± 0.82	6.00 ± 0.82
PDA	4.67 ± 0.54	6.00 ± 0.00
Put	6.00 ± 0.82	6.33 ± 0.27
Cad	6.67 ± 0.27	6.33 ± 0.72
HDA	5.33 ± 0.27	5.33 ± 0.72
ODA	4.67 ± 0.72	6.67 ± 1.09
DETA	6.67 ± 0.72	8.00 ± 0.94
Spd	6.33 ± 0.27	8.00 ± 1.41
TETA	6.67 ± 0.54	8.00 ± 0.00
Spm	6.67 ± 1.10	6.67 ± 0.98

The enzyme hyperactivation of ChT by amine compounds was seen with high dosage of additives (several mM) (Figure 3.2.2), which were much higher than those of cationic polyeletctrolytes, such as several μM of poly(allylamine) [20]. This difference was attributed to the multivalency and hydrophobicity of modulators. Enzyme hyperactivation of ChT by amine compounds was dependent on both the number of amine units and hydrophobicity of amine compounds (Figure 3.2.3B). Compared to the low molecular weight amine compounds, cationic poly(allylamine) has many amine units and greater hydrophobicity (log*P* of allylamine is 1.28). Thus, both multivalency and hydrophobicity of modulators are important parameters

for enzyme hyperactivation of ChT. The generality of the simple correlation suggests the applicability to the other enzymes, as well as serine protease, with enhancement of activity by design of the substrate-additive pair.

The interactions of amine compounds with proteins affect the structure and function of the proteins. For example, Hoyer et al. reported that amine compounds induced fibril aggregation of α-synuclein due to the formation of α-synuclein/amine compound complexes [43, 44]. Our results suggested the weak binding of amine compound onto the surface of ChT in MD simulation (Figure 3.2.5, Table 3.2.1). Thus, it was suggested that the weak intermolecular interaction between amine compounds and ChT contributed to the hyperactivation of ChT. Interestingly, a kinetic study indicated that amine compounds increased the catalytic constant (k_{cat}) and specific constant (k_{cat}/K_M) depending on multivalency and hydrophobicity of amine compounds (Figure 3.2.4). It is possible that amine compounds also stabilize the intermediate state in the catalytic reaction of ChT or decrease the activation energy of the substrate.

3.2.5. Conclusion

In summary, I demonstrated enzyme hyperactivation of ChT using polyamines and their analogs. The activation effects of amine compounds were dependent on the multivalency and hydrophobicity of the structures. This study provided extended design parameters for artificial modulators of enzyme hyperactivation. Furthermore, the present results also demonstrated the novel function of polyamines as enzyme activators *in vitro*, implying that the unclear function of polyamines in living cell system existed. Although the detailed mechanisms underlying the enzyme hyperactivation induced by the charged substrate/modulator pairs remain unclear, it is noteworthy that enzyme activity was affected by small compounds as well as polyelectrolytes. This paper suggests the possibility that enzyme activities in crude and complex conditions, typical of those *in vivo*, are quite different from those seen under simple *in vitro* experimental conditions. Finally, I emphasize that the enzyme hyperactivation by several modulators,

including polyamines, could expand the potential uses of enzymes in biomedical and biotechnological applications.

3.2.6. References

[1] Sintra, T. E.; Ventura, S. P.M.; Coutinho, J. A. P. Superactivity Induced by Micellar Systems as the Key for Boosting the Yield of Enzymatic Reactions *J. Mol. Catal. B: Enzym.* **2014**, *107*, 140-151.

[2] Iyer, P. V.; Ananthanarayan, L. Enzyme Stability and Stabilization-Aqueous and Non-Aqueous Environment *Process. Biochem.* **2008**, *43*, 1019–1032.

[3] Biasutti, M. A.; Abuin, E. B.; Silber, J. J.; Correa, N. M.; Lissi, E. A. Kinetics of Reactions Catalyzed by Enzymes in Solutions of Surfactants. *Adv. Colloid. Interface. Sci.* **2008**, *136*, 1-24.

[4] Naushad, M.; Alothman, Z.A.; Khan, A. B.; Ali, M. Effect of Ionic Liquid on Activity, Stability, and Structure of Enzymes: a Review. *Int. J. Biol. Macromol.* **2012**, *51*, 555-560.

[5] Getzoff, E. D.; Cabelli, D. E.; Fisher, C. L.; Parge, H. E.; Viezzoli, M. S.; Banci, L.; Hallewell, R. A. Faster Superoxide Dismutase Mutants Designed by Enhancing Electrostatic Guidance. *Nature* **1992**, *358*, 347-351.

[6] Imoto, T.; Ueda, T.; Tamura, T.; Isakari, Y.; Abe, Y.; Inoue, M.; Miki, T.; Kawano, K.; Yamada, H. Lysozyme Requires Fluctuation of the Active Site for the Manifestation of Activity. *Protein Eng.*, **1994**, *7*, 743-748.

[7] Shiraki, K.; Norioka, S.; Li, S.; Sakiyama, F. Contribution of an Imidazole-Indole Stack to High Catalytic Potency of a Lysine-Specific Serine Protease, *Achromobacter* Protease I. *J. Biochem.* **2002**, *131*, 213-218.

[8] Murata, H.; Cummings, C. S.; Koepsel, R. R.; Russell, A. J. Polymer-Based Protein Engineering can Rationally Tune Enzyme Activity, pH-Dependence, and Stability. *Biomacromolecules* **2013**, *14*, 1919-1926.

[9] Murata, H.; Cummings, C. S.; Koepsel, R. R.; Russell, A. J. Rational Tailoring of Substrate and Inhibitor Affinity via ATRP Polymer-Based Protein Engineering. *Biomacromolecules* **2014**, *15*, 2817-2823.

[10] Hong, R.; Emrick, T.; Rotello, V. M. Monolayer-Controlled Substrate Selectivity Using Noncovalent Enzyme-Nanoparticle Conjugates. *J. Am. Chem. Soc.* **2004**, *126*, 13572-13573.

[11] Sandanaraj, B. S.; Vutukuri, D. R.; Simard, J. M.; Klaikherd, A.; Hong, R.; Rotello, V. M.; Thayumanavan, S. Noncovalent Modification of Chymotrypsin Surface Using an Amphiphilic Polymer Scaffold: Implications in Modulating Protein Function. *J. Am. Chem. Soc.* **2005**, *127*, 10693-10698.

[12] Roy, R.; Sandanaraj, B. S.; Klaikherd, A.; Thayumanavan, S. Tuning Substrate Selectivity of a Cationic Enzyme Using Cationic Polymers. *Langmuir* **2006**, *22*, 7695-7700.

[13] You, C. C.; Agasti, S. S.; De, M.; Knapp, M. J.; Rotello, V. M. Modulation of the Catalytic Behavior of α-Chymotrypsin at Monolayer-Protected Nanoparticle Surfaces. *J. Am. Chem. Soc.* **2006**, *128*, 14612-14618.

[14] Jin, L.; Yang, K.; Yao, K.; Zhang, S.; Tao, H.; Lee, S. T.; Liu, Z.; Peng, R. Functionalized Graphene Oxide in Enzyme Engineering: A Selective Modulator for Enzyme Activity and Thermostability. *ACS Nano* **2012**, *6*, 4864-4875.

[15] Harada, A.; Kataoka, K. Pronounced Activity of Enzymes through the Incorporation into the Core of Polyion Complex Micelles Made from Charged Block Copolymers. *J. Control. Release* **2001**, *72*, 85-91.

[16] Harada, A.; Kataoka, K. Switching by Pulse Electric Field of the Elevated Enzymatic Reaction in the Core of Polyion Complex Micelles. *J. Am. Chem. Soc.* **2003**, *125*, 15306-15307.

[17] Kawamura, A.; Yoshioka, Y.; Harada, A.; Kono, K. Acceleration of Enzymatic Reaction of Trypsin through the Formation of Water-Soluble Complexes with Poly(ethylene glycol)-*block*-poly(α,β-aspartic acid). *Biomacromolecules* **2005**, *6*, 627-631.

[18] Harada, A.; Yoshioka, Y.; Kawamura, A.; Kojima, C.; Kono, K. Effect of Polycarboxylate Blocks on

the Amidase Activity of Trypsin through Complexation with PEG/Polycarboxylate Block Ionomers. *Macromol. Biosci.* **2007**, *7*, 339-343.

[19] Kawamura, A.; Harada, A.; Kono, K.; Kataoka, K. Self-Assembled Nano-Bioreactor from Block Ionomers with Elevated and Stabilized Enzymatic Function. *Bioconjug. Chem.* **2007**, *18*, 1555-1559.

[20] Kurinomaru, T.; Tomita, S.; Hagihara, Y.; Shiraki, K. Enzyme Hyperactivation System Based on a Complementary Charged Pair of Polyelectrolytes and Substrates. *Langmuir* **2014**, *30*, 3826-3831.

[21] Viparelli, P.; Alfani, F.; Gallifuoco, A.; Cantarella, M. Effect of Quaternary Ammonium Salts on the Hydrolysis of *N*-Glutaryl-L-Phenylalanine Catalysed by α-Chymotrypsin *J. Mol. Catal. B: Enzym.* **2004**, *28*, 101-110.

[22] Spreti, N.; Mancini, V. M.; Germani, R.; Profio, D. P.; Savelli, G. Substrate Effect on α-Chymotrypsin Activity in Aqueous Solutions of Big-Head Ammonium Salts *J. Mol. Catal. B: Enzym.* **2008**, *50*, 1-6.

[23] Spreti, N.; Alfani, F.; Cantarella, M.; D'Amico, F.; Germani, R.; Savelli, G. α-Chymotrypsin Superactivity in Aqueous Solutions of Cationic Surfactants *J. Mol. Catal. B: Enzym.* **1999**, *6*, 99-110.

[24] Viparelli, P.; Alfani, F.; Cantarella, M. Models for Enzyme Superactivity in Aqueous Solutions of Surfactants. *Biochem. J.* **1999**, *344*, 765-773.

[25] Spreti, N.; Di, Profio P.; Marte, L.; Bufali, S.; Brinchi, L.; Savelli, G. Activation and Stabilization of α-Chymotrypsin by Cationic Additives. *Eur. J. Biochem.* **2001**, *268*, 6491-6497.

[26] Viparelli, P.; Alfani, F.; Cantarella, M. Effect of Cationic and Non-Ionic Surfactants on the Hydrolysis of *N*-Glutaryl-L-Phenylalanine Catalysed by Chymotrypsin Iso-Enzymes. *J. Mol. Catal. B: Enzym.* **2003**, *21*, 175-187.

[27] Celej, M. S.; D'Andrea, M. G.; Campana, P. T.; Fidelio, G. D.; Bianconi, M. L. Superactivity and Conformational Changes on α-Chymotrypsin upon Interfacial Binding to Cationic Micelles. *Biochem. J.* **2004**, *378*, 1059-1066.

[28] Kala_c, P.; Krausova, P. A Review of Dietary Polyamines: Formation, Implications for Growth and Health and Occurrence in Foods. *Food Chem.* **2005**, *90*, 219–230.

[29] Kusano, T.; Yamaguchi, K.; Berberich, T.; Takahashi, Y. Advances in Polyamine Research in 2007. *J. Plant. Res.* **2007**, *120*, 345-350.

[30] Kudou, M.; Shiraki, K.; Fujiwara, S.; Imanaka, T.; Takagi, M. Prevention of Thermal Inactivation and Aggregation of Lysozyme by Polyamines. *Eur. J. Biochem.* **2003**, *270*, 4547-4554.

[31] Hamada, H.; Takahashi, R.; Noguchi, T.; Shiraki, K. Differences in the Effects of Solution Additives on Heat- and Refolding-induced Aggregation. *Biotechnol. Prog.* **2008**, *24*, 436-443.

[32] Yasui, K.; Uegaki, M.; Shiraki, K.; Ishimizu, T. Enhanced Solubilization of Membrane Proteins by Alkylamines and Polyamines. *Protein Sci.* **2010**, *19*, 486-493.

[33] Pace, C. N.; Vajdos, F.; Fee, L.; Grimsley, G.; Gray, T. How to Measure and Predict the Molar Absorption Coefficient of a Protein. *Protein Sci.* **1995**, *4*, 2411-2423.

[34] Hornak, V.; Abel, R.; Okur, A.; Strockbine, B.; Roitberg, A.; Simmerling, C. Comparison of Multiple Amber Force Fields and Development of Improved Protein Backbone Parameters. *Proteins* **2006**, *65*, 712-725.

[35] Jorgensen, W. L.; Chandrasekhar, J.; Madura, J. D.; Impey, R. W.; Klein, M. L. Comparison of Simple Potential Functions for Simulating Liquid Water. *J. Chem. Phys.* **1983**, *79*, 926─935.

[36] Wang, J.; Wolf, R. M.; Caldwell, J. W.; Kollman, P. A.; Case, D. A. Development and Testing of a General Amber Force Field. *J. Comput. Chem.* **2004**, *25*, 1157-1174.

[37] Bayly, C. I.; Cieplak, P.; Cornell, W. D.; Kollman, P. A. A Well- Behaved Electrostatic Potential Based Method Using Charge Restraints for Deriving. *J. Phys. Chem.* **1993**, *97*, 10269─10280.

[38] Parrinello, M Rahman A. Polymorphic Transitions in Single Crystals: A New Molecular Dynamics Method. *J. Appl. Phys.* **1981**, *52*, 7182–7190.

[39] Essmann, U.; Perera, L.; Berkowitz, M. L.; Darden, T.; Lee, H.; Pedersen, L. G. A Smooth Particle Mesh Ewald Method. *J. Chem. Phys.* **1995**, *103*, 8577─8593.

[40] Hess, B.; Bekker, H.; Berendsen, H. J. C.; Fraaije, J. G. E. M. LINCS: A Linear Constraint Solver for Molecular Simulations. *J. Comput. Chem.* **1997**, *18*, 1463─1472.

[41] Hess, B.; Kutzner, C.; van, der Spoel D.; Lindahl, E. GROMACS 4: Algorithms for Highly Efficient, Load-Balanced, and Scalable Molecular Simulation. *J. Chem. Theory. Comput.* **2008**, *4*, 435─447.

[42] Tetko, I. V.; Gasteiger, J.; Todeschini, R.; Mauri, A.; Livingstone, D.; Ertl, P.; Palyulin, V. A.; Radchenko, E. V.; Zefirov, N. S.; Makarenko, A. S.; Tanchuk, V. Y.; Prokopenko, V. V. Virtual Computational Chemistry Laboratory-Design and Description. *J. Comput. Aided. Mol. Des.* **2005**, *19*, 453-463.

[43] Antony, T.; Hoyer, W.; Cherny, D.; Heim, G.; Jovin, T. M.; Subramaniam, V. Cellular Polyamines Promote the Aggregation of α-synuclein. *J. Biol. Chem.* **2003**, *278*, 3235-3240.

[44] Fernandez, C. O.; Hoyer, W.; Zweckstetter, M.; Jares-Erijman, E. A.; Subramaniam, V.; Griesinger, C.; Jovin, T. M. NMR of α-Synuclein-Polyamine Complexes Elucidates the Mechanism and Kinetics of Induced Aggregation. *EMBO. J.* **2004**, *23*, 2039-2046.

Chapter 4. Precipitation-redissolution Method

4.1. Protein-Poly(amino acid) Complex Precipitation for High-concentration Protein Formulation

4.1.1. Introduction

Therapeutic proteins have increased dramatically in both number and frequency of use [1]. At present, more than 200 different biopharmaceutical agents are approved for clinical application by the US Food and Drug Administration, and many more are currently in the development [2]. In some cases, effective therapy using proteins requires preparation of a high-concentration protein solution. For example, the desired concentration of proteins is above 100 mg/mL with a volume limitation of 1.5 mL for subcutaneous injection of therapeutic antibodies [3,4]. The simplest method for producing high-concentration protein formulations is dissolution of lyophilized formulation in a low volume of physiological saline. However, the lyophilized formulation requires a long dissolution time, which places a limitation on its practical usage [5].

Methods for concentration of protein solutions play important roles in the preparation of high-concentration protein formulations. The industrial development of high-concentration protein formulations has been achieved by various conventional separation techniques such as ultrafiltration, drying, chromatography, and dialysis [3] Recently, novel laboratory scale concentration methods such as gelation,6 crystallization [7], nanoparticle formation [8], liquid-liquid phase separation [9], and combination with suspension and spray drying [10,11] have been reported for therapeutic proteins. Precipitation has great potential as an alternative concentration method for both ease and scalability. If the protein precipitate can be fully redissolved in some way, such precipitated protein represents a concentrated state of protein. Matheus et al. [12] reported the feasibility of high-concentration antibody formulation by the

precipitation-redissolution method using typical precipitants such as sodium citrate, ammonium sulfate, and poly(ethylene glycol) (PEG) 4000. However, high concentrations of the precipitants are required and therefore the precipitation-redissolution method remains limited to *in vitro* experiments.

Polyelectrolytes have also been used as precipitants in biological and biotechnological methods, including protein purification [13–18]. The polyelectrolyte interacts strongly with complementary charged protein through multiple electrostatic interactions, resulting in the formation of various types of protein-polyelectrolyte complexes (PPC) [19]. PPCs are prone to form precipitates depending on several factors such as stoichiometric ratio, pH, temperature, and ionic strength. Our group have recently shown that the formation of PPCs could be achieved to regulate enzyme activity and to stabilize protein structure [20–23]. To our knowledge, however, few studies concerning PPCs precipitation of therapeutic proteins have been reported because of the pharmaceutical demerit of protein precipitation such as irreversible aggregation or cytotoxicity.

In this study, a precipitation-redissolution method using poly(amino acid) as a precipitant was developed for several types of pharmaceutical proteins, including therapeutic enzymes, antibodies, and hormones. All proteins were fully precipitated by poly-L-lysine or poly-L-glutamic acid at low ionic strength, and the precipitates were then dissolved at physiological ionic strength of 150 mM sodium chloride (NaCl). The redissolved proteins retained the original activity and native secondary structure. The feasibility of the precipitation-redissolution method using poly(amino acid) for concentration of protein is discussed.

4.1.2. Materials and Methods

Materials

Proteins: L-Asparaginase was purchased from Kyowa Hakko Kirin Company Ltd. (Tokyo, Japan) and used without further purification. Adalimumab (Eisai Company, Ltd., Tokyo, Japan), infliximab (Mitsubishi-Tanabe Pharmaceutical Company, Ltd., Osaka, Japan), omalizumab (Novartis Pharma KK,

Tokyo, Japan), and rituximab (Zenyaku Kogyo Company, Ltd., Tokyo, Japan) were obtained via reagent distributors and purified on a Protein A column to remove the cosolutes. Etanercept (Takeda Pharmaceutical Company, Ltd., Osaka, Japan) and panitumumab (Takeda Pharmaceutical Company) were obtained via reagent distributors and purified on a dextran gel column to remove the salts. Human IgG was from Equitech-Bio, Inc. (Kernville, Texas) and dialyzed to remove the cosolutes. Carperitide was from Daiichi-Sankyo Company, Ltd. (Tokyo, Japan) and purified on a silica gel column to remove the cosolutes. Thyroglobulin was separated from molecular weight standards (151-1901; Bio-Rad Laboratories, Hercules, California) by size-exclusion chromatography.

Others: Ammonium sulfate, L-asparagine (L-Asn), citrate, Nessler's reagent, sodium chloride (NaCl), and trichloroacetic acid (TCA) were from Kanto Chemical Company, Inc. (Tokyo, Japan). Polysorbate 20 was from Wako Pure Chemical Ind., Ltd. (Osaka, Japan). 3-(*N*-morpholino)Propanesulfonic acid (MOPS) was from Nacalai Tesque, Inc. (Kyoto, Japan). Tris(hydroxymethyl)aminomethane (Tris) was from Bio-Rad Laboratories. Biotinylated anti-human IgG, poly-L-glutamic acid sodium salt with average molecular weight of 1.5-5.5 kDa (polyE1) and 3.0-15 kDa (polyE2), and poly-L-lysine hydrobromide with average molecular weight of 4.0-15 kDa (polyK1) and above 30 kDa (polyK2) were from Sigma Chemical Company (St. Louis, Missouri). Human IgE was from Abcam (Cambridge, Massachusetts). Human tumor necrosis factor α (TNF-α) was from Gibco Life Technologies Ltd. (Grand Island, New York). Streptavidin-labeled horseradish peroxidase was from Thermo Fisher Scientific (Waltham, Massachusetts). 3,3',5,5'-Tetramethylbenzidine (TMB) was from KPL (Gennep, the Netherlands). These chemicals were of high- quality analytical grade, and were used as received.

Precipitation-Redissolution Method

Aliquots of 200 μL of precipitant solution containing 0-1.0 mg/mL poly(amino acid) (polyK1, polyK2, polyE1, or polyE2) and 10 mM buffer [citrate (pH 5.0-5.4), MOPS (pH 6.5-7.0), or Tris (pH 8.0-8.7)] were mixed with 200 μL of proteins in the same buffer, and then the samples were centrifuged at 15,000g for 20

min at 25°C. Subsequently, 360 μL of supernatant was replaced with another buffer containing 10 mM buffer and 167 mM NaCl. The concentrations of proteins were determined form the absorbance at 280 nm using a spectrom- eter (SpectraMax Plus384; Molecular Devices Company, Ltd., Sunnyvale, California).

Enzyme Assay

The enzyme activity of L-asparaginase was measured as follows. An aliquot of 50 μL of L-asparaginase solution was incubated with 950 μL of the substrate solution containing 22 mM L-Asn at 37°C for 15 min. The reaction was stopped by the addition of 250 μL of 1.5 M TCA to the assay mixture. Subsequently, the sample was mixed with Nessler's reagent to measure the amount of ammonia released after L-Asn hydrolysis. The absorbance was monitored spectrophotometrically at 450 nm. The concentration of ammonia produced by the enzyme reaction was determined from a reference curve using ammonium sulfate as the standard. One unit of enzyme activity was defined as the amount of enzyme required to produce 1.0 μmol ammonia per minute at 37°C.

Immunoassay

The immnunoreactivities of four types of antibodies were measured as follows. The wells of polystyrene 96-well ELISA microplates (Sumitomo Bakelite Company, Ltd., Tokyo, Japan) were coated with antigens (human TNF-α for adalimumab, etanercept, and infliximab; human IgE for omalizumab), and the plates were incubated at 4°C overnight. The wells were washed five times by the addition of washing buffer containing 24.8 mM Tris, 136.9 mM NaCl, 2.7 mM potassium chloride, and 0.1% polysorbate 20 (pH 7.4). The wells were then blocked with Blocking One (Nacalai Tesque) at room temperature for 1 h. After washing of the wells, 100 μL of the antibody solutions with different concentrations was added to the wells and incubated at room temperature for 1 h. After washing of the wells, 100 μL of biotinylated anti-human IgG was added to each well and incubated at room temperature for 1 h. After washing of the wells, 100 μL of streptavidin-labeled horseradish peroxidase was added to each well and incubated at room temperature for

30 min. After washing of the well, 100 μL of TMB was added to each well and incubated in the dark at room temperature for more than 15 min. Finally, 100 μL of 0.1% HCl was added, and the absorbance at 450 nm was determined using a microplate reader (SpectraMax Plus384; Molecular Devices).

Circular Dichroism

Circular dichroism (CD) experiments were performed in a 1-mm path-length quartz cuvette using a spectropolarimeter (J- 720; Japan Spectroscopic Company, Ltd., Tokyo, Japan). The spectra of redissolved proteins were measured at 25^{o}C. The CD spectra of the samples were corrected by subtracting the corresponding spectra of the buffers in the absence of proteins.

4.1.3. Results

Precipitation-redissolution methods for proteins were performed using four types of poly(amino acids), that is, cationic poly-L-lysine with average molecular weight of 4.0-15 kDa (polyK1) and above 30 kDa (polyK2) or anionic poly-L-glutamic acid with average molecular weight of 1.5-5.5 kDa (polyE1) and 3.0-15 kDa (polyE2). The examination procedures are shown in Figure 4.1.1. First, poly(amino acid) was added to the protein solution in buffer without NaCl (Stage 1) and immediately suspended (Stage 2). Subsequently, the suspensions were precipitated by centrifugation (Stage 3), followed by removal of the supernatant (Stage 4). Finally, other buffers with NaCl were added to the precipitants, which were fully dissolved (Stage 5). The final concentration of NaCl (150 mM) corresponded to physiological ionic strength.

First, the precipitation-redissolution method was investigated for two proteins, L-asparaginase (*p*I = 4.7) that is used for acute lymphoblastic leukemia and adalimumab (*p*I = 8.7) that is used for rheumatoid arthritis. Anionic L-asparaginase with cationic polyK1 in 10 mM MOPS (pH 7.0) and cationic adalimumab with anionic polyE2 in 10 mM MOPS (pH 6.5) were chosen as models. The solutions of 0.5 mg/mL L-asparaginase with various concentrations of polyK1 were mixed. The protein solution with 0.025 mg/mL

(0.05 eq.) polyK1 showed a visible suspension, whereas that with above 0.3 mg/mL (>0.6 eq.) polyK1 became clear. After centrifugation, the supernatant (90% of the total volume) was removed, and the same volume of 10 mM MOPS (pH 7.0) with final concentration of 150 mM NaCl was added to the precipitate, which was completely dissolved. Figure 4.1.2a shows the concentration of L-asparaginase at Stage 5 (C_{Stage5}). The C_{Stage5} of L-asparaginase without polyK1 was 0.05 mg/mL, whereas that in the presence of 0.025 mg/mL (0.05 eq.) polyK1 was 0.5 mg/mL, indicating that almost all of the L-asparaginase was precipitated. When a high concentration of polyK1 was added to the protein solution, C_{Stage5} decreased by 0.07 mg/mL in the presence of 0.5 mg/mL (1.0 eq.) polyK1. The decrease in C_{Stage5} corresponded to the decrease in suspension at Stage 2. A similar tendency was observed in cationic adalimumab with anionic polyE2 (Figure 4.1.2b). The C_{Stage5} of adalimumab with 0.025 mg/mL (0.05 eq.) polyE2 increased to 0.51 mg/mL, whereas it decreased with further addition of polyE2. These results suggested that cationic polyK and anionic polyE significantly precipitated anionic and cationic proteins, respectively.

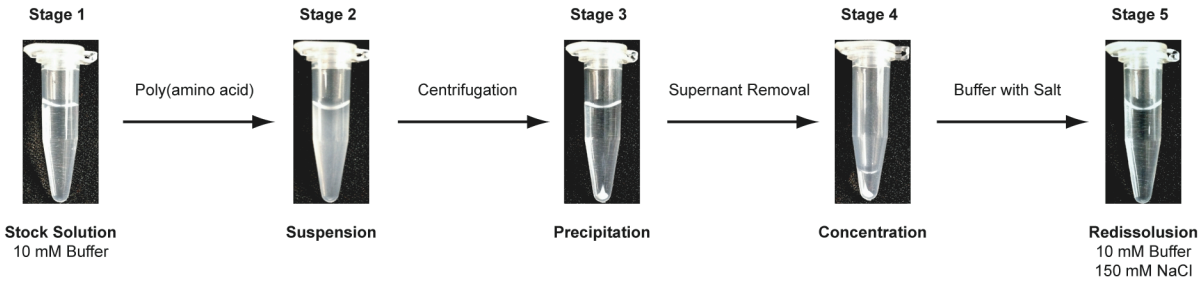

Figure 4.1.1. Outline of precipitation-redissolution method for L-asparaginase. Stock solution containing 1.0 mg/mL L-asparaginase in 10 mM MOPS (pH 7.0) (Stage 1). Aliquots of 200 μL of poly(amino acid) were added to 200 μL of stock solution at low ionic strength (Stage 2). After centrifugation (Stage 3), 360 μL of supernatant was removed (Stage 4) and then added to 360 μL of buffer containing NaCl (Stage 5).

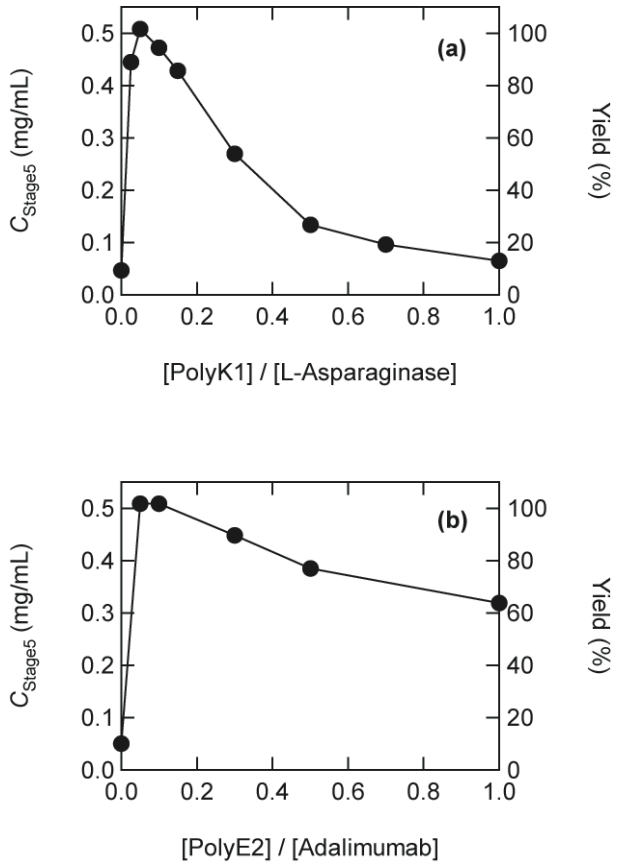

Figure 4.1.2. Concentrations at Stage 5 for two types of proteins by poly(amino acid). Various concentrations of polyK1 or polyE2 were added to solutions containing 0.5 mg/mL L-asparaginase **(a)** or adalimumab **(b)**, respectively, at Stage 2.

To confirm the generality of the precipitation-redissolution method, similar experiments were performed using eight pharmaceutical proteins, that is, panitumumab (*p*I = 6.9), etanercept (*p*I = 8.0), thyroglobulin (*p*I = 5.5), carperitide (*p*I = 10.5), infliximab (*p*I = 8.7), rituximab (*p*I = 8.7), omalizumab (*p*I = 7.6), and IgG (*p*I = 6.9). Table 4.1.1 lists the experimental conditions with precipitant poly(amino acid), pH, and stoichiometric ratio for each protein. Note that precipitation occurred only when poly(amino acid) had a charge complementary to that of the protein at experimental pH, that is, positively charged polyK precipitated negatively charged proteins, and vice versa. Thus, conditions were screened based on electrostatic pairing between protein and poly(amino acid) as a function of pH. As expected, anionic panitumumab and etanercept at pH 8.7 and thyroglobulin at pH 7.0 were precipitated with the addition of

cationic polyK; the highest yields of the anionic proteins were above 86%. Similarly, cationic carperitide at pH 7.0, infliximab and rituximab at pH 6.5, omalizumab at pH 5.5, and IgG at pH 5.0 were precipitated with the addition of anionic polyE; the highest yields of the cationic proteins were above 89%. Therefore, It was suggested that the precipitation-redissolution method was effective for various types of proteins.

Table 4.1.1. Experimental conditions with the highest yields of several types of protein.

Protein (p*I*)	Precipitant	Buffer (pH)	[Precipitant] / [Protein]	C_{Stage2} (mg/mL)	C_{Stage5} (mg/mL)	Yield (%)
Panitumumab (6.9)	polyK1	Tris (8.7)	0.100	0.50	0.49	98
Etanercept (8.0)	polyK2	Tris (8.7)	0.080	1.00	0.86	86
Thyroglobulin (5.5)	polyK1	Tris (8.0)	0.050	0.25	0.22	88
L-Asparaginase (4.7)	polyK1	MOPS (7.0)	0.050	0.50	0.51	102
Carperitide (10.5)	polyE1	MOPS (7.0)	0.300	0.50	0.47	94
Adalimumab (8.7)	polyE2	MOPS (6.5)	0.050	0.50	0.51	100
Infliximab (8.7)	polyE2	MOPS (6.5)	0.050	1.00	1.03	103
Rituximab (8.7)	polyE2	MOPS (6.5)	0.075	1.00	1.00	100
Omalizumab (7.6)	polyE2	Citrate (5.5)	0.050	1.00	0.95	95
IgG (7.3)	polyE2	Citrate (5.0)	0.150	1.00	0.89	89

Table 4.1.2. Enzyme activities or immunoreactivities of redissolved proteins.

Protein (p*I*)	Precipitant	Buffer (pH)	[Precipitant] / [Protein]	$Activity_{Control}$	$Activity_{Stage5}$	Relative Activity (%)
L-Asparaginase (4.7)	polyK1	MOPS (7.0)	0.05	2065 (U/mg) [a]	1943 (U/mg) [a]	94
Etanercept (8.0)	polyK2	Tris (8.7)	0.08	179 (pM) [b]	171 (pM) [b]	105
Adalimumab (8.7)	polyE2	MOPS (6.5)	0.05	279 (pM) [b]	271 (pM) [b]	103
Infliximab (8.7)	polyE2	MOPS (6.5)	0.05	354 (pM) [b]	368 (pM) [b]	96
Omalizumab (7.6)	polyE2	Citrate (5.5)	0.05	70 (pM) [b]	71 (pM) [b]	99

[a] One unit of enzyme activity is the amount of enzyme required to produce 1.0 μmol ammonia per 1 min at 37°C.

[b] The 50 % effective concentration (EC_{50}).

Subsequently, the protein activities at Stage 5 were measured to determine whether the redissolved proteins retained their original activities. The enzyme activity of L-asparaginase at Stage 5 was comparable to that without polyK1 (Table 4.1.2). Similarly, there was no significant change in antigen-binding activity; the 50% effective concentration values of the antibodies at Stage 5 were equivalent to those without poly(amino acid) (Figure 4.1.3, Table 4.1.2). These results indicated that the precipitation-redissolution process did not affect protein activities.

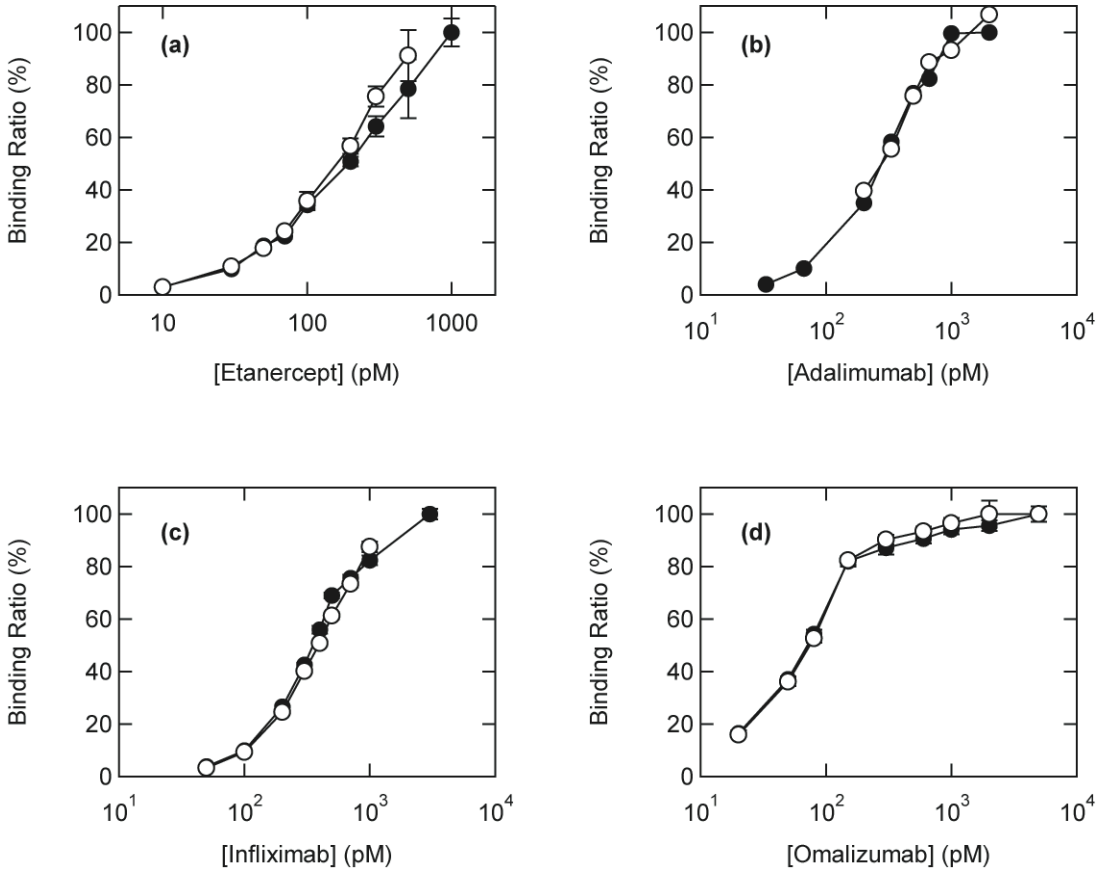

Figure 4.1.3. Immunoreactivities of etanercept **(a)**, adalimumab **(b)**, infliximab **(c)**, and omalizumab **(d)** at Stage 5. Proteins were mixed with poly(amino acid) (shown in Table 4.1.1). Native proteins, closed circles; redissolved proteins, open circles.

Figure 4.1.4 shows the far-UV CD spectra of proteins at Stage 5 to determine whether any conformational changes occurred in the proteins. The far-UV CD spectra of antibodies at Stage 5 were identical to those of native proteins, although slight changes were observed in the far-UV CD spectra of panitumumab and IgG at Stage 5. These results suggested that the secondary structures of redissolved antibodies were significantly maintained. In contrast, far-UV CD spectra of L-asparaginase and thyroglobulin at Stage 5 seemed to have subtle peak shifts, indicating that the effect of secondary structure by precipitation-redissolution method was dependent on the properties of the protein.

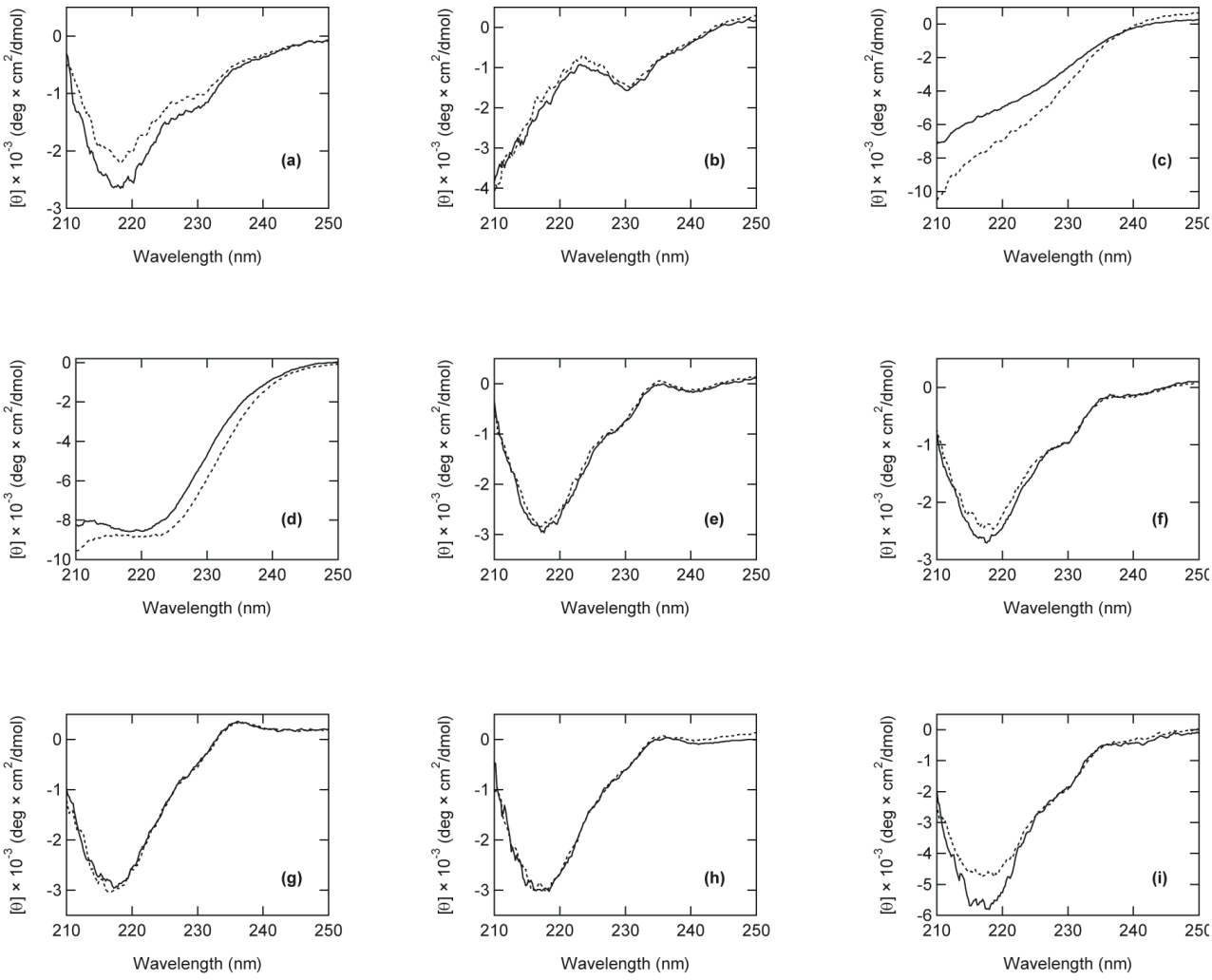

Figure 4.1.4. Far-UV CD spectra of panitumumab **(a)**, etanercept **(b)**, thyroglobulin **(c)**, L-asparaginase **(d)**, adalimumab **(e)**, infliximab **(f)**, rituximab **(g)**, omalizumab **(h)**, and IgG **(i)** at Stage 5. Proteins were mixed with poly(amino acid) (shown in Table 4.1.1). Native proteins, solid lines; redissolved proteins, dotted lines.

4.1.4. Discussion

This paper described a precipitation-redissolution method using poly(amino acid). All types of proteins examined, including a pharmaceutically important enzyme, antibody, and hormone, were fully precipitated by poly(amino acid) (Table 4.1.1). The precipitant was dissolved under physiological ionic strength at 150 mM NaCl. The most important observation was that the activities of redissolved proteins after precipitation were comparable to those of the respective native proteins (Figure 4.1.3, Table 4.1.2). Previous studies showed that polyelectrolytes inhibited enzyme activities at low ionic strength [20–23], because of the formation of PPCs. Thus, the recoveries of protein activities by buffer exchange observed in the present study indicated that proteins were released from PPCs, and hence redissolved proteins retained their native states. Accordingly, the redissolved proteins are likely to be applicable for protein therapy.

The precipitation-redissolution method using poly(amino acid) is summarized in Figure 4.1.5. Poly(amino acid) binds to oppositely charged protein surfaces through electrostatic interactions at low ionic strength, and thus precipitable PPCs are formed [24,25]. The salts at high ionic concentration shield the electrostatic interaction between proteins and poly(amino acid), resulting in disruption of PPC precipitation [24,25] The salt responsiveness of protein precipitate is not observed by commonly used precipitants, including salt, organic solvent, or uncharged polymer, because of the differences in the mechanism of protein precipitation [26–29]. It should be noted that PPC precipitants were occurred in the pH range of $| \mathrm{pH} - p\mathrm{I} | \approx 2$. A similar tendency was reported in the precipitation ratio of antibodies by polyelectrolytes as a function of pH [16], indicating that the PPCs were likely to precipitate under these conditions.

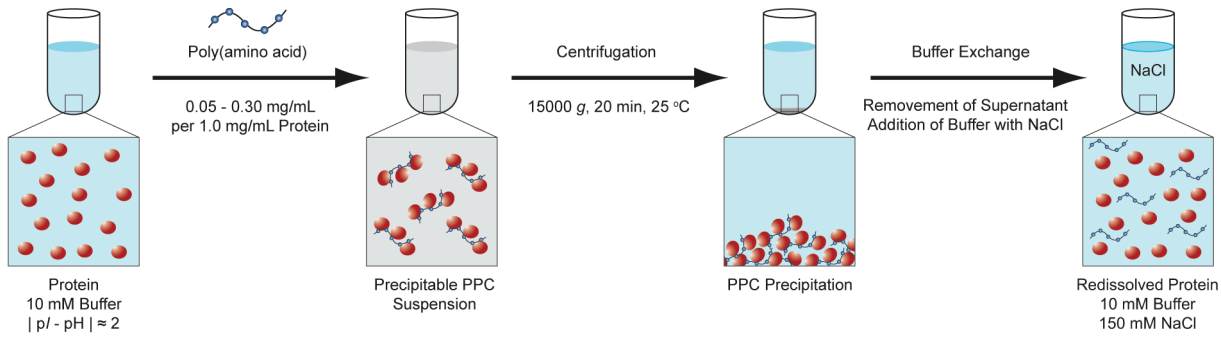

Figure 4.1.5. Schematic illustration of the precipitation–redissolution method by poly(amino acid).

Another significant advantage of the precipitation-redissolution method using poly(amino acid) is the low dosage of poly(amino acid) required to precipitate a protein. For example, proteins at 1.0 mg/mL were fully precipitated by the addition of 0.05-0.3 mg/mL poly(amino acid) (Table 4.1.1), which is much lower than the dosages of conventional precipitants used such as 200 mg/mL ammonium sulfate and 90 mg/mL PEG [12]. Low dosage of poly(amino acid) may be preferable for protein formulation from a pharmaceutical perspective, as high concentrations of additives result in several practical limitations for cytotoxicity. On the contrary, the yield of PPC precipitation decreased with further addition of poly(amino acid) (Figure 4.1.2). This behavior is similar to the previous studies [25,30] in that an excess of polyelectrolyte increased protein molecules per unit of polyelectrolyte, resulting in repulsion between PPCs and a decline in precipitable PPCs. From a mechanistic viewpoint, it is reasonable that low concentrations of poly(amino acid) are required for PPC precipitation.

Interestingly, peak shifts of the far-UV CD spectra were observed for redissolved oligomer proteins such as L-asparaginase and thyroglobulin, whereas those of redissolved antibodies were almost identical to the native state, although there were slight changes for panitumumab and IgG (Figure 4.1.4). This difference may arise from the following properties. First, the residual interactions between poly(amino acid) and proteins may affect the secondary structure of redissolved proteins at physiological ionic strength [25]. Second, the tertiary structures of proteins may be due to the differences in structural stability of redissolved proteins; oligomeric protein contain assembly homo- or heterosubunits through non-covalent interactions, whereas antibodies are roughly Y-shaped with a disulfide bond between two heavy chains and two light

chains. Although it is difficult to further discuss the dominant factors of poly(amino acid) on secondary structure of protein, antibodies may be more suitable for the precipitation-redissolution method than other proteins.

In summary, this paper presented a unique precipitation-redissolution method using poly(amino acid) for several types of therapeutic proteins. As dilute proteins can be fully precipitated at low ionic strength, it is possible to prepare high-concentration protein formulations by redissolution in a lower volume of salt-containing buffer. In addition, the precipitation-redissolution method does not require particular instruments and therefore process development and scale-up may be feasible. Therefore, this system could be expanded for the concentration of therapeutic proteins as well as for protein purification.

4.1.5. References

[1] Leader, B.; Baca, Q. J.; Golan, D. E. Protein Therapeutics: a Summary and Pharmacological Classification. *Nat. Rev. Drug. Discov.* **2008**, *7*, 21-39.

[2] Walsh, G. Biopharmaceutical Benchmarks 2010. *Nat. Biotechnol.* **2010**, *28*, 917-924.

[3] Shire, S. J.; Shahrokh, Z.; Liu, J. Challenges in the Development of High Protein Concentration Formulations. *J. Pharm. Sci.* **2004**, *93*, 1390-1402.

[4] Harris, R. J.; Shire, S. J.; Winter, C. Commercial Manufacturing Scale Formulation and Analytical Characterization of Therapeutic Recombinant Antibodies *Drug. Dev. Res.* **2004**, *61*, 137-154.

[5] Bhambhani, A.; Blue, J. T. Lyophilization Strategies for Development of a High-Concentration Monoclonal Antibody Formulation: Benefits and Pitfalls *American. Pharmaceutical. Review.* **2010**, *13*, 31–32, 34–38.

[6] Johnson, H. R.; Lenhoff, A. M. Characterization and Suitability of Therapeutic Antibody Dense Phases for Subcutaneous Delivery. *Mol. Pharm.* **2013**, *10*, 3582-3591.

[7] Yang, M. X.; Shenoy, B.; Disttler, M.; Patel, R.; McGrath, M.; Pechenov, S.; Margolin, A. L.

Crystalline Monoclonal Antibodies for Subcutaneous Delivery. *Proc. Natl. Acad. Sci. U. S. A.* **2003**, *100*, 6934-6939.

[8] Bromberg, L.; Rashba-Step, J.; Scott, T. Insulin Particle Formation in Supersaturated Aqueous Solutions of Poly(ethylene glycol). *Biophys. J.* **2005**, *89*, 3424-3433.

[9] Nishi, H.; Miyajima, M.; Nakagami, H.; Noda, M.; Uchiyama, S.; Fukui, K. Phase Separation of an IgG1 Antibody Solution under a Low Ionic Strength Condition. *Pharm. Res.* **2010**, *27*, 1348-1360.

[10] Dani, B.; Platz, R.; Tzannis, S. T. High Concentration Formulation Feasibility of Human Immunoglubulin G for Subcutaneous Administration. *J. Pharm. Sci.* **2007**, *96*, 1504-1517.

[11] Bowen, M.; Armstrong, N.; Maa, Y. F. Investigating High-Concentration Monoclonal Antibody Powder Suspension in Nonaqueous Suspension Vehicles for Subcutaneous Injection. *J. Pharm. Sci.* **2012**, *101*, 4433-4443.

[12] Matheus, S.; Friess, W.; Schwartz, D.; Mahler, H. C. Liquid High Concentration IgG1 Antibody Formulations by Precipitation. *J. Pharm. Sci.* **2009**, *98*, 3043-3057.

[13] Wang, Y. F.; Gao, J. Y.; Dubin, P. L. Protein Separation via Polyelectrolyte Coacervation: Selectivity and Efficiency. *Biotechnol. Prog.* **1996**, *12*, 356─363.

[14] Zhang, C.; Lillie, R.; Cotter, J.; Vaughan, D. Lysozyme Purification from Tobacco Extract by Polyelectrolyte Precipitation. *J. Chromatogr. A* **2005**, *1069*, 107-112.

[15] Boeris, V.; Spelzini, D.; Farruggia, B.; Pico´, G. Aqueous Two-Phase Extraction and Polyelectrolyte Precipitation Combination: A Simple and Economically Technologies for Pepsin Isolation from Bovine Abomasum Homogenate *Process. Biochem.* **2009**, *44*, 1260–1264.

[16] McDonald, P.; Victa, C.; Carter-Franklin, J. N.; Fahrner, R. Selective Antibody Precipitation Using Polyelectrolytes: a Novel Approach to the Purification of Monoclonal Antibodies. *Biotechnol. Bioeng.* **2009**, *102*, 1141-1151.

[17] Peram, T.; McDonald, P.; Carter-Franklin, J.; Fahrner, R. Monoclonal Antibody Purification Using Cationic Polyelectrolytes: an Alternative to Column Chromatography. *Biotechnol. Prog.* **2010**, *26*,

1322-1331.

[18] Capito, F.; Bauer, J.; Rapp, A.; Schröter, C.; Kolmar, H.; Stanislawski, B. Feasibility Study of Semi-Selective Protein Precipitation with Salt-Tolerant Copolymers for Industrial Purification of Therapeutic Antibodies. *Biotechnol. Bioeng.* **2013**, *110*, 2915-2927.

[19] Kayitmazer, A. B.; Seeman, D.; Minsky, B. B.; Dubin, P. L.; Xu, Y. Protein–polyelectrolyte interactions. *Soft Matter* **2013**, *9*, 2553-2583.

[20] Ganguli, S.; Yoshimoto, K.; Tomita, S.; Sakuma, H.; Matsuoka, T.; Shiraki, K.; Nagasaki, Y. Regulation of Lysozyme Activity Based on Thermotolerant Protein/Smart Polymer Complex Formation. *J. Am. Chem. Soc.* **2009**, *131*, 6549-6553.

[21] Tomita, S.; Ito, L.; Yamaguchi, H.; Konishi, G.; Nagasaki, Y.; Shiraki, K. Enzyme Switch by Complementary Polymer Pair System (CPPS) *Soft Matter* **2010**, *6*, 5320-5326.

[22] Tomita, S.; Shiraki, K. Poly(acrylic acid) is a Common Noncompetitive Inhibitor for Cationic Enzymes with High Affinity and Reversibility. *J. Polym. Sci. Part A: Polym. Chem.* **2011**, *49*, 3835-3841.

[23] Kurinomaru, T.; Tomita, S.; Kudo, S.; Ganguli, S.; Nagasaki, Y.; Shiraki, K. Improved Complementary Polymer Pair System: Switching for Enzyme Activity by PEGylated Polymers. *Langmuir* **2012**, *28*, 4334-4338.

[24] Tsuboi, A.; Izumi, T.; Hirata, M.; Xia, J.; Dubin, P. L.; Kokufuta, E. Complexation of Proteins with a Strong Polyanion in an Aqueous Salt-free System. *Langmuir* **1999**, *12*, 6295-6303.

[25] Carlsson, F.; Malmsten, M.; Linse, P. Protein-Polyelectrolyte Cluster Formation and Redissolution: a Monte Carlo Study. *J. Am. Chem. Soc.* **2003**, *125*, 3140-3149.

[26] Melander, W.; Horvath, C. Salt Effect on Hydrophobic Interactions in Precipitation and Chromatography of Proteins: an Interpretation of the Lyotropic Series. *Arch. Biochem. Biophys.* **1977**, *183*, 200-215.

[27] Atha, D. H.; Ingham, K. C. Mechanism of Precipitation of Proteins by Polyethylene Glycols. Analysis in Terms of Excluded Volume. *J. Biol. Chem.* **1981**, *256*, 12108-12117.

[28] Arakawa, T.; Timasheff, S. N. Mechanism of Protein Salting In and Salting Out by Divalent Cation Salts: Balance between Hydration and Salt Binding. *Biochemistry.* **1984**, *23*, 5912-5923.

[29] Yoshikawa, H.; Hirano, A.; Arakawa, T.; Shiraki, K. Mechanistic Insights into Protein Precipitation by Alcohol. *Int. J. Biol. Macromol.* **2012**, *50*, 865-871.

[30] Morawetz, H.; Walter L. Hughes, J. The Interaction of Proteins with Synthetic Polyelectrolytes I. Complexing of Povine Serum Albumin. *J. Phys. Chem.* **1952**, *56*, 64─69.

4.2. Feasibility of Antibody-Poly(glutamic acid) Complexes: Preparation of High-concentration Antibody Formulations and Their Pharmaceutical Properties

4.2.1. Introduction

Monoclonal antibodies have generated considerable interest as biopharmaceuticals over the past two decades because of their high target specificity and biocompatibility. At present, over 20 types of monoclonal antibody have been approved by the US Food and Drug Administration [1] and used for several types of disease, such as cancer and autoimmune diseases [2–5]. Despite the advances in antibody drug development, the routes of administration for these antibodies remain challenging. The major route of delivery for antibodies has been intravenous administration due to the high bioavailability [6]. In contrast, subcutaneous administration has been in great demand as an alternative route that allows at-home administration by patients and improves compliance rates [7–10]. However, the desirable concentration of antibodies for subcutaneous administration is usually above 100 mg/mL with a volume limitation of 1.5 mL [9, 10].

Several methods have been developed to obtain high-concentration protein solutions that would enable proteins to be used in formulations, for example with additives such as arginine or other amino acids [11, 12], ultrafiltration [13], gelation [14], crystallization [15], liquid–liquid phase separation [16], and spray drying [6, 17]. However, these methods are still time-consuming and costly. Methods for the suspension or precipitation of protein have also been reported for use in concentrated protein formulations [18, 19]. If the precipitates of protein can be fully resolubilized by the simple method, such precipitates can be used as concentrated protein solutions. Recently, our group have demonstrated the precipitation–redissolution method with poly(amino acid) as a precipitant [20]. Briefly, charged polyelectrolytes, including poly-L-lysine and poly-L-glutamic acid, interact strongly with complementary charged proteins through

multiple electrostatic interactions, resulting in the formation of a protein–polyelectrolyte complex (PPC) [20–26], which can often be precipitated depending on the experimental conditions, such as pH, ionic strength, and stoichiometric ratio [24, 27, 28]. PPC precipitates are then redissolved by the addition of buffer with high ionic strength such that the final concentration reaches 150 mM, which corresponds to physiological conditions [20, 28, 29]. This simple system has been applied successfully for several types of therapeutic protein, including enzymes, antibodies, and peptide hormones [20]. However, the utility of this precipitation–redissolution method for protein therapy is still unclear.

In this study, the feasibility of the complex precipitation–redissolution method using poly(amino acid) was demonstrated for high-concentration antibody formulation. As described below, antibody formulations with concentrations over 100 mg/mL of adalimumab for autoimmune disease and omalizumab for allergic asthma could be prepared by addition of poly-L-glutamic acid (polyE). The formation of antibody−polyE complex and precipitation–redissolution processes did not significantly change the immunoactivity or secondary structure of the antibodies, and did not result in undesirable aggregation. Comparison of time required, yield, and aggregate ratio indicated that the precipitation–redissolution method was more effective for application than the conventional concentration methods, including lyophilization–redissolution, evaporation–redissolution, and ultrafiltration. The precipitation–redissolution method was successfully performed from a scale of 400 μL to 1.0 L, indicating that this method could be scaled up to 2500-fold. Finally, the general toxicity and pharmacokinetic profiles of the antibody–polyE complex formulation were similar to those of conventional antibody formulations. These results suggested that this simple method represents a new strategy for preparing high-concentration antibody formulations, and it is expected that this method and complex formulations would be applicable for medicinal use.

4.2.2. Materials and Methods

Materials

Adalimumab was obtained from transfected Chinese hamster ovary (CHO) cell cultures and purified on a protein-A column. Omalizumab was purchased from Novartis Pharma KK (Tokyo, Japan) and purified on a protein-A column to remove the additives. Citrate, sodium chloride (NaCl), sodium phosphate, and potassium chloride (KCl) were from Kanto Chemical Co., Inc. (Tokyo, Japan). Polysorbate 20 was from Wako Pure Chemical. Ind., Ltd. (Osaka, Japan). 3-(*N*-morpholino)Propanesulfonic acid (MOPS) and Blocking One were from Nacalai Tesque, Inc. (Kyoto, Japan). Tris(hydroxymethyl)aminomethane (Tris) was from Bio-Rad Laboratories (Hercules, CA). Biotinylated anti-human IgG monoclonal antibody, rat IgG, and poly-L-glutamic acid sodium salt with average molecular weights of 3000 – 15000 Da (polyE1) and 50000 – 100000 Da (polyE2) were from Sigma Chemical Co. (St. Louis, MO). Human IgE was from Abcam (Cambridge, MA). Biotinylated anti-human IgE monoclonal antibody was from Miltenyi Biotec GmbH (Bergisch Gladbach, Germany). Human tumor necrosis factor α (TNF-α) was from Gibco Life Technologies Ltd. (Grand Island, NY). Human high-affinity immunoglobulin epsilon receptor subunit α (FcεRIα) was from Sino Biological Inc. (Beijing, China). Streptavidin-labeled horseradish peroxidase (Avidin-HRP) was from Thermo Fisher Scientific (Waltham, MA). 3,3',5,5'-Tetramethylbenzidine (TMB) was from KPL (Gennep, the Netherlands). Human IgG1 Therapeutic EIA Kit was from Cayman Chemical Co. (Ann Arbor, MI). Sucrose was from Dai-Nippon Meiji Sugar Co., Ltd. (Tokyo, Japan). L-Histidine hydrochloride was from Mitsubishi Tanabe Pharma Co. (Osaka, Japan). L-Histidine was from Kyowa Hakko Bio Co., Ltd. (Tokyo, Japan). Glucose 50% injection was from Terumo Co. (Tokyo Japan). These chemicals were of high-quality analytical grade and were used as received.

Preparation of Antibody-Poly(amino acid) Complex and Redissolution

The procedure of precipitation and redissolution of antibody−polyE1 complex were described as follows (Figure 4.2.1). *Step 1:* The antibody stock solutions containing low (1.0 mg/mL) and high (30 mg/mL)

concentration antibodies in 10 mM buffer (MOPS at pH 6.5, for adalimumab; citrate at pH 5.5 for omalizumab) were prepared. *Step 2:* Aliquots of 200 μL of various concentrations of polyE1 in 10 mM buffer (MOPS at pH 6.5, for adalimumab; citrate at pH 5.5 for omalizumab) were mixed with aliquots of 200 μL antibody stock solution in same buffer. *Step 3:* the samples of antibody−polyE mixture were centrifuged at 1000 × g for 3 minutes at 25°C. *Step 4:* The supernatant of 370 μL was removed and precipitates were resuspended by vortexing. The nominal value of the samples was 30 μL. *Step 5:* 10 μL of 600 mM NaCl in 10 mM buffer was added. The concentrations of antibodies for each step were determined from the absorbance at 280 nm using a spectrometer (SpectraMax Plus384; Molecular Devices Co., Ltd., Sunnyvale, CA). The immnoreactivity, secondary structure, and aggregation ratio were determined as described below.

In addition to the above original scale experiments (400 μL), both 50-fold scale up (20 mL; medium scale) and 2500-fold scale up (1.0 L; large scale) experiments were performed. Table 4.2.3 shows the volumes of these scales at Step 2. A concentration of 0.2 mg/mL polyE1 solution was mixed with 2.0 mg/mL adalimumab solution, and then precipitation–redissolution procedures were performed as described above. It is note that the final concentration of antibody at Step 5 is five times higher than that at Step 1. The containers and centrifuges used for each scale were 1.5 mL centrifuge tubes (MS-4215M; Sumitomo Bakelite Co., Ltd., Tokyo, Japan) and Kubota 3740 for mini-scale, 50 mL centrifuge tubes (430829; Corning Inc., Corning, NY) and Kubota 5220 for medium-scale, and 1 L Nalgene Polycarbonate Centrifuge Bottles (3122-1010; Thermo Fisher Scientific Inc., Waltham, MA) and Kubota 9900 for large-scale. All centrifuges were purchased from Kubota Co. (Tokyo, Japan).

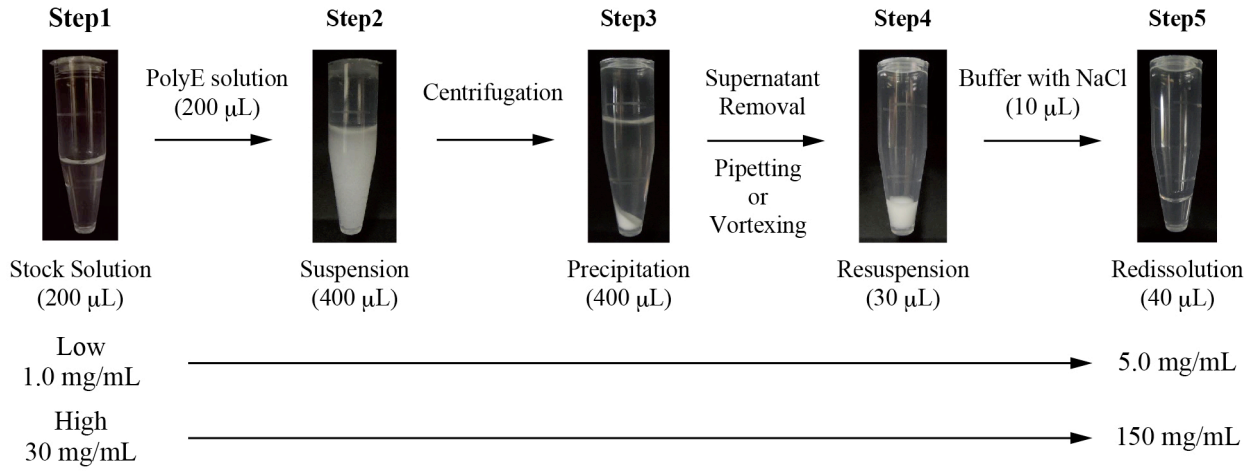

Figure 4.2.1. Outline of the precipitation–redissolution method for antibody drugs. Aliquots of 200 μL of polyE solution in 10 mM buffer were added to 200 μL of stock solution containing low (1.0 mg/mL) or high (30 mg/mL) concentration of antibody in the same buffer (Step 1), and antibody–polyE complex suspension was formed immediately (Step 2). After centrifugation (Step 3), 370 μL of supernatant was removed and the precipitate was resuspended by pipetting or vortexing (Step 4) followed by addition of buffer containing NaCl (Step 5).

Concentration of Antibody Solutions by Several Methods

To compare the efficiencies of the concentration methods, 150 mg/mL omalizumab and adalimumab solutions were prepared by the following methods. *i) Precipitation–redissolution*: 250 μL of 0.15 mg/mL polyE1 in 10 mM buffer (MOPS, pH 6.5, for adalimumab; citrate, pH 5.5 for omalizumab) and 250 μL of 30 mg/mL antibodies in same buffer. The samples of antibody−polyE mixture were centrifuged at 1000 × g for 3 minutes at 25°C. 462.5 μL of supernatant was removed 37.5 μL of 600 mM NaCl in 10 mM buffer was added. The final volume of the concentrated antibodies was 50 μL. *ii) Lyophilization−redissolution*: 250 μL of 30 mg/mL antibodies in 10 mM buffer were added to vials and lyophilized by vacuum freeze-drying (Drying Chamber DRC-1100; Tokyo Rikakikai Co., Ltd., Tokyo, Japan). After lyophylization, 50 μL of 10 mM buffer were added to the vials to redissolve the lyophilized cakes. *iii) Evaporation−redissolution*: 250 μL of 30 mg/mL antibodies in 10 mM buffer were added to tubes and evaporated in a rotatory evaporator (Centrifugal vaporizer CVE-100D; Tokyo Rikakikai). After evaporation, 50 μL of 10 mM buffer were added to the tube to redissolve the cakes. *iv) Ultrafiltration*: 250 μL of 30 mg/mL antibodies in 10 mM

buffer were put into an ultrafiltration unit with a 50 kDa cut-off (UFC5050; Millipore Co., Ltd., Billerica, MA) and centrifuged at 14000 × *g* at 4°C until the volume was decreased to 50 μL. The time required, final concentration, and aggregation ratio were determined as described below.

Immunoassay

The immunoreactivities of omalizumab were measured by competitive enzyme-linked immunosorbent assay (ELISA) to confirm structural integrity of redissolved antibody. Two types of omalizumab with or without precipitation−redissolution method were used, as described above. The wells of 96-well ELISA microplates (Sumitomo Bakelite Co., Ltd., Tokyo, Japan) were coated with human FcεRIα, and the plates were incubated at 4°C overnight. The wells were washed a total of five times by addition of washing buffer containing 24.8 mM Tris, 136.9 mM NaCl, 2.7 mM KCl, and 0.1% polysorbate 20 (pH 7.4). The wells were then blocked with Blocking One at room temperature for 1 hour. After washing of the wells, solutions containing human IgE at a constant concentration and omalizumab of different concentrations were added to the wells and incubated at room temperature for 1 hour. After washing of the wells, 100 μL of biotinylated anti-human IgE monoclonal antibody was added to each well and plates were incubated at room temperature for 1 hour. After washing of the wells, 100 μL of streptavidin-labeled horseradish peroxidase was added to each well and plates were incubated at room temperature for 30 minutes. After washing of the wells, 100 μL of TMB was added to each well and plates were incubated at room temperature for more than 15 minutes. Finally, 100 μL of 0.1% HCl was added and the absorbance at 450 nm was determined using a microplate reader (SpectraMax Plus384; Molecular Devices).

The immunoreactivities of adalimumab were measured by ELISA. Two types of adalimumab with or without precipitation−redissolution method were used, as described above. The wells of polystyrene 96-well ELISA microplates were coated with human TNF-α, and the plates were incubated at 4°C overnight. After washing of the wells, Blocking One were added and plates were incubated at room temperature for 1 hour. After washing of the wells, 100 μL of adalimumab solutions with or without precipitation−redissolution

process of different concentrations were added to the wells and plates were incubated at room temperature for 1 hour. After washing of the wells, 100 μL of biotinylated anti-human IgG monoclonal antibody was added to each well and plates were incubated at room temperature for 1 hour. Subsequent procedures were as described above.

Circular Dichroism

Circular dichroism (CD) experiments were performed using a spectropolarimeter (J-720; Japan Spectroscopic Co., Ltd., Tokyo, Japan). Two types of antibodies with or without precipitation−redissolution method were used, as described above. The samples containing 1.0 mg/mL antibodies in 10 mM buffer were added to a 1-mm path length quartz cuvette, and then CD spectra of antibodies were measured at 25°C. Scans were taken from 195 to 250 nm at a rate of 100 nm/min with a sample interval of 0.2 nm, 0.25 s response, and 1.0 nm bandwidth. 50 scans were averaged. Obtained far-UV CD spectra were plotted in the wavelength range of 210 – 250 nm because of the large noise below 210 nm. The CD spectra of the samples were corrected by subtracting the corresponding spectra of the buffers in the absence of antibodies.

Size Exclusion Chromatography (SEC)

Two types of antibodies with or without precipitation−redissolution method were used, as described above. The samples containing 1.0 mg/mL antibodies in 10 mM buffer were centrifuged at 14000 × *g* for 10 minutes, and then the supernatant was analyzed by SEC mode HPLC. The analysis was performed on an SEC column (Yarra 3u SEC-3000; Phenomenex Inc., Torrance, CA) on the HPLC system (LC-20A; Shimadzu Corp., Kyoto, Japan) at a constant flow rate of 0.5 mL/min. The mobile phase consisted of 100 mM sodium phosphate buffer and 0.5 M NaCl (pH 6.8).

General toxicity test

General toxicity tests were evaluated using two types of samples, IgG–polyE2 complex formulation and conventional IgG formulation as a control. Each formulation was prepared as described below. *IgG−polyE2 complex formulation:* Aliquots of 4.5 mL of 0.24 mg/mL polyE2, 8.0% glucose, and 10 mM citrate (pH 5.0) were added to 4.5 mL of 2.0 mg/mL IgG and 10 mM citrate (pH 5.0) aseptically. The samples of antibody−polyE mixture were centrifuged at 1000 × g for 3 minutes at 25°C. 8.1 mL of supernatant was removed and precipitates were resuspended by vortexing. The nominal value of the samples was 900 μL containing 10 mg/mL IgG, 1.2 mg/mL polyE2, 4.0 % glucose, 10 mM citrate (pH 5.0). *Conventional IgG formulation:* Aliquots of 500 μL of 10 mg/mL IgG, 4.0 % glucose, 10 mM citrate (pH 5.0) was prepared.

Five-week-old Crl:CD (SD) rats were from Charles River Laboratories Japan, Inc. (Kanagawa, Japan). The samples were injected subcutaneously into the backs of six rats in two groups at 50 mg/kg (333 nmol/kg). The body weights of the rat were measured for 0 – 14 days. Weight checks of the organs (heart, lung, liver, spleen, and kidney), pathology assessment, and blood test were performed for 1 and 2 weeks after injection. In the pathology assessment, the above organs and administration site were assessed. In the blood test, the following items were measured: white blood cell count (WBC), red blood cell count (RBC), hemoglobin (HGB), hematocrit (HCT), mean corpuscular volume (MCV), mean corpuscular hemoglobin (MCH), mean corpuscular hemoglobin concentration (MCHC), platelets (PLT), activated partial thromboplastin time (APTT), prothrombin time (PT), alkaline phosphatase (ALP), aspartate aminotransferase (AST), alanine aminotransferase (ALT), lactase dehydrogenase (LDH), total bilirubin (TB), total protein (TP), albumin (ALB), total cholesterol (TC), triglyceride (TG), phospholipid (PL), glucose (GLC), blood urea nitrogen (BUN), creatinine (CRE), inorganic phosphorus (Pi), calcium (Ca), sodium (Na), potassium (K), and chlorine (Cl).

Pharmacokinetic Profile

Pharmacokinetic studies were evaluated using two types of samples, omalizumab−polyE2 complex formulation and conventional omalizumab formulation as a control. Each formulation was prepared as described below. *Omalizumab−polyE2 complex formulation:* Aliquots of 2.5 mL of 0.24 mg/mL polyE2, 8.0% glucose, and 20 mM citrate (pH 5.5) were added to 2.5 mL of 2.0 mg/mL omalizumab and 20 mM citrate (pH 5.5) aseptically. The samples of antibody−polyE mixture were centrifuged at 1000 × g for 3 minutes at 25°C. 4.5 mL of supernatant was removed and precipitates were resuspended by vortexing. The nominal value of the samples was 500 μL containing 10 mg/mL omalizumab, 1.2 mg/mL polyE2, 4.0 % glucose, 20 mM citrate (pH 5.5). *Conventional omalizumab formulation:* Aliquots of 500 μL of 10 mg/mL omalizumab, 10.4% sucrose, 0.20% L-histidine hydrochloride, 0.13% L-histidine, and 0.04% polysorbate 20 was prepared. Sterile syringes were filled with the samples. Each sample, conventional, and complex formulation of omalizumab was injected subcutaneously into the backs of three rats at 10 mg/kg (66.7 nmol/kg), and the animals were kept in cages for 0 – 22 days. Blood was collected from the tail vein at 0 – 22 days after injection. Finally, blood concentration of omalizumab was measured using a Human IgG1 Therapeutic EIA Kit (Cayman Chemical Co., Ann Arbor, MI). All animal experiments were approved by the institutional animal care and use committee of Terumo Corp. before the experiments.

4.2.3. Results

Preparation of High-concentration Antibody Solution by Precipitation-redissolution Method

Previously, our group reported a precipitation–redissolution method using poly(amino acid), which enables the preparation of salt-dissociable precipitates of protein–poly(amino acid) complexes [20]. To evaluate the efficiency of antibody concentration by the precipitation–redissolution method, two antibody drugs: adalimumab (p*I* = 8.7; for autoimmune disease) and omalizumab (*p*I =7.6; for allergic asthma), were selected. Anionic poly-L-glutamic acid with average molecular weight of 3000 – 15000 Da (polyE1) was selected for

cationic antibodies at pH 5.5 – 6.5, because protein–poly(amino acid) complexes were formed only when poly(amino acid) had a charge complementary to that of the protein at experimental pH. Two types of stock solution containing low (1.0 mg/mL) or high (30 mg/mL) concentrations of antibodies were mixed with the polyE1 solutions. The yield of antibody under the milder condition (1,000 g for 3 minutes at 25°C) was identical to that under the harder condition (15,000 g for 20 minutes at 25°C). Thus, the centrifugation condition was selected at 1,000 g for 3 minutes at 25°C in this study. Figure 4.2.2 shows the final concentration of antibodies at Step 5. In Figure 4.2.1A, final concentration of antibodies increased sharply with increasing concentration of polyE1, and reached a plateau at around 0.05 eq., which was consistent with the previous report [20]. Similar profiles were observed even at high concentration of stock solution (Figure 4.2.2B); final concentration values of omalizumab and adalimumab reached about 150 mg/mL at 0.05 eq. The yields of these antibodies were also about 100% even at high protein concentration (150 mg/mL) as well as low concentration (5 mg/mL).

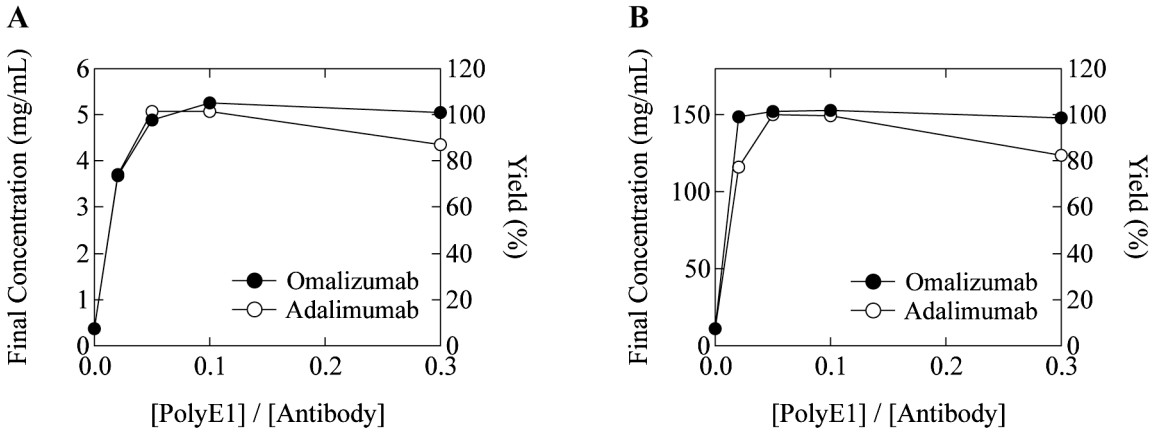

Figure 4.2.2. Precipitation–redissolution profiles of antibodies by polyE1. Various concentrations of polyE1 were added to stock solutions containing 1.0 mg/mL (low) (**A**) or 30 mg/mL (high) (**B**) antibodyes in 10 mM buffer. The final concentrations of antibodies at Step 5 in the presence of polyE1 were measured. The final concentration of antibodies in the absence of polyE1 was lower than that of stock solution due to the dilution of precipitation–redissolution process. Closed circles, omalizumab; open circles, adalimumab.

Subsequently, the activity and structure of the redissolved antibodies were characterized. As shown in Figures 4.2.2A and 4.2.2B, the immunoreactivities of redissolved omalizumab and adalimumab were identical to those of native antibodies; the 50% inhibitory concentration values (IC_{50}) of omalizumab and the 50% effective concentration values (EC_{50}) of adalimumab were equivalent to those without polyE1 (Table 4.2.1, Figure 4.2.3A,B). Thus, the activities of the antibodies were not altered by the concentration and redissolution process. In addition, far-UV circular dichroism (CD) spectra of redissolved antibodies were identical to those of the native antibodies (Figure 4.2.3C,D), although slight changes were observed in the far-UV CD spectra of adalimumab at 218 nm. These results suggested that the secondary structure of the antibodies were significantly maintained even in the redissolved state. Furthermore, SEC analysis indicated that the soluble aggregates were not increased in the redissolved antibody solutions (Figure 4.2.3E,F). These results suggested that redissolved antibodies retained the original activity, structure, and aggregation properties.

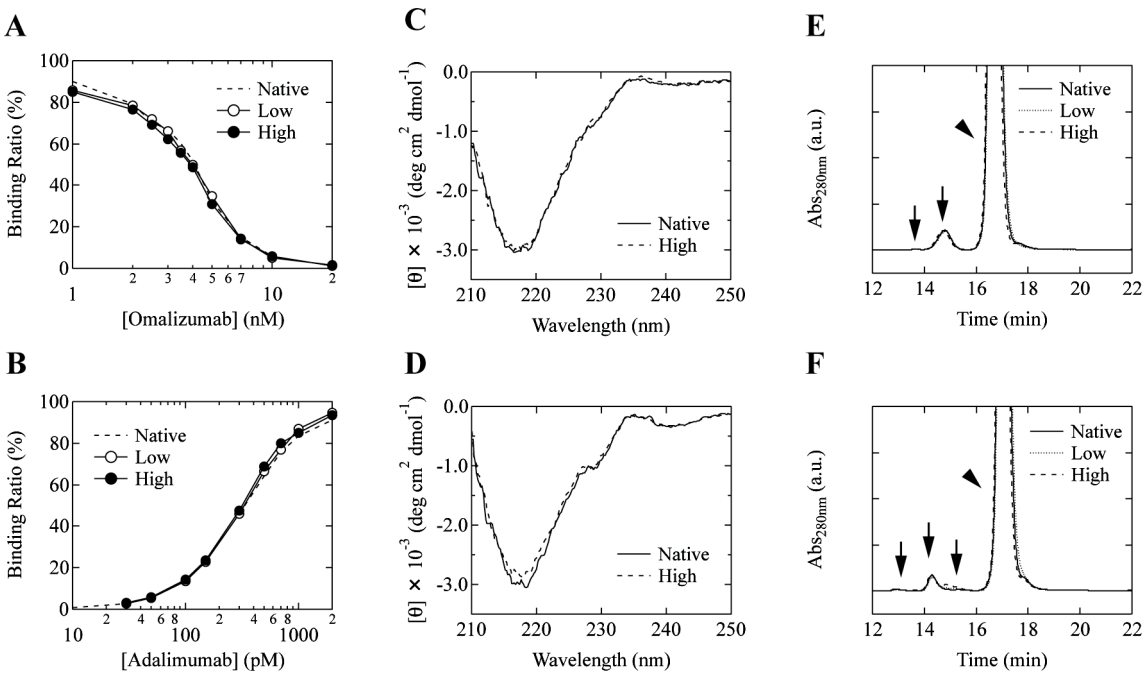

Figure 4.2.3. Characterization of omalizumab (**A,C,E**) and adalimumab (**B,D,F**) with or witout precipitation−redissolution method. (**A,B**) Binding curve of antibodies. dashed lines; native antibodies, open circles; low-concentration redissolved antibodies and closed circles; high-concentration redissolved antibodies. (**C,D**) Far-UV CD spectra of antibodies. solid lines; native antibodies and dushed lines; high-concentration redissolved antibodies. (**E,F**) SEC chromatograms of antibodies, solid lines; native antibodies, dotted lines; low-concentration redissolved antibodies ans dushed lines; high-concentration redissolved antibodies, arrowhead; monomer peak and arrow; aggregate peak.

Table 4.2.1. Immunoreactivities of redissolved antibodies.

Antibody	Concentration	$Activity_{control}$	$Activity_{Step5}$
Omalizumab	Low	3.99 (nM) [a]	3.92 (nM) [a]
	High		3.77 (nM) [a]
Adalimumab	Low	327 (pM) [b]	321 (nM) [b]
	High		309 (pM) [b]

[a] 50% inhibitory concentration.

[b] 50% effective concentration.

Feasibility Studies of Precipitation-redissolution Method

The feasibility studies of the precipitation–redissolution method using poly(amino acid) were performed to confirm its utility for pharmaceutical applications. First, the efficiency of the precipitation–redissolution method was compared to three conventional concentration methods, i.e., lyophilization–redissolution, evaporation–redissolution, and ultrafiltration. As expected, 150 mg/mL antibody solutions were obtained by the precipitation–redissolution method (Table 4.2.2). On the other hand, the final concentrations of antibody solutions obtained by the conventional methods were 72.7 – 136 mg/mL, suggesting that some antibody was lost in the concentration process in these methods. The time required for the precipitation–redissolution method was about 2 hours, which was shorter than those of lyophilization and evaporation (Table 4.2.2). Furthermore, SEC analysis revealed that soluble aggregates did not increase in the concentrated antibody solutions prepared by the precipitation–redissolution method and ultrafiltration, but increased in those prepared by lyophilization and evaporation (Table 4.2.2). These results suggested that the precipitation–redissolution method is a good alternative to the well-known concentration methods.

Table 4.2.2. Comparison of the precipitation–redissolution method with conventional concentration methods.

		Adalimumab		Omalizumab	
Concentration method	Time Required (hours)	Final concentration (mg/mL)	Aggregation peak ratio (%)	Final concentration (mg/mL)	Aggregation peak ratio (%)
Precipitation-redissolution	2	151	9.67	154	3.98
Lyophilization-redissolution	18	136	12.7	86.0	7.35
Evapolation-redissolution	5	133	19.4	96.1	8.61
Ultrafiltration	2	131	7.29	72.7	3.58

Table 4.2.3. Scaling up of the precipitation–redissolution method for preparation of 10 mg/mL adalimumab from 2.0 mg/mL stock solution

Scale	Final concentration (mg/mL)	Immnoreactivity (pM)	Aggregates peak ratio (%)
Mini (400 μL)	10.2	302	8.09
Medium (20 mL)	10.1	317	8.42
Large (1.0 L)	10.4	289	8.52

To examine whether the precipitation–redissolution method could be scaled up, 10 mg/mL adalimumab solutions from 2.0 mg/mL adalimumab were prepared by the addition of 0.1 mg/mL polyE1 at three different scales−original-scale (400 μL), 50-fold scale up (20 mL; medium-scale), and 2500-fold scale up (1.0 L; large-scale). Similar to the original-scale, the adalimumab–polyE mixed solution formed a complex and was suspended immediately at the medium- (data not shown) and large-scales (Figure 4.2.3 Step 2) At the large scale, the complex was spontaneously precipitated almost completely in 2 hours at Step 2. After centrifugation (Step 3), the supernatant was removed and resuspended by mild agitation (Step 4). Finally, the suspension was fully dissolved by the addition of NaCl in the same buffer (Step 5). ELISA and SEC analysis revealed that the immunoreactivities and the amounts of soluble aggregates of redissolved adalimumab at medium and large scales were similar to those at the original-scale (Table 4.2.3), suggesting that the properties of redissolved antibody were independent of the scale. Thus, it was indicated that the precipitation–redissolution method could be scaled up by 2500-fold.

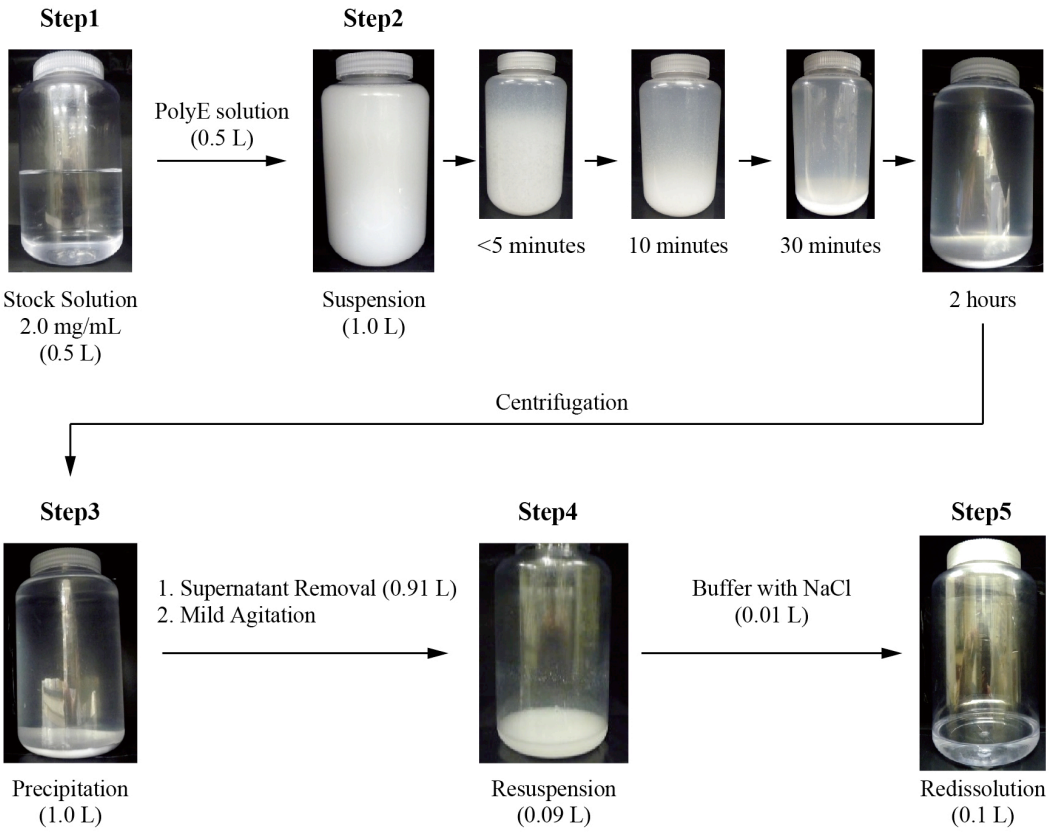

Figure 4.2.4. Outline of precipitation–redissolution method for adalimumab at the scale of 1.0 L. Aliquots of 0.5 L of 0.2 mg/mL polyE1 solution in 10 mM MOPS (pH 6.5) was added to 0.5 L of stock solution containing 2.0 mg/mL adalimumab in the same buffer (Step 1), and antibody–polyE complex suspension was formed immediately (Step 2). After centrifugation (Step 3), 0.91 L of supernatant was removed and the precipitate was resuspended by mild agitation (Step 4) followed by addition of 0.01 L buffer containing NaCl (Step 5).

Finally, to test the potential of antibody–poly(amino acid) complexes for medicinal use, general toxicity tests of the antibody–poly(amino acid) complex suspension (Step 4) were performed. Anionic poly-L-glutamic acid with average molecular weight of 50000 – 100000 Da (polyE2) was selected because it was speculated that poly(amino acids) with larger molecular weight would have longer blood half-lives and stronger influence [30]. In addition, rat IgG (pI ≈ 7.0) was selected to avoid immune reaction in rats. Suspensions of the complex containing 10 mg/mL rat IgG and 1.2 mg/mL polyE2 (Step 4) were prepared by the precipitation–redissolution method, and then injected subcutaneously into rats at 50 mg/kg (333 nmol/kg). Comparison of administration of conventional IgG formulation and IgG–polyE2 complex formulation

indicated no significant difference in rat body weight or the weights of several organs (heart, lung, liver, spleen, and kidney) between the two groups (Figure 4.2.4A,B). In addition, no significant differences in pathological findings or blood composition were observed between the two groups (data not shown). These results suggested that antibody–polyE complexes did not have general toxicity in these experimental animals. Furthermore, pharmacokinetic analysis were performed to compare the behaviors of the conventional omalizumab and omalizumab–polyE2 complex formulation in blood. Figure 4.2.4C shows the plasma concentration of omalizumab–time curve in rats after subcutaneous administration. The curve of omalizumab–polyE2 complex (Step 4) corresponded to that of the conventional omalizumab. These results indicated that the antibody–polyE complex formulation did not affect the bioavailability of the therapeutic antibody.

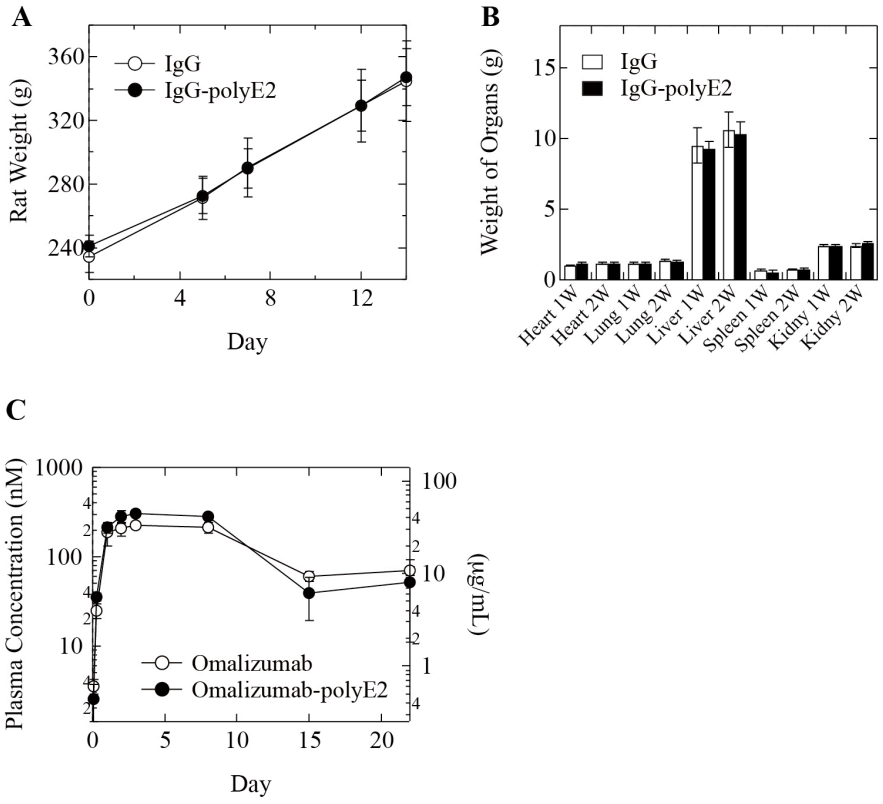

Figure 4.2.5. General toxicity tests in rats; body weight of rats (A) and weight of organs (B). Conventional IgG formulation, closed symbols; IgG-polyE2 complex fomulation, open symbols. (C) Plasma concentration of omalizumab–time curve in rats after subcutaneous administration. Conventional omalizumab formulation, open circles; omalizumab–polyE2 complex formulation, closed circles.

4.2.4. Discussion

High-concentration (> 100 mg/mL) antibody formulations are indispensable for subcutaneous administration because of the limitation of injection volume (typically 1.5 mL) [9, 10]. As demonstrated above, 150 mg/mL antibody formulations were successfully prepared from 30 mg/mL antibody solutions using the precipitation–redissolution method with poly(amino acid) (Figure 4.2.2). It is emphasized that the procedures involved in the precipitation–redissolution method are quite simple: (i) polyE is added to the antibody solution, resulting in precipitation of the antibody–polyE complex; (ii) the antibody–polyE precipitates can be suspended easily; (iii) the antibody–polyE complexes can be redissolved with saline solution. Note that the protein concentration was changed from 1.0 mg/mL to 30 mg/mL, indicating that the precipitation–redissolution method could be used for preparation of desirable concentrations of antibody formulations. In addition, the precipitation–redissolution method would be applicable for several types of therapeutic protein, including enzymes, antibodies, and peptide hormones [20].

It is possible that quality of redissolved antibody formulation is comparable to the conventional antibody formulation. ELISA revealed that the immunoreactivity of redissolved antibodies was similar to that of native antibodies (Table 4.2.1, Figure 4.2.3A,B). Far-UV CD spectra suggested that the secondary structure of antibodies did not significantly change by the precipitation−redissolution process (Figure 4.2.3C,D). In addition, SEC analysis showed that soluble aggregates of redissolved antibodies were similar to those of native antibodies (Figure 4.2.3E,F). Furthermore, pharmacokinetic profile of omalizumab/polyE complex formulation was similar to that of conventional omalizumab formulation (Figure 4.2.5C). Although further investigation of structural and colloidal properties remains unclear, these *in vitro* and *in vivo* evaluations supported that the redissolved antibodies are likely to be applicable for protein therapy.

Comparison with conventional concentration methods indicated significant advantages of the precipitation–redissolution method with regard to time required and yield (Table 4.2.2). The precipitation–redissolution method successfully prepared antibody solutions of about 150 mg/mL within 2 hours, whereas lyophilization–redissolution, evaporation–redissolution, and ultrafiltration failed to reach this

concentration (Table 4.2.2). Although visible aggregates were not observed in the adalimumab concentrated by the conventional methods, the final concentrations were lower than 150 mg/mL. The loss of adalimumab in these methods were due to the unfavorable influences of these processes, such as adsorption to the container or ultrafiltration membrane [31–34] or the generation of water-ice crystals at the periphery of the container [35]. The final concentrations of omalizumab obtained by the conventional methods were significantly lower than that achieved by the precipitation–redissolution method (Table 4.2.2), which may have been due to the instability of omalizumab compared to adalimumab. Indeed, visible aggregates were observed in the omalizumab solution during the concentration process, suggesting that the aggregates decreased the yield of concentrated omalizumab. Thus, the precipitation–redissolution method enables prompt and successful concentration of antibodies without soluble aggregates.

The precipitation–redissolution method has another significant advantage with regard to scalability. The adalimumab solutions with different volume scale were successfully concentrated 5-fold without loss of quality (Table 4.2.3). Interestingly, centrifugation is not always necessary to prepare highly concentrated antibody formulations on a large scale. As shown in Figure 4.2.4, the adalimumab–polyE complex was formed and the solution was suspended immediately. The suspension began to precipitate spontaneously a few minutes later and precipitated almost completely within 2 hours (Step 2). The supernatant of the precipitation solution without centrifugation did not contain any antibody (data not shown). The volume of supernatant collected was 0.98 L, meaning that the theoretical maximum concentration of redissolved adalimumab was > 5-fold even without centrifugation. This is important for the application of the precipitation–redissolution method for industrialization, e.g., to reduce the costs associated with centrifuges.

Poly(amino acids) are not listed on the Inactive Ingredient Search for Approved Drug Products of the US Food and Drug Administration, although poly(amino acids) have been used as biocompatible materials [36–39]. Nevertheless, *in vivo* tests revealed that the general toxicity and pharmacokinetic profile of the antibody–polyE complex formulations were identical to those of the conventional antibody formulation (Figure 4.2.5). The antibody–polyE complex could be easily dissociated by saline solution; the salts at

physiological ionic concentration (150 mM) shielded the electrostatic interaction between antibody and polyE and then dissociated the precipitable complexes [28, 29]. Accordingly, it was suggested that the suspension of antibody–polyE complex injected into rats was immediately dissolved to antibody and polyE at physiological ionic strength in the subdermal space. Therefore, it was suggested that the high-concentration antibody–poly(amino acid) complex has biocompatibility for application in protein therapy.

In summary, this study indicated the feasibility of the precipitation–redissolution method for preparation of antibody–poly(amino acid) complex formulations. This simple, quick, and scalable method allows the formation of high-concentration protein solutions without loss of structure or function. More importantly, antibody–polyE complex formulations have the same level of biocompatibility as conventional antibody formulations. Due to its several advantages, the precipitation–redissolution method could be beneficial in medical applications. It is expected that protein–poly(amino acid) complex formulations prepared by this method could be used in protein therapy.

4.2.5. References

[1] Wang, W.; Singh, S.; Zeng, D. L.; King, K.; Nema, S. Antibody Structure, Instability, and Formulation. *J. Pharm. Sci.* **2007**, *96*, 1-26.

[2] Reichert, J. M.; Rosensweig, C. J.; Faden, L. B.; Dewitz, M.C. Monoclonal Antibody Successes in the Clinic. *Nat. Biotechnol.* **2005**, *23*,1073-1078.

[3] Chan, A.C.; Carter, P. J. Therapeutic Antibodies for Autoimmunity and Inflammation. *Nat. Rev. Immunol.* **2010**, *10*, 301-316.

[4] Weiner, L. M.; Surana, R.; Wang, S. Monoclonal Antibodies: Versatile Platforms for Cancer Immunotherapy. *Nat. Rev. Immunol.* **2010**, *10*, 317-327.

[5] Sliwkowski, M. X.; Mellman, I. Antibody Therapeutics in Cancer. *Science* **2013**, *341*,1192-1198.

[6] Dani, B.; Platz, R.; Tzannis, S. T. High Concentration Formulation Feasibility of Human Immunoglubulin G for Subcutaneous Administration. *J. Pharm. Sci.* **2007**, *96*, 1504-1517.

[7] Genovese, M. C.; Covarrubias, A. Leon, G.; Mysler, E.; Keiserman, M.; Valente, R.; Nash, P.; Simon-Campos, J. A.; Porawska, W.; Box, J.; Legerton, C. III; Nasonov, E.; Durez, P.; Aranda, R.; Pappu, R.; Delaet, I.; Teng, J.; Alten, R. Subcutaneous Abatacept Versus Intravenous Abatacept: a Phase IIIb Noninferiority Study in Patients with an Inadequate Response to Methotrexate. *Arthritis Rheum.* **2011**, *63*, 2854-2864.

[8] Wells, A. F.; Jodat, N.; Schiff, M. A Critical Evaluation of the Role of Subcutaneous Abatacept in the Treatment of Rheumatoid Arthritis: Patient Considerations. *Biologics* **2014**, *8*, 41-55.

[9] Shire, S. J.; Shahrokh, Z.; Liu, J. Challenges in the Development of High Protein Concentration Formulations. *J. Pharm. Sci.* **2004**, *93*, 1390-1402.

[10] Harris, R. J.; Shire, S. J.; Winter, C. Commercial Manufacturing Scale Formulation and Analytical Characterization of Therapeutic Recombinant Antibodies. *Drug. Dev. Res.* **2004**, *61*, 137-154.

[11] Inoue, N.; Takai, E.; Arakawa, T.; Shiraki, K. Arginine and Lysine Reduce the High Viscosity of Serum Albumin Solutions for Pharmaceutical Injection. *J. Biosci. Bioeng.* **2014**, *117*, 539-543

[12] Inoue, N.; Takai, E.; Arakawa, T.; Shiraki, K. Specific Decrease in Solution Viscosity of Antibodies by Arginine for Therapeutic Formulations. *Mol. Pharm.* **2014**, *11*, 1889-1896.

[13] Rosenberga, E.; Hepbildikler, S.; Kuhnea, W.; Winter, G. Ultrafiltration concentration of monoclonal antibody solutions: Development of an Optimized Method Minimizing Aggregation. *J. Memb. Sci.* **2009**, *342*, 50–59.

[14] Johnson, H. R.; Lenhoff, A. M. Characterization and Suitability of Therapeutic Antibody Dense Phases for Subcutaneous Delivery. *Mol. Pharm.* **2013**, *10*, 3582-3591.

[15] Yang, M. X.; Shenoy, B.; Disttler, M.; Patel, R.; McGrath, M.; Pechenov, S.; Margolin, A. L. Crystalline Monoclonal Antibodies for Subcutaneous Delivery. *Proc. Natl. Acad. Sci. U. S. A.* **2003**, *100*, 6934-6939.

[16] Nishi, H.; Miyajima, M.; Nakagami, H.; Noda, M.; Uchiyama, S.; Fukui, K. Phase Separation of an IgG1 Antibody Solution under a Low Ionic Strength Condition. *Pharm. Res.* **2010**, *27*, 1348-1360.

[17] Bowen, M.; Armstrong, N.; Maa, Y. F. Investigating High-Concentration Monoclonal Antibody Powder Suspension in Nonaqueous Suspension Vehicles for Subcutaneous Injection. *J. Pharm. Sci.* **2012**, *101*, 4433-4443.

[18] Bromberg, L.; Rashba-Step, J.; Scott, T. Insulin Particle Formation in Supersaturated Aqueous Solutions of Poly(ethylene glycol). *Biophys. J.* **2005**, *89*, 3424-3433.

[19] Matheus, S.; Friess, W.; Schwartz, D.; Mahler, H. C. Liquid High Concentration IgG1 Antibody Formulations by Precipitation. *J. Pharm. Sci.* **2009**, *98*, 3043-3057.

[20] Kurinomaru, T.; Maruyama, T.; Izaki, S.; Handa, K.; Kimoto, T.; Shiraki, K. Protein-Poly(amino acid) Complex Precipitation for High-Concentration Protein Formulation. *J. Pharm. Sci.* **2014**, *8*, 2248-2254.

[21] Ganguli, S.; Yoshimoto, K.; Tomita, S.; Sakuma, H.; Matsuoka, T.; Shiraki, K.; Nagasaki, Y. Regulation of Lysozyme Activity Based on Thermotolerant Protein/Smart Polymer Complex Formation. *J. Am. Chem. Soc.* **2009**, *131*, 6549-6553.

[22] Tomita, S.; Ito, L.; Yamaguchi, H.; Konishi, G.; Nagasaki, Y.; Shiraki, K. Enzyme Switch by Complementary Polymer Pair System (CPPS) *Soft Matter* **2010**, *6*, 5320-5326.

[23] Tomita, S.; Shiraki, K. Poly(acrylic acid) is a Common Noncompetitive Inhibitor for Cationic Enzymes with High Affinity and Reversibility. *J. Polym. Sci. Part A: Polym. Chem.* **2011**, *49*, 3835-3841.

[24] Kurinomaru, T.; Tomita, S.; Kudo, S.; Ganguli, S.; Nagasaki, Y.; Shiraki, K. Improved Complementary Polymer Pair System: Switching for Enzyme Activity by PEGylated Polymers. *Langmuir* **2012**, *28*, 4334-4338.

[25] Kayitmazer, A. B.; Seeman, D.; Minsky, B. B.; Dubin, P. L.; Xu, Y. Protein–polyelectrolyte interactions. *Soft Matter* **2013**, *9*, 2553-2583.

[26] Kurinomaru, T.; Tomita, S.; Hagihara, Y.; Shiraki, K. Enzyme Hyperactivation System Based on a Complementary Charged Pair of Polyelectrolytes and Substrates. *Langmuir* **2014**, *30*, 3826-3831.

[27] Tsuboi, A.; Izumi, T.; Hirata, M.; Xia, J.; Dubin, P. L.; Kokufuta, E. Complexation of Proteins with a Strong Polyanion in an Aqueous Salt-free System. *Langmuir* **1999**, *12*, 6295-6303.

[28] Carlsson, F.; Malmsten, M.; Linse, P. Protein-Polyelectrolyte Cluster Formation and Redissolution: a Monte Carlo Study. *J. Am. Chem. Soc.* **2003**, *125*, 3140-3149.

[29] Ni, R.; Cao, D.; Wang, W. Release of Lysozyme from the Branched Polyelectrolyte-Lysozyme Complexation. *J. Phys. Chem. B* **2008**, *112*, 4393-4400.

[30] Kontermann, R. E. Strategies to Extend Plasma Half-Lives of Recombinant Antibodies. *BioDrugs* **2009**, *23*, 93-109.

[31] Petty, C.; Cunningham, N. L. Insulin Adsorption by Glass Infusion Bottles, Polyvinylchloride Infusion Containers, and Intravenous Tubing. *Anesthesiology* **1974**, *40*, 400-404.

[32] Duncan, M. R.; Lee, J. M.; Warchol, M. P. Influence of Surfactants upon Protein/Peptide Adsorption to Glass and Polypropylene. *Int. J. Pharm.* **1995**, *120*, 179-188.

[33] Norde, W.; Haynes, C. A. Reversibility and the Mechanism of Protein Adsorption. *ACS Symposium Series* **1995**, *602*, 26-40.

[34] Tomisawa, N.; Yamashita, A. C. Amount of Adsorbed Albumin Loss by Dialysis Membranes with Protein Adsorption. *J. Artif. Organs* **2009**, *12*, 194-199.

[35] Teh, L. C.; Murphy, L. J.; Huq, N.L.; Surus, A. S.; Friesen, H. G.; Lazarus, L.; Chapman, G. E. Methionine Oxidation in Human Growth Hormone and Human Chorionic Somatomammotropin. Effects on Receptor Binding and Biological Activities. *J. Biol. Chem.* **1987**, *262*, 6472-6477.

[36] Kakizawa, Y.; Kataoka, K. Block Copolymer Micelles for Delivery of Gene and Related Compounds. *Adv. Drug. Deliv. Rev.* **2002**, *54*, 203-222.

[37] Osada, K.; Christie, R. J.; Kataoka, K. Polymeric Micelles from Poly(ethylene glycol)-Poly(amino acid) Block Copolymer for Drug and Gene Delivery. *J. R. Soc. Interface 6 Suppl.* **2009**, *3*, S325-39.

[38] Bae, Y.; Kataoka, K. Intelligent Polymeric Micelles from Functional Poly(ethylene glycol)-Poly(amino acid) Block Copolymers. *Adv. Drug. Deliv. Rev.* **2009**, *61*, 768-784.

[39] Lavasanifar, A.; Samuel, J.; Kwon, G. S. Poly(ethylene oxide)-*block*-Poly(L-amino acid) Micelles for Drug Delivery. *Adv. Drug. Deliv. Rev.* **2002**, *54*, 169-190.

Chapter 5. General Discussion

Proteins are useful materials for various applications in biotechnology and biomedicine. Protein-polyelectrolyte complexes (PPC) have a great potential for expanding the applications of proteins. Although there have been several fundamental and practical studies of PPC, practical techniques related to protein handling have remained insufficient. Here, various techniques were developed using which enable to improve conventional protein handling techniques. A general discussion, paerspectives, and future directions of this research are presented below.

1. PEGylated polyelectrolytes

PEGylated polyelectrolytes are composed of ionic polyelectrolyte segments and non-ionic PEG segments. The polyelectrolyte segments can bind to the protein surface through electrostatic interactions, whereas PEG provides a steric stabilizing effect due to its strong hydration and high conformational flexibility. Taking advantage of these properties, on/off switching of enzyme activity (Chapter 2.1) and stabilization of protein against stress (Chapter 2.2) were achieved using PEGylated polyelectrolyte. The common point of these results is the formation of soluble PPC. The soluble PPC with PEGylated polyelectrolyte is primarily attributed with to the steric repulsion effect of the PEG segment in PEGylated polyelectrolyte. In fact, PPC with non-PEGylated polyelectrolyte (i.e., PAA or PAMA) aggregated, resulting in failure of on/off switching and stabilization of proteins. Accordingly, PEGylated polyelectrolyte is a new candidate for functionalization and stabilization of proteins.

Interestingly, the formation of soluble PPC with ASNase/PEG-*b*-PAMA did not affect the enzyme activity, whereas α-amylase and β-galactosidase were inactivated. Taking account of not only enzyme-polyelectrolyte but also substrate, this difference may have been due to the following properties: **(i)**

the molecular weight (M_w) of the ASNase substrate is smaller than those of α-amylase and β-galactosidase substrates [ASNase, L-asparagine (M_w = 132.1 g/mol); α-amylase, *p*-nitrophenyl-α-D-maltoside (PNPM, M_w = 463.3 g/mol); β-galactosidase, *o*-nitrophenyl-β-D -galactopyranoside (ONPG, M_w = 271.2 g/mol)]; **(ii)** PNPM and ONPG have dye molecules released by substrate, whereas L-asparagine do not; **(iii)** the surface distribution of charged amino acid on the proteins; and **(iv)** the affinity between the proteins and their substrate. Although it is difficult to further discuss the detailed mechanism of inactivation of proteins by polyelectrolyte, soluble PPC with PEGylated polyelectrolyte may be applied on a case-by-case basis, e.g., drug delivery systems or biosensors.

2. Enzyme hyperactivation phenomenon

Enzyme hyperactivation occurred in the presence of not only polyelectrolyte with high M_w (Chapter 3.1), but also charged molecules with low M_w, including polyamine (Chapter 3.2). These results suggested that the combination of complementary charged pair between molecules and substrates is a key factor in this phenomenon. In fact, preliminary experiments indicated that subtilisin activity toward anionic substrates increased with the addition of cationic polyelectrolyte. Another interesting point is that cationic ChT was hyperactivated not only by the addition of both anionic and cationic polyelectrolytes, suggesting that the formation of PPC is not important for the enzyme hyperactivation phenomenon. It should be noted that enzyme hyperactivation phenomenon does not require laborious mutagenesis or chemical modification of enzymes, and may expand the potential use of enzymes in biotechnological applications as biosensors and bioreactors.

Unfortunately, the detailed mechanism underlying the enzyme hyperactivation phenomenon remains unclear. In particular, the enhancement of ChT activity by cationic polyelectrolytes is difficult to explain because theoretically cationic polyelectrolyte does not form a PPC with cationic ChT. However, molecular dynamics simulation showed that cationic amine compounds bound to the ChT surface, suggesting that cationic polyelectrolyte may interact with the ChT surface through not only electrostatic but also

hydrophobic interactions. The interaction between enzyme and polyelectrolyte may contribute to the accumulation of charged substrate, which is attracted by polyelectrolyte on the enzyme through electrostatic interaction. Furthermore, preliminary experiments indicated that hyperactivation of different enzymes, such as elastase and trypsin, did not occur despite the presence of complementary charged substrate and polyelectrolyte, suggesting that there may be other systematic rules. Thus, further studies are required to gain a fundamental understanding of the enzyme hyperactivation phenomenon.

3. Precipitation-redissolution method

In contrast to the above studies associated with soluble PPC, there have been few investigation regarding use of insoluble PPC. To extend the possibility of using insoluble PPC, a precipitation-redissolution method was developed using poly(amino acid) for formulation of high-concentration therapeutic protein. Insoluble PPCs with ten types of therapeutic proteins were obtained by screening experimental conditions, and then precipitated by centrifugation. The precipitate of insoluble PPC was redissolved by exchanging solvent containing saline due to the electrostatic shield by increasing ionic strength. The redissolved proteins had native structures and functions, and did not form undesirable aggregates. Furthermore, *in vivo* experiments indicated that the general toxicity and pharmacokinetic profiles of redissolved antibodies corresponded to those of a conventional antibody formulation. Therefore, the protein formulation produced by the precipitation-redissolution method would be applicable for biomedical use.

In general, protein precipitation has attracted little attention as a general formulation method. However, these data indicate that PPC precipitation is superior as a novel method for concentration of protein formulations. In addition, the PPC precipitate stabilized protein against several types of stress, including heat, agitation, and oxidation. Use of the precipitation-redissolution method may facilitate use of protein precipitation for biomedical applications.

Chapter 6. General Conclusion

This thesis described various techniques using protein-polyelectrolyte complexes (PPC) for improvement of protein handling. Chapter 2 showed that on/off switching of enzyme activity for large and unstable enzymes was possible using PEGylated polyelectrolyte due to the formation of soluble PPC. Based on these findings, a stabilizing method designated as non-covalent PEGylation was developed to protect therapeutic L-asparaginase against proteolytic degradation and shaking-induced aggregation. These finding indicated that soluble PPC with PEGylated complex is applicable to biosensors or drug delivery systems. Chapter 3 presented an investigation of the enzyme hyperactivation phenomenon, which resulted in a marked increase in α-chymotrypsin (ChT) activity by addition of complementary charged pair between substrate and polyelectrolyte. In addition, the hyperactivation of ChT using a library of cationic amine compounds with different numbers of amine groups and alkyl chains suggested that both of multivalency and hydrophobicity of charged compounds were important factors for the enzyme hyperactivation phenomenon. The application of enzyme hyperactivation for tumor markers with enzyme activity, such as prostate-specific antigen, may facilitate the development of novel sensing methods using enzyme activity as a signal. Chapter 4 showed the feasibility of precipitation-redissolution method, which enables the preparation of various types of high-concentration protein formulation both easily and quickly. This technique should contribute to the development of a novel type of protein formulation, i.e., PPC precipitate formulaton.

Despite the many fundamental studies regarding PPC, there have been few reports of practical techniques using PPC for protein applications. The findings of this study will facilitate the development of novel biotechnology and biomedicine applications. For application of the techniques discussed in this thesis, a fundamental understanding of the underlying mechanisms is essential, especially the enzyme hyperactivation phenomenon. Protein-handling techniques using PPC are likely to be widely adopted in various research fields in the near future.

List of Publications

Related Publications

[1] **Takaaki, Kurinomaru;** Shunsuke, Tomita; Shinpei, Kudo; Sumon, Ganguli; Yukio, Nagasaki; Kentaro, Shiraki Improved Complementary Polymer Pair System: Switching for Enzyme Activity by PEGylated Polymers. *Langmuir* **2012**, *28*, 4334-4338.

[2] **Takaaki, Kurinomaru;** Shunsuke, Tomita; Kentaro, Shiraki Enzyme Hyperactivation System Based on a Complementary Charged Pair of Polyelectrolytes and Substrates. *Langmuir* **2014**, *30*, 3826-3831.

[3] **Takaaki, Kurinomaru;** Takuya, Maruyama; Shunsuke, Izaki; Kenji, Handa; Tomoaki, Kimoto; Kentaro, Shiraki; Protein-Poly(amino acid) Complex Precipitation for High-Concentration Protein Formulation. *Journal of Pharmaceutical Sciences* **2014**, *8*, 2248-2254.

[4] **Takaaki, Kurinomaru**; Kentaro, Shiraki Non-Covalent PEGylation of L-Asparaginase Using PEGylated Polyelectrolyte. *Journal of Pharmaceutical Sciences* **2014**, *in press*.

[5] Shunsuke, Izaki[1]; **Takaaki, Kurinomaru**[1]; Takuya, Maruyama; Takayuki, Uchida; Kenji, Handa; Tomoaki, Kimoto; Kentaro, Shiraki Feasibility of Antibody-Poly(glutamic acid) Complexes: Preparation of High-Concentration Antibody Formulations and Their Pharmaceutical Properties. *in submitted*. [1]These authors contributed equally to this paper.

[6] **Takaaki, Kurinomaru**; Tomoshi, Kameda; Kentaro, Shiraki Effects of Multivalency and Hydrophobicity of Polyamines on Enzyme Hyperactivation of α-Chymotrypsin. *in submitted*.

Other Publications

[1] Takuya, Maruyama[1]; Shunsuke, Izaki[1]; **Takaaki, Kurinomaru**; Kenji, Handa; Tomoaki, Kimoto; Kentaro, Shiraki Protein-Poly(amino acid) Precipitation Stabilizes Therapeutic Protein against Physicochemical Stress. *in submitted*. [1]These authors contributed equally to this paper.

[2] Shunsuke, Izaki; **Takaaki, Kurinomaru**; Kenji, Handa; Tomoaki, Kimoto; Kentaro, Shiraki Stress Tolerance of Antibody-Poly(amino acid) Complexes: for Improving the Stability of High Concentration Antibody Formulations. *in preparation*.

Acknowledgements

I have been very fortunate to have met and had the help of so many people. This work performed during the course of study at the University of Tsukuba would not have been possible without their devoted efforts.

First, I would like to express my deepest gratitude to the chief examiner of my thesis, Associate Professor Kentaro Shiraki (University of Tsukuba). He has been continually supportive and understanding, and I am especially grateful for the countless hours of consultation and the freedom to explore many of my own interests during this work.

I am also indebted to Professor Yukio Nagasaki (University of Tsukuba), Professor Toshiaki Hattori (University of Tsukuba), and Associate Professor Muneaki Hase (University of Tsukuba) for useful insights from a range of diverse perspectives.

I have also benefited from the work of many collaborators: Professor Yukio Nagasaki and Mr. Shinpei Kudo (University of Tsukuba); Dr. Tomoshi Kameda, Dr. Yoshihisa Hagihara, and Dr. Shunsuke Tomita (National Institute of Advanced Industrial Science and Technology (AIST)); Mr. Tomoaki Kimoto, Mr. Kenji Handa, Mr. Shunsuke Izaki, Mr. Shiuhei Mieda, and Mr. Takayuki Uchida (Terumo Corporation); and Dr. Sumon Ganguli (University of Chittagong) provided expert assistance with equipment, experiments and invaluable discussions, and were always helpful.

I would also like to thank the members of Associated Professor Shiraki's laboratory I would also like to thank the Shiraki Grope members—Dr. Atsushi Hirano, Dr. Shunsuke Tomita, Dr. Eisuke Takai, Mr. Ryosuke Ariki, Mr. Soichiro Kayano, Mr. Shuhei Matsushita, Mr. Kohei Kabei, Mr. Hiroki Yoshikawa, Ms. Chie Yamamoto, Ms. Yui Shikiya, Mr. Daisuke Shinozaki, Ms. Chie Tanaka, Ms. Yuri Kamiyama, Mr. Masato Shimada, Ms. Yumiko Tanabe, Mr. Naoto Inoue, Mr. Gai Ohashi, Mr. Takuya Maruyama, Mr. Shunsuke Yoshizawa, Mr. Kazuki Iwashita, Mr. Kengo Kuwada, Ms. Ayumi Matsuda, Ms. Takumi Miyatake. I would not have been able to accomplish the goal without our friendly rivalry.

I am grateful to my parents, sister, brother, and Ms. Mariko Sakamoto without whom none of the achievements in this course of study would have been possible. In particular, my parents strongly encouraged me to follow my dreams and did everything they could to ensure that these dreams came true.

Finally, I would like to extend my deepest gratitude to all of my friends for their continued support and encouragement. I am grateful for everyone's time and effort in making this thesis possible.

Takaaki Kurinomaru

February 2015